Author:
Goldmann, Wolfgang Heinrich

Title:
Pressure and temperature perturbation studies of the interaction between actin and myosin and between calcium and troponin C

PRESSURE AND TEMPERATURE PERTURBATION STUDIES OF THE INTERACTION BETWEEN ACTIN AND MYOSIN AND BETWEEN CALCIUM AND TROPONIN C

A dissertation submitted to the University of Bristol in candidature for the degree of Doctor of Philosophy

by

Wolfgang Heinrich GOLDMANN

Department of Biochemistry

University of Bristol

July, 1990

SUMMARY

Coates et al. (1985) have shown that the association reaction of actin with myosin subfragment 1 (S1) consists of at least two steps following the formation of a collision complex;

$$A + M \overset{K_o}{\longleftrightarrow} A\,M \overset{K_1}{\longleftrightarrow} A\text{-}M \overset{K_2}{\longleftrightarrow} AM$$

The influence of monovalent anions, ionic strength, organic solvents, nucleotide and temperature on this reaction is examined by various kinetic techniques (stopped flow, pressure jump and slow temperature jump).

Increases in ionic strength above 0.1M, the presence of ethylene glycol or dimethylsulphoxide or the addition of nucleotide reduce K_2. In contrast, K_oK_1 is relatively unaffected by these treatments. However, specific monovalent anions above 0.1M do reduce K_oK_1 by increasing k_{-1}. The differential effect of these parameters to stabilize actomyosin intermediates for structural analysis is discussed.

Geeves & Ranatunga (1990) have demonstrated that high pressure augments twitch tension in intact muscle fibres. Studies of troponin C in solution by pressure jump method show that the binding to calcium is not affected by 100atm pressure. This suggests, assuming that the effect of pressure is no different to that in fibres, that muscle is "switched on" to a larger extent per stimulus at high pressure by either increased release of

calcium from the sarcoplasmic reticulum or by a change in the inhibitory function of the regulatory proteins.

The rate binding properties of fluorescent labelled TnC to calcium are investigated by pressure jump and fast temperature jump methods.

Fuer meine kleine Maus,

Sousan

PREFACE

The studies presented here were carried out in the Department of Biochemistry, University of Bristol, between February 1987 and July 1990. The work forms no part of any thesis previously submitted and apart from exceptions noted, was carried out unaided.

ACKNOWLEDGEMENTS

I gratefully acknowledge the discussion and advice of my supervisor, Dr. M.A. Geeves during the preparation of this thesis and would like to thank him very much for all his help during my research.

I would also like to thank Prof. H. Gutfreund for advice and financial help to carry out this project.

I like to thank Mr. Rick Border and Dr. T.E. Jeffries for technical advice with protein preparations during the early stages of this work, Mrs. M. Bray for clean glassware and Drs. M.A. Geeves, D.J. Halsall and Mr. D. McKillop for the use of the computer software to analyse data. A special thanks goes to Dr. M.A. Geeves, Prof. H. Gutfreund and Drs. N.S. Fortune and J. Hancock for their critical reading of this manuscript.

Finally, I thank Dr. E. Davies, Mr. Paul Connibear and all the others in the Inner Court for the friendly working atmosphere.

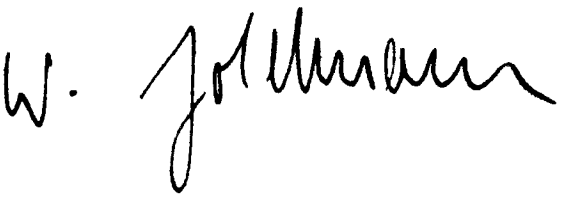

PUBLICATIONS

1. The influence of anions, ionic strength and organic solvents on the interaction between actin and myosin subfragment 1. M.A. Geeves & W.H. Goldmann (1990), Biochem. Soc. Transactions, Vol.18, 585-586

2. A "slow" temperature jump apparatus built from a stopped flow machine. W.H. Goldmann & M.A. Geeves (1990). Submitted to Anal. Biochem.

CONTENTS

ABBREVIATIONS

The abbreviations in this thesis are in accordance with the guide to authors for submission to the Biochemical Journal with the following additions:

A	F-actin
ADP	Adenosine 5'diphosphate
Ap5A	p^1,p^5, diadenosine 5'pentaphosphate
atm	atmosphere
ATP	Adenosine 5'triphosphate
ATPase	Adenosine 5'triphosphatase
DANZ	Dansylaziridine
DEAE	Diethylaminoethyl
DMF	Dimethylformamide
DTT	Dithiothreitol
DMSO	Dimethylsulphoxide
EDTA	Ethylenediaminetetra-acetic acid
EGTA	Ethyleneglycol-bis-(β aminoethyl ether) N,N,N',N'-tetra acetic acid
EHT	Extra high tension
EPR	Electron paramagnetic resonance
F-actin	Filamentous actin
FPLC	Fast protein liquid chromatography
FRET	Fluorescence resonance energy transfer
G-actin	Globular actin
HMM	Heavy meromyosin
LMM	Light meromyosin

M	Myosin
MPa	Mega-pascal
N	Nucleotide
PMSF	Phenylmethylsulphonylfluoride
Pyrene	N-(1-pyrenyl)iodoacetamide
Pyr-actin	Pyrene labelled actin at CYS 374
Pi	Inorganic phosphate
S1	Myosin subfragment 1
S2	Myosin subfragment 2
SDS-page	Sodium dodecyl sulphate, polyacryamide gel electrophoresis
τ	Relaxation time
Tn/Tm	Troponin and tropomyosin complex
Tm	Tropomyosin
Tn	Troponin
TnC	Troponin C
TnI	Troponin I
TnT	Troponin T
Tris	Tris[hydroxymethyl]aminomethane

The n^{th} step of a reaction k_{+n} is the forward rate constant, k_{-n} is the reverse rate constant and $K_n = k_{+n}/k_{-n}$ is the equilibrium constant. Stopped flow experiment concentrations are referred to as reaction chamber concentrations. For pressure jump studies equilibrium constants are quoted at atmospheric pressure. Bars denote equilibrium free protein concentration.

CHAPTER 1 INTRODUCTION

Inherent movement is the prime sign in life. For this and many other reasons, man has shown a perpetual curiosity about the organs of locomotion in his own body and in those of other creatures since the times of Greek anatomists. Indeed, some of the earliest scientific experiments known, concerned muscle and its functions. Although a large number of different techniques have been employed, the problem of energy transduction from chemical reaction into mechanical work is still not fully understood today.

Muscle is a highly efficient and versatile energy-converting device, with remarkable engineering and performance characteristics. The conversion of the chemical energy of ATP into the mechanical energy required to bring about contraction, translocation and propulsion, is still one of the most challenging problems in modern biochemistry.

The study of muscular contraction has encompassed many different scientific disciplines. Biochemists, physiologists, biophysicists, electron-microscopists have all been involved in the investigation of muscle contraction. Most of the recent advances in muscle research have derived from correlation of these disciplines, with the main approaches being structural, mechanical and biochemical.

The work presented in this thesis is concerned with the biochemical events of protein-protein interaction in muscle. Current theories in this field and the contribution to other disciplines will be discussed in this introduction.

MUSCLES

Muscle types

Movement is one of the essential properties of a living organism and is made by cellular contractility. In a unicellular organism, movement is one of several functions of the single cell, but in coelenterates it becomes a specialised function of certain surface epithelial cells. When examining more complex animals, specialised muscle cells can be found, which contract to produce coordinated movements under the control of some type of nervous organization. In vertebrates muscle, cells are further specialised and three distinctive types of muscle may be recognised: smooth muscle, which is regulated involuntarily and shows little well-defined structure; cardiac muscle, which is regulated spontaneously and functions continuously throughout life and skeletal muscle, which is under voluntary control and forms a major part of the body mass.

The morphology and function of skeletal muscle is much better understood than our corresponding knowledge of smooth and of cardiac muscle. While the known differences between these three fundamental muscle types can not be ignored, much of the information on the anatomical structure, on the physiology of contraction and on the biochemistry of action of muscle proves relevant to all three forms of muscle.

This thesis is concerned solely with rabbit skeletal muscle, although biochemical studies have been performed on other skeletal muscles from frogs, chickens, fish and insects.

Muscle structure

The substructure of striated muscle, explored by light microscope, is shown schematically in fig. 1.1. Muscle fibres are composed of longitudinal fibrils, approx 1-2um in diameter, with alternating dark and light bands. The dense bands are birefringent and are called the A (anisotropic) bands; the light bands are known as I (isotropic) bands. Within the I-band lies the dense Z line, about 80nm thick, which is continuous across the width of the fibre, holding the fibrils together and keeping the A and I bands of the many fibrils in register. A package of myofibrils from Z line to Z line is a sarcomere.

COMPONENTS OF MUSCLE

The thick filament

Myosin is one of the principal protein components of the contractile system and comprises of approx 50% of the total protein in skeletal muscles. It is a relatively large (approx 500kDa Mwt.), asymmetric, hexameric protein containing several structural and functional domains (Cooke, 1986). Under denaturing conditions myosin dissociates into two heavy chains of approx 230kDa Mwt. and four light chains of 16-20kDa Mwt. (Harrington & Rodgers, 1984). A diagrammatic representation of the myosin structure is shown in fig. 1.2a.

At physiological salt concentrations myosin aggregates to form bipolar thick filaments, which are insoluble below 0.3M ionic strength (Margossian & Lowey, 1982). The molecule contains

Figure 1.1 The micro-anatomy of vertebrate skeletal muscle (from Harold, 1986)

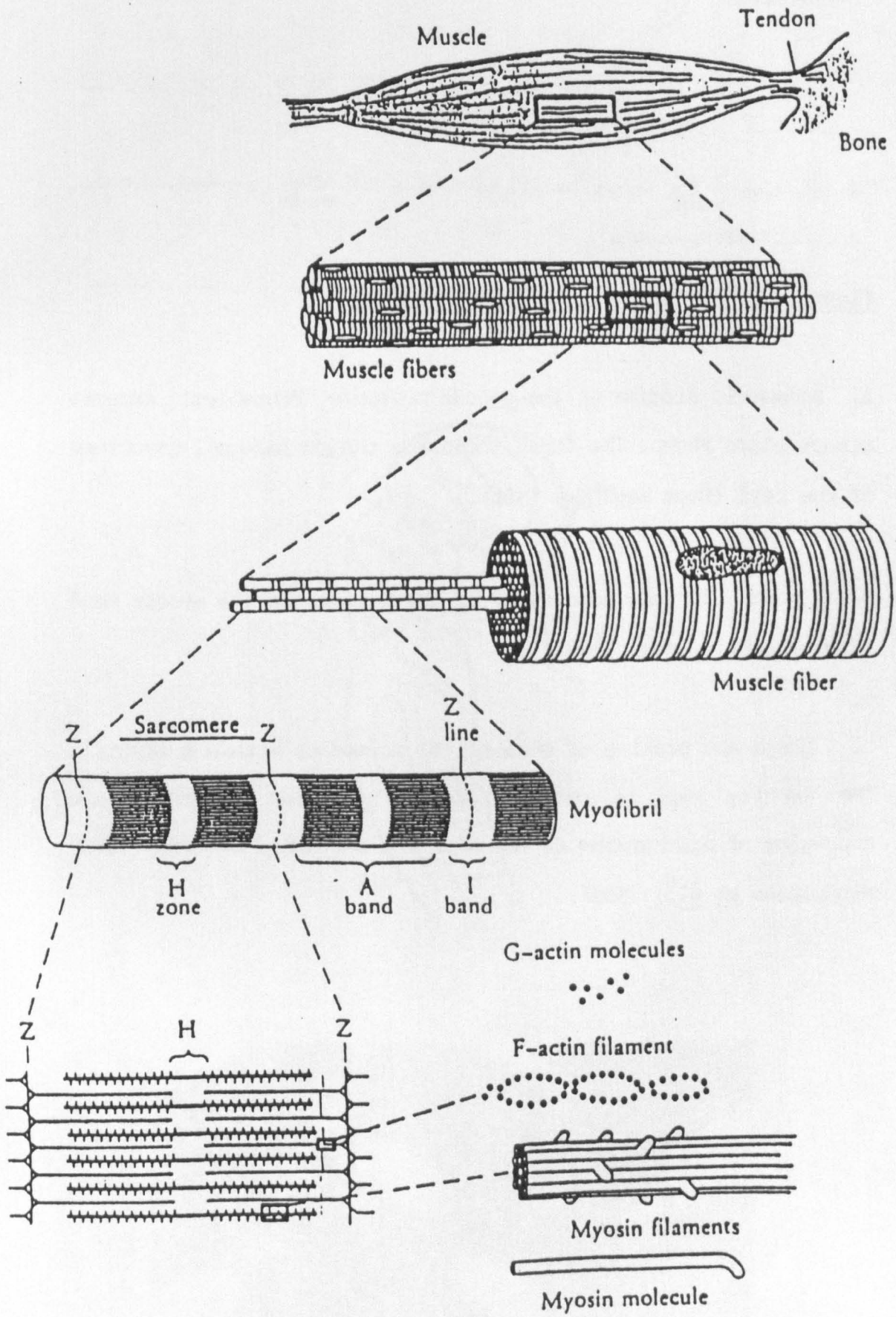
Muscle
Tendon
Bone
Muscle fibers
Muscle fiber
Z
Sarcomere
Z
Z
line
Myofibril
H
zone
A
band
I
band
G-actin molecules
Z
H
Z
F-actin filament
Myosin filaments
Myosin molecule

Figure 1.2 Myosin and its subfragments

A. Schematic diagram of the myosin molecule. Proteolytic enzymes attack where shown. The inset indicates the coiled-coil structure of the tail (from Bagshaw, 1982).

B. A model for the topography of the domains in the myosin head (from Vibert & Cohen, 1988).

C. Shape and packing of skeletal S1 molecules within a crystal. The density map is reconstructed by computer filtering and averaging of micrographs of embedded and sectioned material (from Winkelmann et al., 1985).

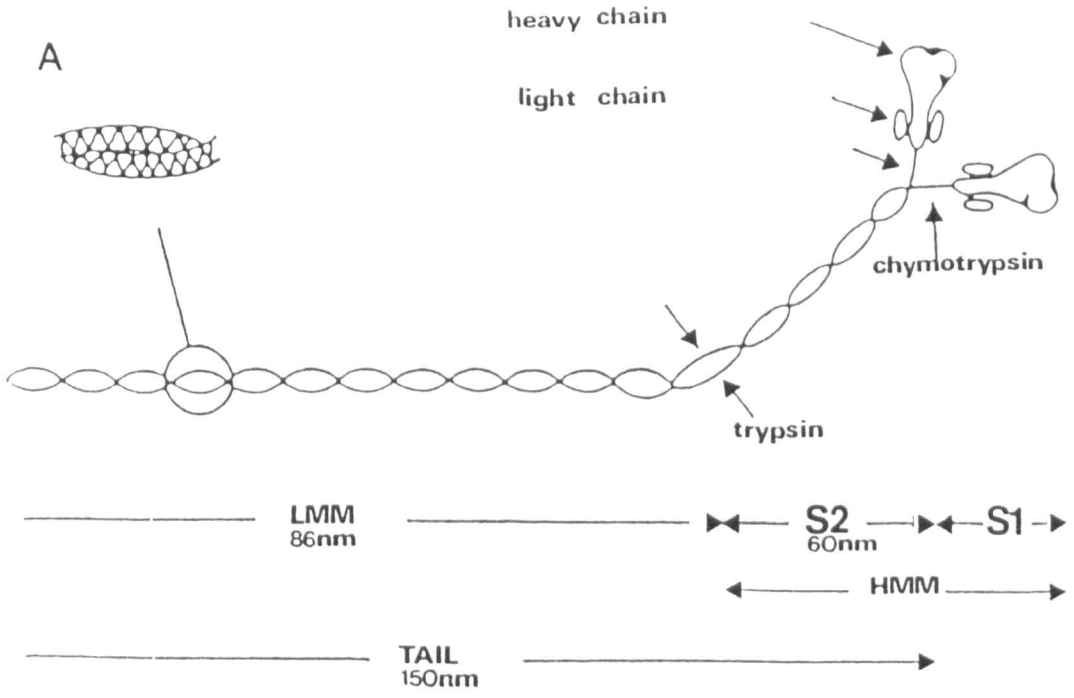
A
heavy chain
light chain
chymotrypsin
trypsin
LMM
86nm
S2
60nm
S1
HMM
TAIL
150nm

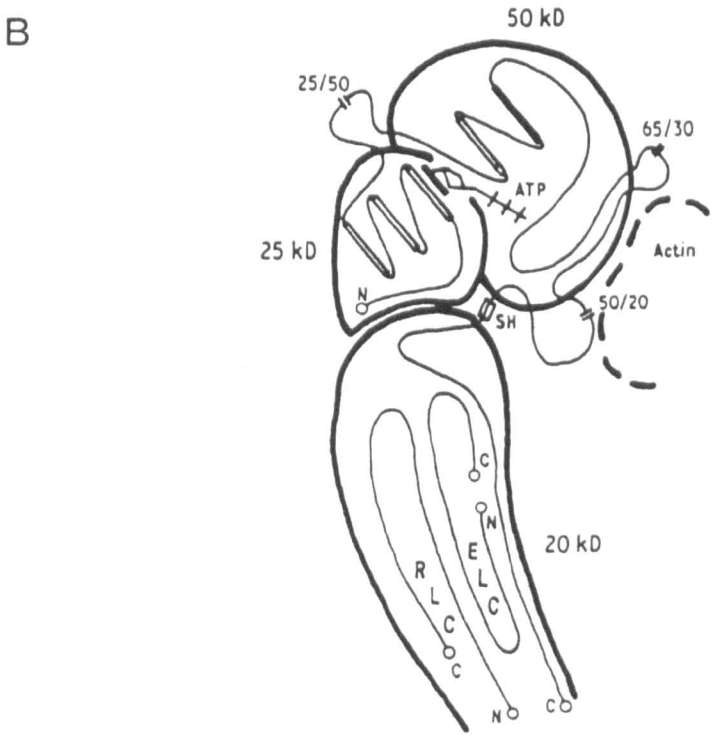
B
50 kD
25/50
65/30
ATP
25 kD
Actin
N
SH
50/20
C
N
20 kD
E
L
C
R
L
C
C
N
C

C

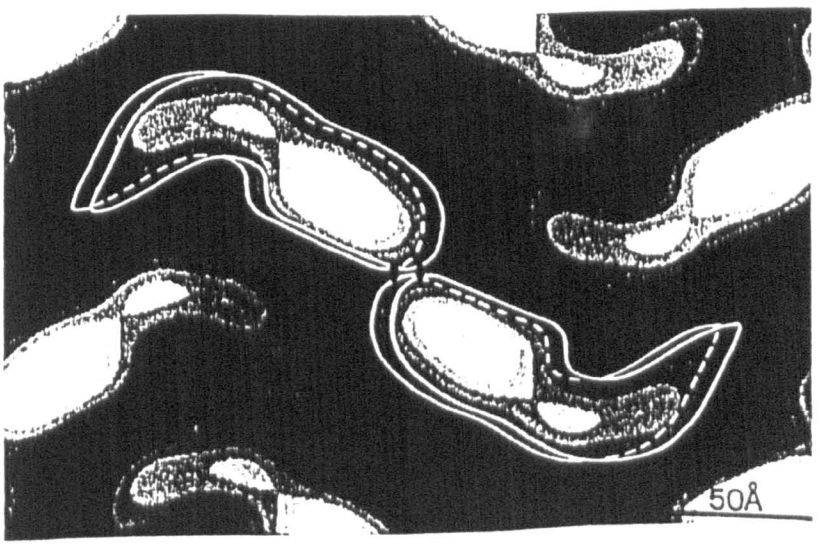
50Å

three main regions, which are sensitive to proteolysis. Chymotryptic digestion in the presence of divalent metal ions results in the cleavage of the tail region or "light meromyosin" (LMM) and "heavy meromyosin" (HMM). LMM is 86nm long and insoluble at physiological ionic strength while the soluble HMM consists of the "S2" region, which is 60nm long and the "S1" head region (Stewart & Edwards, 1984). The junction between the "S2" region and the globular "S1" head region is susceptible to proteolysis in the absence of divalent metal ions.

LMM consists of two heavy chains in a coiled-coil α-helical structure, which is highly repetitive (Karn et al., 1983). The hydrophobic residues on the inside of the helix form the interface between the two strands of the coiled-coil. The amino acid sequence of this portion has provided at least a partial explanation of the forces that hold the core of the thick filament together (McLachlan, 1984).

The "S2" section is thought to contain the flexible region, which links the "S1" with the rigid tail region. The sequence of the rod basically favours the strong α-helical secondary structure, however, weaker parts have been found at the junction between LMM and "S2". This region is susceptible to proteolysis and thought to be essential for the functioning of the protein, allowing the head group to interact cyclically with the actin filament (Applegate & Reisler, 1984).

The "S1" head region can be cleaved into three segments with molecular weights of 50, 25 and 20kDa, respectively (Balint et al., 1978). The N-terminal 25kDa fragment binds nucleotide and

has sequence homology with other nucleotide binding proteins. The 50kDa and 20kDa segments can be cross-linked to actin (Mornet et al., 1981a;b; Sutoh, 1983; Vibert & Cohen, 1988). The 20kDa region extends to the "swivel", an area, which connects the head with the rod and which binds both of the light chains. The region contains two highly reactive sulphydryls, SH-1 and SH-2 (fig. 1.2b).

Each "S1" head contains two classes of light chains; the P-light chain, which can be phosphorylated and the alkali A-light chain, which exists in two different forms referred to as A1 and A2. The P-light chain is involved in the regulation of contraction (Adelstein & Eisenberg, 1980). In smooth and some non-muscle cells this is achieved via phosphorylation of this chain, and in skeletal and cardiac muscle, the contraction is modulated by the phosphorylation. The A-light chain was first thought to be essential for the myosin ATPase activity, however, now it is known, myosin devoid of both light chains retains an actin activated ATPase activity similar to intact myosin. The two isoforms of A-light chains, A1 and A2 have been found in skeletal muscles, which confer different ATPase activities (Sivaramakrishnam & Burke, 1982; Wagner & Stone, 1983) and actin binding on S1 at low ionic strength (Trayer et al., 1985).

Winkelmann et al. (1985) have crystalized S1 and determined the overall length of the molecule to be 16nm. Electron micrographs of the crystals have indicated two domains, one of higher and one of lower density. The higher density region has a prominent mass at one end with dimensions of 6 x 4nm. The region of lower density forms a curved neck region and extents from one

end of the mass. This mass probably comprises of 20kDa portion of the heavy chain and the two light chains (Baker & Winkelmann, 1986) (fig. 1.2c).

OTHER COMPONENTS OF THE THICK FILAMENT

Although myosin is the main component of the thick filament of vertebrate striated muscle, it is not the only one. In electron micrographs of A bands a set of 11 stripes, 43nm apart, may be seen in each half of the A band, occupying a region 0.25-0.50μm from the centre (Craig, 1977). Some, but not all, of the components have now been identified: B-protein, which is a component of the M-line; C-protein; F-protein has been identified as the enzyme phosphofructokinase; H-protein and X-protein (Starr & Offer, 1982). A group of giant myofibrillar proteins are present in abundance in a wide range of vertebrate and invertebrate striated muscles: titin and nebulin. These proteins are unusual not only in their giant sizes, but also in their solubility and their localisation in the sarcomere. The function of all these proteins is not fully understood today, but they could be involved as regulators of cross-bridge movements, in a mechanical or structural function or in filament assembly (Trinick et al., 1984; Wang & Greaser, 1985; Marayama et al., 1989).

THE THIN FILAMENT

Actin is a globular protein with a single polypeptide chain, which in skeletal muscle is composed of 375 amino acids and has a

molecular weight of 42 kDa (Collins & Elzinga, 1975). It forms the backbone of the thin filament and has been shown to occur in every eukaryotic cell studied sofar (Clarke & Spudich, 1977). The complete amino acid sequence has been determined and showed a remarkable degree of homology in muscle and non-muscle cells with only a few amino acid substitutions predominantly near the N-terminus of the chain (Vandekerckhove & Weber, 1979).

At physiological salt concentration, actin polymerizes to filamentous (F)-actin. F-actin is a double-stranded helix linked by non-covalent bonds and with 13-15 molecules of globular (G)-actin for one full turn (fig. 1.3a). In solution the filaments are in dynamic equilibrium with the monomeric actin and the association of the monomers occur preferentially from one end of the filament.

In (1981) Suck et al. determined the structure of monomeric actin from rabbit skeletal muscle by X-ray crystallography at 6 Angstrom resolution. The structure showed that the molecule is asymmetric with dimensions of approx 7nm x 4nm x 3nm and composed of two different size domains, which are separated by a cleft. Recent reconstructions of actin polymers have resolved the actin monomer into a major and a minor domain, similar to those determined from X-ray crystallography (O'Brien et al., 1983) (fig. 1.3b), despite the ambiguity about the situation of the domains nearest to the filament axis (Egelman, 1985). Attempts to determine an actin structure at 3 Angstrom resolution have been made by Kabsch & Holmes (1990) and preliminary results have been published.

Figure 1.3 Actin structure

A. Schematic representation of F-actin, troponin and tropomyosin with measurements. The intertwined strands cross over approx every 38nm and the filament width has been estimated at approx 9.5nm with an approx 5.9nm pitch (from Cooke, 1986).

B. Three-dimensional reconstruction of F-actin from electron micrographs of filaments embedded in amorphous ice (from Egelman, 1985).

A

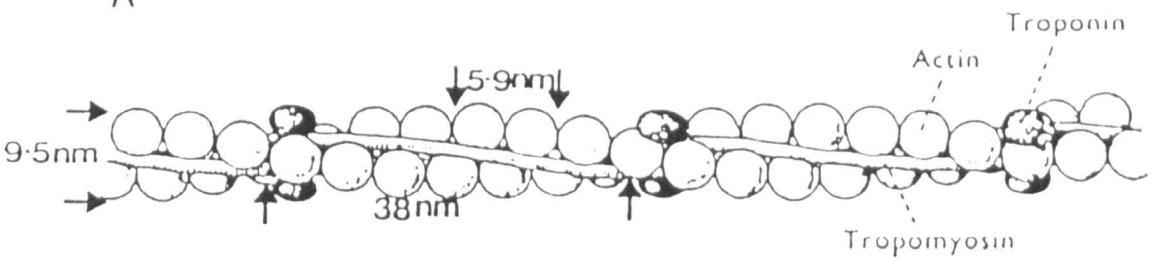

B

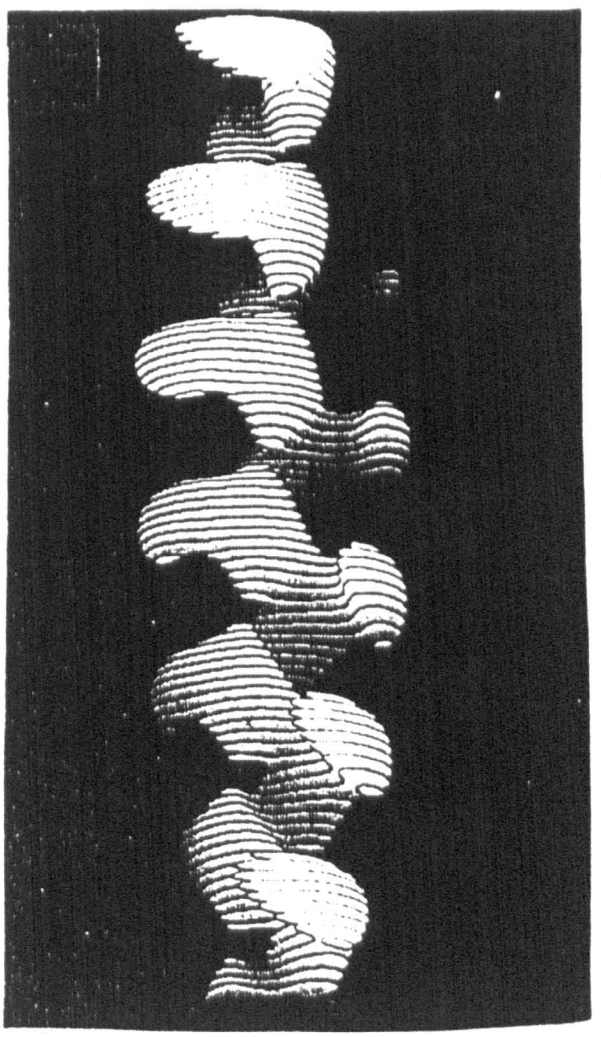

OTHER COMPONENTS OF THE THIN FILAMENT

Tropomyosin

Tropomyosin (Tm) is a key protein in the regulation of muscle contraction and is found in a wide range of non-muscle cells. It exists as a dimer of two polypeptide subunits, which associate in register in a coiled-coil fashion (Graceffa & Lehrer, 1980). The subunits of 284 amino acid residues and 33kDa each have very similar amino acid sequences (Hodges et al., 1972). Crystals of tropomyosin have been formed to about 4 Angstrom resolution, in which the 400 Angstrom long molecule appears to bonded head-to-tail to form continuous filaments. X-ray diffraction pattern showed second order helical layer lines arising from the 140 Angstrom pitch of the two-stranded coiled-coil, which suggests that Tm can bind actin by winding around the actin filament. The eight or nine residue head-to-tail overlap of tropomyosin molecules is crucial to Tm polymerization and binding to actin (Phillips et al., 1986) (fig. 1.4a).

Troponin

Ebashi & Kodama (1966) and Endo & Ebashi (1966) first demonstrated that the Ca^{2+} dependence of actomyosin ATPase activity required a protein, which they called troponin (Tn). The exact composition of troponin was uncertain for several years until Greaser & Gergely (1971; 1973) established that troponin consists of three non-identical subunits, which led to the following terminology: (TnT), which binds tropomyosin and attaches the troponin complex to the thin filament, (TnI), which

Figure 1.4 Troponin, tropomyosin and actin interactions

A. A model for the protein components of the vertebrate thin filament, incorporating bi-lobal actin monomers, the two-stranded α-helical coiled-coil of tropomyosin and the elongated head and tail structure of the troponin complex (from Philips et al., 1986)

B. A diagrammatic representation of troponin/tropomyosin (from Flicker et al., 1982).

C. Folding of troponin C from the 0.28nm X-ray diffraction map (from Herzberg & James, 1985).

A

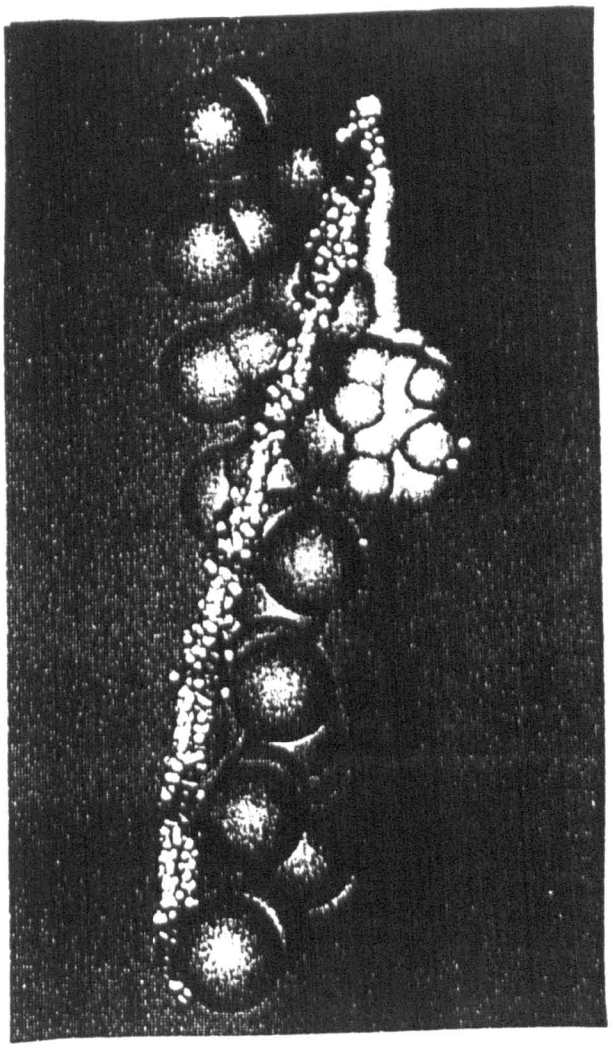

B

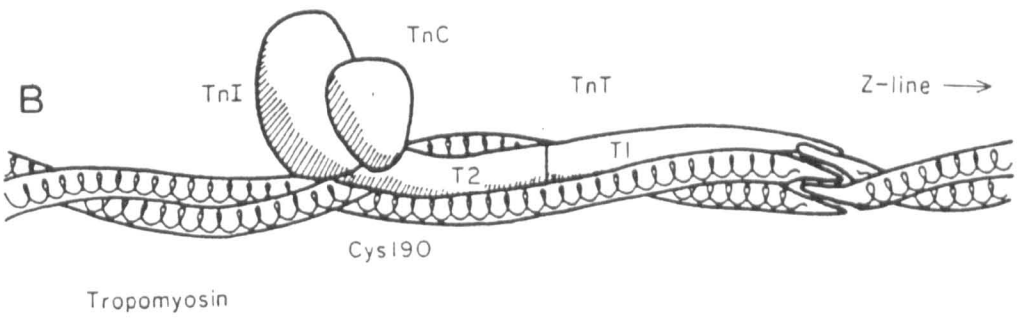
TnC
TnI
TnT
Z-line
T1
T2
Cys190
Tropomyosin

C

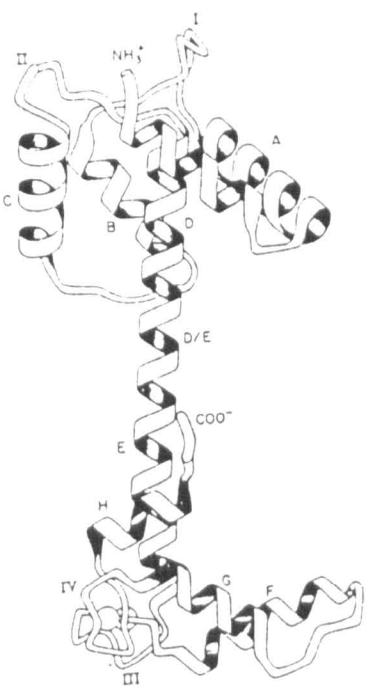
I
II
NH3+
A
C
B
D
D/E
COO-
E
H
IV
G
F
III

inhibits the actin.subfragment 1 (acto.S1) ATPase and (TnC), which binds Ca^{2+}. The subunits interact with tropomyosin and are situated one third of the distance from the carboxyl-terminal end of the (Tm) molecule (fig. 1.4b).

Troponin T

Troponin T (TnT) is the largest subunit of troponin with a calculated molecular weight of 30,503 Daltons and 259 amino acid residues (Pearlstone et al., 1976). This globular protein with a rod-shaped tail is highly polar near the amino and carboxyl termini and links the troponin complex to tropomyosin. It has direct interactions with TnI, TnC and tropomyosin and confers a Ca^{2+}-sensitive inhibition of ATPase activity (Greaser & Gergely, 1971). Crystals of TnT and Tm have been formed to 17 Angstrom resolution by White et al. (1987).

Troponin I

Troponin I (TnI) has a calculated molecular weight of 20,864 Daltons and consists of 179 amino acids (Wilkinson & Grand, 1975). This rod-shaped molecule has two segments, which are significant in the regulatory thin filament interactions. Functionally, TnI inhibits the actomyosin Mg^{2+}-ATPase. In the absence of tropomyosin or troponin, one TnI molecule per actin monomer is required to inhibit activity. This inhibition is abolished by the presence of TnC, irrespective of $[Ca^{2+}]$ (Greaser & Gergely, 1971).

Troponin C

Troponin C (TnC) is composed of 159 amino acid residues with

a calculated molecular weight of 17,846 Daltons (Collins et al., 1973). Crystal structures to a resolution of 2.2 Angstroms have been produced, which have revealed two distinct domains: one containing the amino-terminal Ca^{2+}-specific sites and the other containing the carboxyl-terminal Ca^{2+}-Mg^{2+}-sites. These sites are separated by a long nine turn α-helix, producing a dumb-bell shaped molecule about 75 Angstrom long (Herzberg & James, 1985) (fig. 1.4c). Potter & Gergely (1975) had found four Ca^{2+}-binding sites on (TnC), which fitted best two classes of sites: two low-affinity sites that selectively bind Ca^{2+} over Mg^{2+} (Ca^{2+}-specific sites; K_{Ca} approx 10^5 M^{-1}) and two high-affinity sites that bind Ca^{2+} and Mg^{2+} competively (Ca^{2+} - Mg^{2+} sites; K_{Ca} approx 10^7 M^{-1}; K_{Mg} approx 10^3 M^{-1}). The interactions between TnC and TnI and actin are central to the Ca^{2+}-dependent regulation of contraction. TnC and TnI interact both in the presence and absence of Ca^{2+}.

MUSCLE CONTRACTION

Cross-bridge theories

A vertebrate skeletal muscle fibre is made up of many sarcomeres, which are approx 2.4um long and contain an interdigitating array of thick and thin filaments stacked end-to-end. On muscle shortening, the thick and thin filaments slide passed each other, leaving the length of filaments constant. This was first observed by H.E. Huxley & Hanson (1954), using interference microscopy and by A.F. Huxley & Niedergerke (1954), using phase contrast microscopy and led to the sliding filament

model of muscle contraction.

In (1957) A.F. Huxley proposed the existence of an elastic element attached to one filament, which could cyclically interact with the other filament, depending on the tension in the fibre and the presence and absence of ATP. H.E. Huxley (1957) identified these elastic elements by high-resolution electron micrographs as "cross-bridges" between neighbouring thick and thin filaments, which were later recognized as the S1 heads of myosin (fig. 1.5a).

In the (1957) theory of A.F. Huxley, force production was accommodated by making the rates of attachment and detachment of force generating links (now cross-bridges) sensitive to position. The rate constants for these two processes were believed to be dependent on the relative axial positions of the myosin-based projections and the actin-based attachment sites. Attachment would be faster than detachment in regions where cross-bridges generated positive tension, but detachment would be much faster from positions, in which the cross-bridges exerted a force opposed to the normal shortening motion. Cross-bridges could not attach directly in positions that exerted negative tension and could reach such positions only through the sliding of the filaments relative to each other during shortening. With the values for attachment and detachment, it was possible to fit quantitatively the experimental data to the mechanical and energetic steady-state properties of muscle that were available at the time. However, rapid transient changes seen in muscle were not included in this theory.

Huxley & Simmons (1971) added this extra feature to the

Figure 1.5 Models of muscle contraction

A. The cross-bridge model of A.F. Huxley (1957). This model proposed the existance of a "side piece" (later cross-bridge) connected to the thick filament, which could attach and detach from the thin filament in a cyclic fashion, depending of the tension in the fibre and the presence or absence of ATP (from Woledge et al. 1985).

B. The cross-bridge model of Huxley & Simmons (1971). The attached cross-bridge head can take up a number of distinct conformations. The transition between these conformations involve rotation of the cross-bridge head. This produces a change in length of the elastic element (from Woledge et al., 1985).

C. Cross-bridge cycle and its relation to the actomyosin ATPase based on the model by Lymn & Taylor (1971). The myosin head prefers two orientations (45^{o} and 90^{o}) in the attached state depending on the presence of nucleotide. The dissociated heads are mobile with freedom of rotational motion (from Hibberd & Trentham, 1986).

D. Cross-bridge model of Eisenberg & Greene (1980). In contrast with the Lymn-Taylor scheme, the reaction AM.ATP $\longleftrightarrow$ AM.ADP.Pi is now a significant step in the mechanism. In both these state myosin is weakly bound to actin; each is in rapid equilibrium with the corresponding myosin state (M.ATP or M.ADP.Pi) (from Eisenberg & Hill, 1985).

A

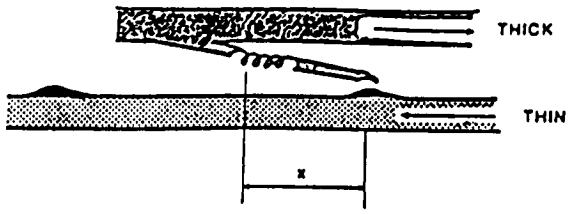
THICK
THIN
x

B

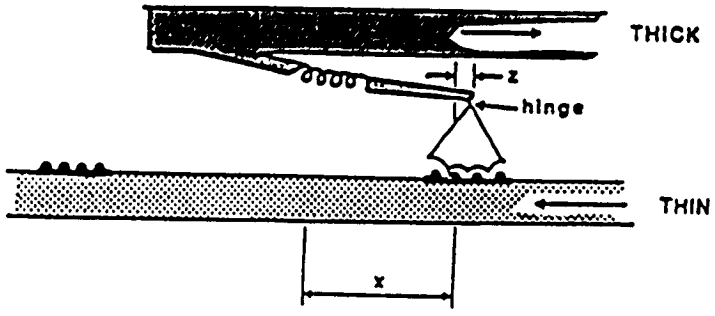
THICK
z
hinge
THIN
x

C

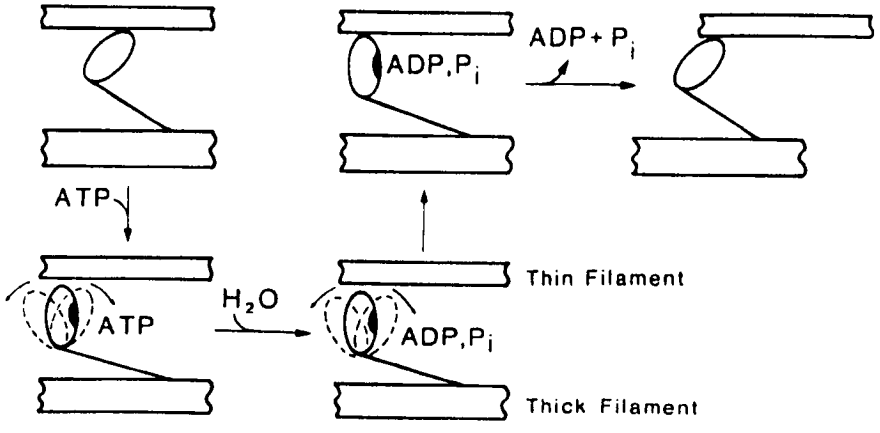
ADP,Pi
ADP + Pi
ATP
Thin Filament
H2O
ATP
ADP,Pi
Thick Filament

D

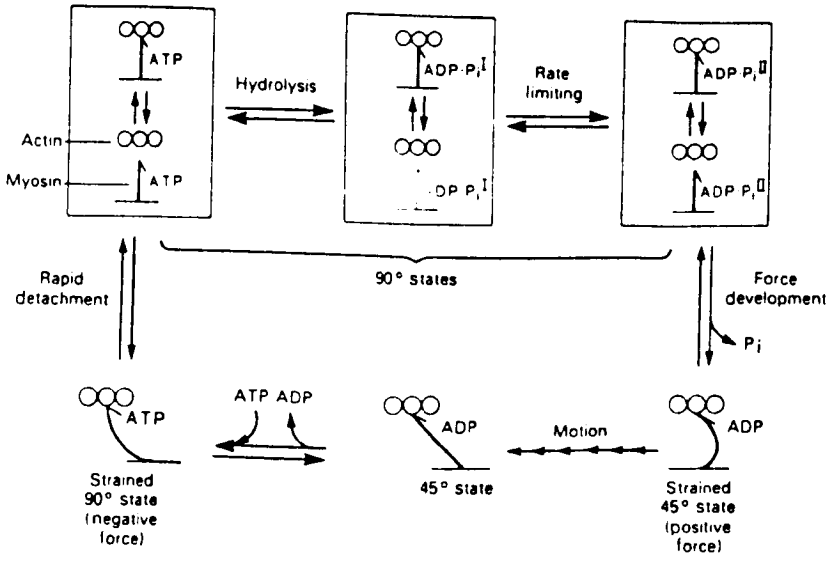
ATP
Actin
Myosin
ATP
Hydrolysis
ADP·Pi I
DP Pi I
Rate limiting
ADP·Pi II
ADP Pi II
Rapid detachment
90° states
Force development
Pi
ATP
Strained 90° state (negative force)
ATP ADP
ADP
45° state
Motion
ADP
Strained 45° state (positive force)

cross-bridge representation used in the A.F. Huxley (1957) theory. The attached cross-bridge head (S1) can now take up a number of different conformations. Rapid tension transients are explained by an elastic element in the cross-bridge arm prior to an orientation change of the cross-bridge (fig. 1.5b).

A widely accepted theory, today, about the mode of action of cross-bridge contracting muscle can be summarized as follows:

a) Cross-bridges cyclically attach to and detach from thin filaments.
b) Force can be generated in the attached cross-bridge, pulling the thin filaments along in the direction that produces muscle shortening.
c) ATP hydrolysis is coupled to such a cycle, providing the energy of contraction.

This theory has been developed to describe quantitatively many mechanical, energetic, biochemical and structural properties of muscle. It is convenient to discuss experimental results in these terms (see also Woledge et al., 1985).

BIOCHEMICAL STUDIES

Many studies have been carried out on muscle proteins with biochemical techniques and correlated with structural and mechanical properties in fibres (Hibberd & Trentham 1986; Irving, 1987). Proteolytic digestion of myosin has made the biochemical approach a powerful tool. By using these methods, myosin retains

its actin binding and ATPase activity and has proved valuable in attempting to elucidate the mechanism of muscle contraction. In interpretating biochemical results, it is important to take into account, the effects of solubilising and digesting muscle proteins.

A common criticism of biochemical studies of actin and myosin subfragment 1 (S1) is that the local concentration of proteins will be much higher in the filament. Further, that solution studies are normally performed at ionic strengths lower than physiological conditions. Also steric contraints in the filament will affect the rates of some of the muscle protein interactions. As proteins in solution can do no work, free energy of ATP hydrolysis must be dissipated as heat. Therefore, solution studies are often compared to muscles contracting under no load. Experiments to compare the solution studies with *in vivo* observations will be discussed (Geeves, 1990; Millar & Homsher, 1990).

THE LYMN-TAYLOR SCHEME

The basic model for the biochemical mechanism of the actomyosin ATPase reaction is the Lymn-Taylor scheme (Lymn & Taylor, 1971). This scheme gives a relatively simple view of how the chemistry of ATP hydrolysis could be related to cycling cross-bridges. The basis of the scheme is as follows: Following ATP binding to actomyosin (AM), actin (A) dissociates from the (AM.ATP) complex faster than ATP is hydrolysed, so the intermediate (M.ATP) is formed. After ATP hydrolysis the myosin products complex (M.ADP.Pi) can rebind to actin, so that there is

a rapid equilibrium between the states (M.ADP.Pi) and (AM.ADP.Pi). Release of the products occurs much faster from (AM.ADP.Pi) than from (M.ADP.Pi), giving the strongly bound (AM.ADP) or (AM) states and completing the cycle and giving it a direction. Fig. 1.5c shows the structural correlations that were proposed to accompany the biochemical events.

THE MODEL OF EISENBERG & GREENE

Stein et al. (1979) tested the Lymn-Taylor scheme and showed that it does not describe the pathway of ATP hydrolysis in solution accurately under all conditions. It was observed that, when actin concentration is increased to nearer the concentration in muscle, it could reversibly bind to all intermediates of the ATPase pathway. Furthermore, ATP binding to actomyosin at low ionic strength does not necessarily lead to actin dissociation before ATP hydrolysis. In contrast to the Lymn-Taylor scheme, the reaction (AM.ATP $\longleftrightarrow$ AM.ADP.Pi) now became an important step in the mechanism. In both these states, myosin is weakly bound to actin; each is in rapid equilibrium with the corresponding myosin state (M.ATP or M.ADP.Pi).

Eisenberg & Greene (1980) proposed a cross-bridge model on the basis of the kinetic scheme by Stein et al. (1979) (fig. 1.5d). Free cross-bridges are in rapid equilibrium with actin-bound cross-bridges. In the weak-binding 90^{o} conformation of the cross-bridge two kinetic events occur (ATP hydrolysis and a "rate-limiting" step). This is followed in the cross-bridge cycle by the transition from the weak-binding 90^{o} to the strong-binding

45^{o} conformation with tension development, Pi release and force production, which is different in muscle and solution as there is no restraint in solution. It was suggested by Eisenberg & Greene (1980) that in muscle tension development and movement occur in two steps. Both steps are a result of the nature of attachment of many cross-bridges instead of one. During tension development a strained 45^{o} attachment exists, exerting positive tension, which is only relieved by the gradual and relative movement of the filaments. The release of ADP from the cross-bridge is slow only until the cross-bridge reaches the stable 45^{o} conformation, then ADP release becomes as rapid as in solution. With the release of ADP, ATP binds to the cross-bridge causing it to return to the 90^{o} state. This state exerts negative tension, but M.ATP detaches rapidly from AM.ATP and no significant tension is developed.

THE MODEL OF GEEVES, GOODY AND GUTFREUND

The transition between weak and strong actin binding states were discussed further by Geeves et al. (1984) and interpreted in the following two step model;

$$A + MN \underset{}{\overset{K_1}{\longrightarrow}} A\text{-}MN \underset{}{\overset{K_2}{\longrightarrow}} AMN$$

(A=actin; M=myosin; N=nucleotide)

In the first step actin binds to form a weakly "attached" ternary complex with an association constant of 10^{3} to 10^{4} M^{-1} and then isomerizes to a "rigor-like" complex. It was proposed

that the first step is relatively independent of nucleotide. The second step, however, was dependent upon the nucleotide present at the myosin subfragment 1 (S1) nucleotide binding site. The equilibrium constant (K_2) of the second step dictates whether the ternary complex exists in either the strong or weak binding state. If $K_2 > 1$ the strong complex predominates, if $K_2 < 1$ the weak complex predominates. The isomerization step is believed to be related to the force generating event in muscle. Eisenberg & Greene (1980) had suggested the transition from the weak 90° state to the strong 45° state to be responsible for tension generation.

Geeves et al. (1984) discussed the kinetic data available at the time in terms of two different models: a direct coupling model suggesting that the steps in the ATPase cycle are directly responsible for conformational changes that represent tension generation in muscle; and an indirect coupling model, in which changes in affinity of actin for myosin at different stages throughout the ATPase cycle determine the time, the myosin molecule would spend in the attached and rigor-like state. The change in both environments is followed by the power stroke.

Several pieces of indirect biochemical evidence for the existence of two states of actin and myosin subfragment 1 (S1) have been provided by various workers with different techniques and under different conditions.

In (1980) Sleep & Hutton studied the oxygen exchange of inorganic phosphate (Pi) and ATP in the presence of acto.S1 and demonstrated that the exchange was greater with hydrolysis of ATP

than when ADP and Pi were only present in the system. The existence of two ADP states were proposed under steady state conditions, one of which could not be formed upon addition of ADP. The kinetics of the interaction between actin and S1.ADP or S1.ethenoADP has also been studied by stopped flow (Marston, 1982; Trybus & Taylor, 1980; Siemankowski & White, 1984; Rosenfeld & Taylor, 1984) and by pressure relaxation methods (Geeves & Gutfreund, 1982). These studies were consistent with a simple one-step binding reaction, preceded by a rapid pre-equilibrium or collision complex.

In the pressure jump study by Geeves & Gutfreund (1982), the interaction of acto.S1 binding was monitored by following the changes in light-scattering. The sensitivity of this method, however, limited the study to conditions (at high salt concentration or in the presence of ADP) where the association constant was between 10^4 and 10^6 M^{-1}.

The use of actin labelled at Cys 374 with a pyrene fluorophore, which has no significant effect on the binding, has enabled characterization of additional acto.S1 and acto.S1-nucleotide complexes (Criddle et al., 1985; Geeves et al., 1986). Employing the specific pyrene probe increased the sensitivity of the pressure jump studies, allowing relaxations at physiological ionic strength and in the absence of nucleotide to be observed. Coates et al. (1985) provided the first direct evidence for this model. It was revealed that two relaxations of acto.S1 were apparent corresponding to two steps in the actin binding reaction with only significant pyrene fluorescence quench on the second, pressure-sensitive step.

More recent work demonstrated that the same two states can be identified when nucleotide or nucleotide analogues are bound to myosin and that the equilibrium constant (K_2) is particular sensitive to the nature of the occupancy of the nucleotide site on myosin (Geeves et al., 1986; Geeves & Jeffries, 1988; Geeves, 1989). The model proposed by Geeves et al. (1984) is shown in fig. 1.6 with experimentally determined or estimated values for (K_1) and (K_2).

RELATION OF BIOCHEMISTRY AND STRUCTURAL STUDIES

The biochemical evidence of intermediates in the actomyosin ATPase cycle might be testable by structural methods, e.g. the fraction of cross-bridges that are attached to actin in a particular mechanical or biochemical state or the existence of two or more configurations of the attached cross-bridge.

Some of the most detailed information about cross-bridge structure has come from electron microscopy. X-ray diffraction is used to gain further information about periodic structural features, whilst X-ray scattering has been used to investigate aperiodic charateristics such as cross-bridge orientation (Irving, 1987). The reactive sulphydryl (SH-1) of myosin subfragment 1 (S1) sites on the cross-bridges can be modified by introducing extrinsic probe molecules, which can be used for optical studies of structure changes. In addition to fluorescence and dichroism studies, extrinsic probes have been used for electron spin resonance (ESR) and electron paramagnetic resonance (EPR) studies of muscle fibres (for references see Cooke, 1986).

Figure 1.6 The two step binding model of Geeves et al. (1984)

The myosin (M) ATPase reaction in the absence of actin is shown in column 1. Equilibrium constants (a.) were taken from Trentham et al. (1976). Each of these states can bind (A) actin weakly to form ternary complexes shown in column 2 and then isomerize to give complexes in column 3. The overall binding constants are given in column 4. This is related to the two binding reaction by the relationship $K_a^{MN} = K_1^{MN} \times (1 + K_2^{MN})$. The equilibrium constants (b.) were assumed to be of the same order for each myosin species as established for myosin.ATP (MT) and myosin.ADP (MDP). The value for the equilibrium constant (c.) was derived from values of the overall binding constant and weak binding constant. This value was determined by Coates et al., 1985; Geeves & Halsall (1986) and chapter 3 between 100-200. Values for (d. and f.) were determined from detailed balance and value for (e.) was established as a minimum (Millar & Geeves, 1983). The equilibrium constant (g.) was obtained by stopped flow (White, 1977) and has been inferred from pressure jump experiments (Geeves et al., 1986). A value of between 10 - 100 for (h.) is compatible with published data (Sleep & Hutton, 1980; Geeves & Gutfreund, 1982; Geeves & Jeffries, 1988). Values for (f.) can be determined from detailed balance. Newly determined values have not been inserted in this scheme.

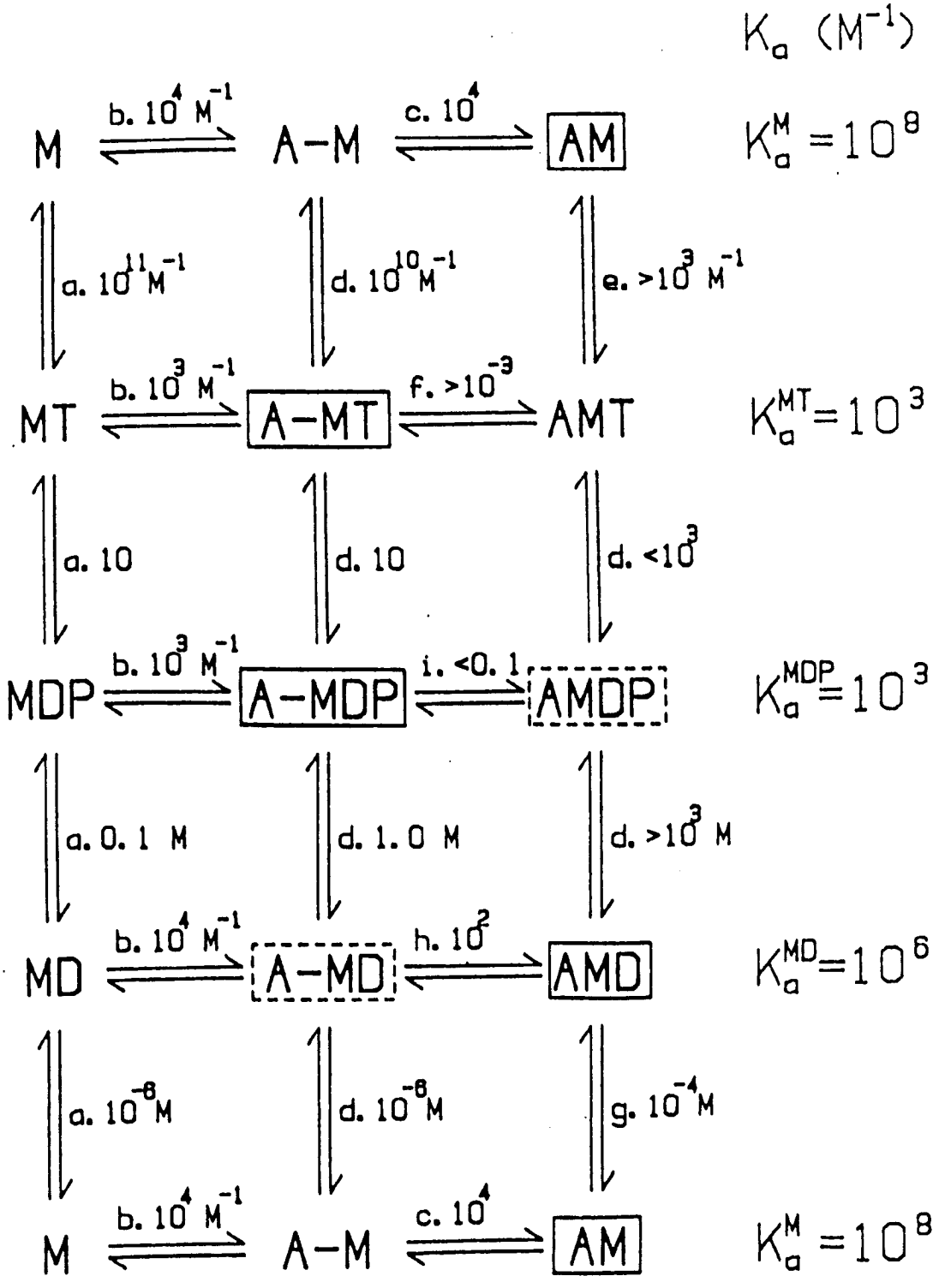
K_a (M^{-1})
M
b. 10^4 M^{-1}
A–M
c. 10^4
AM
$K_a^M = 10^8$
a. 10^{11} M^{-1}
d. 10^{10} M^{-1}
e. $>10^3$ M^{-1}
MT
b. 10^3 M^{-1}
A–MT
f. $>10^{-3}$
AMT
$K_a^{MT} = 10^3$
a. 10
d. 10
d. $<10^3$
MDP
b. 10^3 M^{-1}
A–MDP
i. <0.1
AMDP
$K_a^{MDP} = 10^3$
a. 0.1 M
d. 1.0 M
d. $>10^3$ M
MD
b. 10^4 M^{-1}
A–MD
h. 10^2
AMD
$K_a^{MD} = 10^6$
a. 10^{-8} M
d. 10^{-8} M
g. 10^{-4} M
M
b. 10^4 M^{-1}
A–M
c. 10^4
AM
$K_a^M = 10^8$

Results from electron microscopy in the absence of ATP of actin filaments with myosin (S1) bound to them indicate that heads make an angle of about 45^{o} with the filament axis. X-ray scattering confirms this orientation of 45^{o} to the filament axis (Poulsen & Lowy, 1983) and X-ray diffraction suggests stereospecific attachment of cross-bridge heads. Results from experiments using spin or optical probes attached to S1 support this view. The presence of ADP in rigor muscle has no effect on the mechanical properties in X-ray pattern or orientation of a spin label on myosin (SH-1). Local changes in myosin conformation on addition of ADP have been detected by probes attached to SH-1 (Burghardt et al., 1983).

Actin-based layer lines in electron micrographs of relaxed muscle are weaker than in rigor muscle, suggesting cross-bridge detachment from actin. Extrinsic probes detect a greater disorder of orientation in relaxed than in rigor muscle. X-ray and birefringence measurements estimate an average cross-bridge head angle of 30^{o} with the filament (Irving & Peckham, 1986).

In contracting muscle, X-ray diffraction result suggest 60-80% of cross-bridge attachment to actin (Huxley & Kress, 1985). EPR spectra of isometric contracting muscle indicate 20% of the spin probes on myosin SH-1 are in rigor conformation and 80% remain disordered and mobile. Fluorescence ATP analogue measurements showed 40% of cross-bridge heads in rigor conformation. Differences in these results are interpreted as possible two types of attached cross-bridges.

Clearly, the available structure data are inadequate. It may be necessary to develop new methods to probe the orientations,

mobility or interactions of several defined sites on the cross-bridge to answer questions of structural basis of tension generation (Cooke, 1986).

THE RELATION OF BIOCHEMISTRY TO MECHANICS

An experimental system that allows mechnical observations, while the biochemical milieu of the myofilament is altered, is that of "skinned fibre" preparations: The surface membrane of the muscle fibre is either chemically or mechanically removed and placed in solutions that mimic the intracellular environment. The de-membranated muscle cells with largely intact myofilaments has provided new information about the relationship between mechanical performance (tension development, shortening velocity and response to rapid perturbations) and the chemical environment of the myofilaments. However, caution is required in extrapolating from skinned fibres to intact muscle (Woledge *et al.*, 1985).

The rates of ATP binding and hydrolysis in fibres were measured by Sleep & Smith (1981) and correlated with data from solution studies. The results are ambiguous as protein concentration in fibres and diffusional delays of ATP concentration could not be controlled. Much of the information about actomyosin in muscle has, therefore, come from studies of steady-state and transient mechanical properties of muscle fibres in solutions of various maintained compositions. Cooke & Pate (1985) observed an increase of isometric tension in the presence of ADP, which was consistent with ADP inhibiting the rate, at

which ATP bound to a tension bearing state. The influence of the products of the ATPase reaction (ADP, Pi) on the cross-bridge cycle in muscle has also been explored, suggesting that ADP release could limit the shortening velocity in muscle (Siemankowski & White, 1984; Siemankowski et al., 1985). Oxygen exchange studies were used to elucidate the stages of myosin ATPase in solution and in fibre (Webb et al., 1986). It was observed that exchange occurs at a greater rate in fibres than in solution of purified proteins. It has become possible to study the kinetics of transitions between biochemical states more directly by imposing a rapid step change of ATP concentration within a muscle fibre. This was achieved by allowing ATP protected by a photolabile group, "caged" ATP, to diffuse into the fibre, then illuminating the fibre with an intense pulse of UV-light to generate ATP rapidly in millimolar concentrations (Goldman et al., 1982; Dantzig et al., 1987). Results from these studies indicate that major steady-state intermediates in isometric muscle must have bound hydrolysis products. Time-resolved X-ray diffraction allows the movement of muscle components to be observed directly (Kress et al., 1986) and results indicate a movement of mass towards the thin filament prior to tension increase. More recently, pressure perturbation studies on whole muscle fibres have been carried out and results support the conclusions from solution studies that increased pressure is perturbing a cross-bridge event (Geeves & Ranatunga, 1987; 1990; Fortune et al., 1988; 1989).

A MODEL OF CROSS-BRIDGE ACTION

Based on the models of A.F.Huxley (1957) and Eisenberg & Greene (1980), Pate & Cooke (1989) incorporated all aspects of steady-state kinetics and physiological data obtained from demembranated muscle fibres into a new model of energy transduction.

The authors explain their model, using one single pathway with five states for ATP hydrolysis: three actomyosin attached states (A.M.ADP.Pi; A.M.ADP; and A.M) and two detached states (M.ATP; M.ADP.Pi). This model accounts for the relationship between ATP concentration, steady-state ATPase rate and isometric tension in contracting fibre with a reasonable set of assumptions.

A basic assumption of this model is that the kinetic cycle of ATP hydrolysis is the same in fibres and solution. The free energies of the detached cross-bridge states are not dependent on the relative actin-binding sites. The (A.M.ADP.Pi) state is mechanically the same regarding stiffness, but exerts little force, and the Pi release is seen as the driving force for muscle shortening. Most force is produced by the A.M.ADP state and the rate-limiting step in isometric muscle is the ADP release. The model also defines a linear relationship between the log of Pi concentration, isometric force and ATPase rate.

Premises made in this model conform with most of the data and interpretations of the past few years. However, some ideas and data challenge the traditional view on energy transduction; e.g. the tight coupling between cross-bridge attachment-detachment

cycles and ATP hydrolysis; the cooperative effects between the two independent myosin heads on the energetics of energy transduction mechanism (for all references Pate & Cooke, 1989).

ENVIRONMENTAL CHANGES OF A SOLUTION CONTAINING ACTIN AND S1: THE EFFECT ON THE STRUCTURE, ACTIVITY AND BINDING OF PROTEINS

The understanding of the interaction of actin and myosin under various experimental conditions is important in the study of muscle function. A great amount of evidence has accumulated to illustrate that the interaction of ions or solvents with muscle proteins plays an important role in the contractile process and, therefore, deserves special study. It has been shown that the presence of ions or solvents influence the conformation, the ATPase activity and other physiochemical properties of the actomyosin complex (for all references Stafford, 1985).

Over the last 20 years a considerable body of research has been concerned with the effect of various salts on the conformational stability of a variety of biological macromolecules and macromolecular assemblies in general. The effect was viewed as a shifting, by the added salt, of the transition boundary between an ordered macromolecular structure (in which residue-residue contacts are thermodynamically favoured for at least the groups comprising the "interior" of the macromolecule) and a disordered or "random" coil state, in which residue-solvent contacts for essentially all of the constituent groups (Von Hippel & Wong, 1962). The phase transition boundary may be shifted towards either higher or lower temperatures

relative to the transition temperature of the macromolecule in a dilute aqueous buffer system, depending on whether the added ions tend to stabilize (thermodynamically favour) the ordered or the disordered forms of the macromolecule. The effects of the individual ions on the macromolecular stability were reported to be independent and additive and generally follow the classical Hofmeister series (Hofmeister, 1888; Von Hippel & Schleich, 1969a;b).

Major work has been carried out by various workers on how these effects are brought about. Studies on macromolecules have

made it clear, that the effects do not depend strongly on details of macromolecular conformation or chemistry (Nandi & Robinson, 1972a;b). Therefore, the emphasis of research has turned to an examination of the properties of small molecules e.g. collagen (Von Hippel & Wong, 1962), DNA (Ross & Scruggs, 1964) and myosin (Warren et al., 1966).

The two major forces, which alter the state of interaction of aqueous solutions of biological molecules, are hydrophobic and electrostatic. They play an important role in the transfer of reactants from the bulk-water phase to the surface of the enzyme protein. Further, their interaction with specific protein groups and concomitant conformational changes of the protein make a large contribution to the thermodynamic state of the system. As the accompanying thermodynamic changes provide a useful insight into the processes involving biological molecules, it allows comparison with information on mechanical changes obtained by other analytical methods (Kodama, 1985).

With the development of kinetic techniques for the study of biological systems, much attention has been directed towards the elucidation of distinct intermediates, their rates of interconversion and the characterization of physical properties. The wide range of kinetic techniques today, allows the observation of reactions with different lifetimes and intermediates. Stopped flow, temperature jump and pressure relaxation techniques are the most widely used. Relaxation methods have the advantage over flow techniques, as the time taken to change the concentration of the reactant is not limited by mixing time, which is approx 1msec. Flow, mixing and flow

stopping artefacts are also avoided using relaxation techniques. Temperature jump reactions can be initiated within the nano -and microsecond range and permit observations up to 1sec. In contrast, pressure relaxation reactions can only be observed after 25usec but with no upper time limit. Further advantages over temperature perturbation technique are: no limit of solvent composition, reproducible reactions in rapid succession and no protein denaturation under 1000atm.

Volume changes during biochemical reactions in aqueous media are largely due to changes in solvent structure due to the interaction with solute molecules (Gutfreund, 1972). The formation and disappearance of charged groups accessible to water result in considerable volume changes and hence processes involving such exposed ionising groups show a marked pressure-dependence. These effects can be due either to conformation changes, which result in exposure of a charged group or to pressure-induced change of the pK of a group linked to a conformational rearrangement. Studies of the effect of pressure over a range of conditions allow one to distinguish between the different causes of electrostriction, ionisation, breaking of salt bridges and exposure of buried charged groups. Hydrogen bond transfer from an intrinsic to a water bonded state is generally associated with a small negative volume change.

The aim of relaxation techniques is to perturb the equilibrium so that subsequent rapid reactions can be studied. The perturbation can be mediated through an indirect effect such as the rapid change in pH or of the concentration of some other

reactant species. Studies of amplitudes of relaxations under different conditions can elucidate the volume changes and thermodymanic characteristics of the reaction steps. The amplitude of the change in equilibrium for a pressure change is given by;

$$(\partial \ln K/\partial P)_t = -\Delta V^o/RxT$$

For small pressure changes this approximates to;

$$\Delta K/K = -\Delta P \times \Delta V^o / R \times T$$

(K = equilibrium constant; P = pressure; V^o = standard volume change; R = gas constant; T = absolute temperature)

The study of protein assembly from monomeric units is of interest both because it can give information about the structure and the forces involved in their stability. The potential of pressure relaxation for the study of the assembly of myosin polymers has been demonstrated (Davis & Gutfreund, 1976).

Geeves & Gutfreund (1982) reported that pressure relaxation could be used as a tool to study the mechanism of acto.S1 interactions. Results demonstrated the potential of this method for studying the rate of equilibration of the attachment of S1 for actin by light scattering under various conditions. It was shown that the binding reaction in the presence of ADP, which was treated in terms of a single-step reaction, was sensitive to ionic strength, temperature and pH changes. Similar observations were made for the binding of actin to S1 by the stopped flow

method in the absence of nucleotide (White & Taylor, 1976; Konrad & Goody, 1982; Marston 1982). The marked ionic strength effect on the forward rate constant was interpretated as a significant contribution from charged groups in the binding reaction, in which electrostatic interactions play an important role. The large temperature dependence of the binding indicated a conformational change in the protein and data from the Arrhenius plot suggested an entropy controlled reaction. Konrad & Goody (1982) also interpreted the association of actin and myosin as an entropy driven process. Large values for ΔS^{o} are normally expected for reactions with significant volume changes. Substantial volume changes usually reflect changes in the ordering of water due to changes in the number of exposed charged or hydrophobic groups (Eagland, 1975). This evidence indicated a more complex binding reaction, and the high activation energy (E_a approx 107 kJ/mol) suggested that the first order isomerzation is preceded by a faster diffusion controlled reaction. Further evidence for a more complex reaction has come from the analysis of the observed amplitudes.

The use of fluorescent labelled actin allowed the interaction of actin S1 to be monitored at physiological ionic strength and in the absence of nucleotide by pressure relaxation methods (Coates et al., 1985). Two relaxations were identified, which represented two events in the interaction of actin with S1. However, it was suggested that the first step may be more complex as the reaction did not have the properties associated with a diffusion controlled reaction. Therefore, this step was

considered to comprise the formation of a collision complex before the attached state is formed;

$$A + M \overset{K_o}{\longleftrightarrow} (A\ M) \overset{K_1}{\longleftrightarrow} A\text{--}M \overset{K_2}{\longleftrightarrow} AM$$

and with no direct information on the collison complex, the reaction was discussed in terms of two steps ($K_1' = K_o \times K_1$). It was demonstrated that ionic strength, temperature and organic solvent had a marked effect on the two individual binding steps and that the second step was sensitive to hydrostatic pressure and caused quenching of pyrene fluorescence. The size of perturbations suggested that the equilibrium had an associated volume change of approx 100 cm^3 per mol.

Volume changes of this magnitude normally indicate a change in the hydration sphere of the system caused by the exposure of charged groups to the solvent and must be seen as evidence for a substantial change in conformation of the protein complex or a change in the contact area between the two proteins.

Thermodynamic data of the binding of ATP to myosin subfragment (S1) (Biosca et al., 1983) and acto.S1 (Millar & Geeves, 1983) revealed a large increase in entropy at low temperature. The results were interpretated in terms of temperature induced conformational change in the protein. The entropic control on the free energy is normally the consequence of the hydrophobic interaction dominating the association process at low temperature. The enhancement of solvent structure by the dissolution of non-polar groups in aqueous solution is greatest

at low temperature, and the tendency for hydrophobic association is increased because of this (Ross & Subramanian, 1981).

Many laboratories have used organic solvents to elcuidate the structure of the cross-bridge intermediates in the actomyosin ATPase cycle. The use of organic solvent has been known to weaken the binding of the acto.S1 complex (Marston & Tregear, 1984). Tregear et al. (1984) reported a shift in the S1 structure in the presence of 40% ethylene glycol towards the weak binding conformation. Increasing salt concentration and ethylene glycol concentration furthered this process. Recently, (Mushtaq & Greene, 1989) reported a similar event for controlled actin. No significant effect of 40% ethylene glycol was observed upon the interaction of ATP with acto.S1 (Millar & Geeves, 1983). Geeves & Jeffries (1988) observed that the acto.S1 complex in the presence of 40% ethylene glycol and ADP exists to less than 30% in the weak binding conformation.

The aim of this thesis is to examine the effect of different anions, temperature, solvents, ionic strength and nucleotide in order to understand the nature of the acto.S1 reaction in each step. The differential effect of these parameters could be used to trap actomyosin in the weakly attached state preferentially, facillitating structural studies of the two states.

Results from these studies are evaluated in terms of the two step binding model of Geeves et al. (1984).

CHAPTER 2 MATERIALS AND METHODS

REAGENTS

General reagents were purchased from BDH Chemicals Co., Boehringer Mannheim GmbH., Sigma Chemicals Co. and Aldrich Fine Chemicals, unless otherwise stated. DTT was obtained from Park Scientific and Urea (Enzyme Grade) was supplied by Bethesda Research Lab. (BRL). Fluorescence probe (N-(1-pyrene)iodoacetamide was purchased from Molecular Probes Inc. and N-dansylaziridine was obtained from Pierce Chemicals Co. The chromophoric indicator arsenazo III was a gift from Dr. D. Yates, Bristol University.

GENERAL BUFFERS

Experiments were generally performed at pH 7.0. In pressure jump studies imidazole (pK 7) was used because of its pH stability upon pressure perturbation. Titrations were mainly conducted in tris (pK 8) or cacodylate (pK 6.27) buffers, due to occasional difficulties with background fluorescence caused by impurities in imidazole preparations. Slow and fast temperature jump experiments were usually carried out using cacodylate since this buffer is reasonably insensitive to changes in temperature.

All buffers contained 1mM sodium azide to prevent bacterial and fungal contamination. Double distilled water was used for all buffers. The glassware was rinsed with double distilled water after washing. Magnesium ions were used as described in the appropriate sections.

Ca/EGTA BUFFERS

To keep the concentration of free ionised Ca^{2+} constant in buffers, a series of Ca/EGTA buffers were prepared giving free Ca^{2+} concentrations in the range 0.1 - 10uM at pH 7 and 20°C. The concentration of free Ca^{2+} was calculated, using a binding constant of 4×10^{-8} M^{1} at pH 7, 20°C (Owen, 1976). Solution compositions were determined by using a computer programme for solving multiequilibria (unpublished programme by N.C. Millar). In all experiments involving calcium studies, only acid washed plasticware and double distilled water was used to keep calcium contamination at a minimum.

PIPETTING

For actin concentrations up to 200uM, Gilson direct displacement pipettes were used. For volumes up to 5ml and for larger volumes, Gilson air displacement and graduated glass pipettes were used, respectively.

CHROMOPHORIC DYE ARSENAZO III

Arsenazo III, purified by acid purification, was employed as indicator at 655nm to follow selectively changes in calcium concentration. A binding constant of 10uM for arsenazo III at pH 7 and 20°C was used. The absorbance of arsenazo III is dependent on temperature, and this must either be kept constant or any changes corrected for (for all references Hole, 1980).

NUCLEOTIDES

ATP and ADP were supplied by Boehringer as crystallised disodium or monopotassium salt, respectively and used without further purification. The concentrations were determined, using the molar extinction coefficient of $E_{259} = 15.4\ M^{-1}\ cm^{-1}$ (Bock et al., 1956).

PROTEINS

Proteins were extracted from freshly killed exsanguinated white rabbits. Rabbits were quickly skinned and only muscle from the back and the hind legs was taken. Usually, approx 1kg of muscle was obtained from two rabbits.

MYOSIN

The method described by Margossian & Lowey (1982) was essentially followed to prepare myosin. Myosin was extracted from muscle immediately after mincing in 3 litre of Guba-Straub buffer (0.3M KCl, 0.15M K_2HPO_4/KH_2PO_4, pH 6.5) for exactly 15min at 4°C. Longer extraction times resulted in actin extraction. The suspension was then spun at 5 000 x g in a pre-chilled Mistral 6L centrifuge for 45min at 4°C. The insoluble pellet was used for actin and tropomyosin/troponin preparation, and the supernatant was filtered through a Buchner funnel to remove fats. The funnel contained a 1cm thick pad of Whatman's No.1 filter paper, homogenised in Guba-Straub buffer. The filtrate was collected under vacuum in a flask on ice. Frothing of the filtrate was avoided. The pad was washed with 100ml of Guba-Straub buffer and the filtrate was carefully poured into 10 volumes (30 litres) of

cold single distilled water and left to settle overnight.

The supernatant was siphoned off and the remaining suspension was spun at 5 000 x g, 4°C for 45min for the myosin to pack down. The pellet was then re-dissolved in 167ml of 3M KCl, made up to 1 litre and homogenized. The solution was poured into 10 volumes (10 litre) of cold vortexing single distilled water and left to settle overnight.

The supernatant was siphoned off as before, the myosin was collected and then spun down at 12 000 x g for 30min in the MSE Europa centrifuge. Myosin could be stored at this point for several months at -20°C by dissolving it in 0.5M KCl, 1mM DTT, 10mM K_2HPO_4/KH_2PO_4, pH 6.5 and mixing it with an equal volume of glycerol.

MYOSIN SUBFRAGMENT 1 (S1)

For myosin subfragment 1 (S1) preparations the method described by Weeds & Taylor (1975) was essentially followed. A chymotryptic digest of myosin caused the digestion of the DTNB light chain, but leaving the A-light chain intact.

The digestion was prepared by dissolving myosin in 42ml of 0.3M KCl and only after the suspension was homogenous, 2mM EDTA and 2mM DTT were added. The pH was adjusted to 6.5 by addition of 10mM K_2HPO_4/KH_2PO_4, and the suspension was made up to 1 litre with double distilled water. Myosin concentration was determined by measuring the absorbance at 280nm. Correction for light scattering artefacts was made, by using the absorbance between 360 and 380nm as base line. Values for $E^{1\%}_{280} = 5.6\ cm^{-1}$ and Mwt. of

470kDa were used (Margossian & Lowey, 1982). A concentration of 10 to 20mg/ml myosin was necessary for the digestion. Continuous stirring was required to maintain a homogenous suspension. The digestion was performed at 23°C, by adding 100mg of bovine pancreatic-chymotrypsin in a little water so that the final concentration was 0.1mg/ml. The reaction was stopped after exactly 10min by the addition of 0.5mM PMSF dissolved in 1ml ethanol. The digestion mixture was then dialysed overnight against 10 volumes of 5mM K_2HPO_4/KH_2PO_4, pH 6.5 at 4°C.

Insoluble myosin rods and undigested material were separated by centrifugation at 10 000 x g and 4°C for 1 hour. Concentration of S1 was determined by measuring the absorbance at 280nm using $E^{1\%}_{280} = 7.9\ cm^{-1}$ and Mwt. of 115kDa (Margossian & Lowey, 1982). Between 100 and 200mg of protein per 1g of myosin were gained.

For separation of the two isoenzymes S1(A1) and S1(A2), the solution was loaded onto a 60 x 4.5 cm column (Whatman DE 52), which had previously been equilibrated with a minimum of 500ml of 50mM imidazole, pH 7.0. After loading, a further 50ml of imidazole were pumped onto the column, allowing all protein to adhere to the column resin. Separation was accomplished by elution of a 1 litre linear gradient from 0.05M to 0.2M KCl in 50mM imidazole at 4°C. The flow rate was set at 2-3ml/min and fractions were collected in 80-90 tubes overnight. Protein elution was monitored at 280nm and the salt concentration was detected, using a conductivity meter.

Two protein peaks, representing S1(A1) and S1(A2), were pooled separately and dialysed against 10 volumes of 10mM K_2HPO_4/KH_2PO_4, pH 7.5 at 4°C. Concentration of S1 was determined

by the absorbance at 280nm, using $E^{1\%}_{280}$ of $7.9cm^{-1}$ and Mwt of 115kDa and an equal mass of sucrose was dissolved in the solution to stabilize the protein. The solutions were changed over to 500ml round bottom flasks, rapidly frozen in a CO_2/acetone mixture and then freeze dried under vacuum. Freeze dried flakes were stored at -20°C and could be kept for several months. About 1/3 of the mass of flakes was S1.

For separation of S1, after the chymotryptic digestion, myosin could also be subjected to ammonium sulphate fractionation. Ammonium sulphate was added up to 40% and spun at 7 000 x g for 15min. The pellet was discarded. Ammonium sulphate up to 60% was added to the supernatant, which was then centrifugated at 7 000 x g for 15min. The pellet was re-suspended and dialysed exhaustively against 10 volumes of 10mM K_2HPO_4/KH_2PO_4, pH 7.5 at 4°C. Determination and storage of S1, which was a mixture of (A1) and (A2), was as above.

For experimental use, three times the required mass of protein was weighed out, dissolved in experimental buffer and dialysed against at least 100 volumes of experimental buffer to ensure removal of sucrose and phosphate.

Protein purity was checked, using SDS-polyacrylamide gel electrophoresis. Little variation between preparations was observed and S1 was considered to be pure by this method. A mixture of both isoenzymes was used in experiments.

ACTIN AND TROPONIN/TROPOMYOSIN

The precipitate from the centrifugation of the myosin

preparation was used to prepare acetone powder (Pardee & Spudich, 1982). Actin and troponin/tropomyosin were obtained from this powder.

The pellet was added to 5 litre of 0.4% $NaHCO_3$, 0.1mM $CaCl_2$ and stirred at 4°C for 15min. This mixture was then filtered through cheesecloth, and the precipitate was re-suspended in 1 litre of 10mM $NaHCO_3$, 10mM Na_2CO_3, 0.1mM $CaCl_2$ and stirred at 4°C for 10min. The residue was filtered through cheesecloth and quickly rinsed with 10 litre of distilled water at room temperature. This mixture was passed through cheesecloth to remove most of the water. The pellet was then re-suspended in 2 x 2.5 litre cold acetone, which was stirred each time for 20min. Dehydrated pellets were spread out on filter paper and the acetone was allowed to evaporate. Pieces of connective tissue were removed and the dried material was ground through a plastic sieve. Usually, from two rabbits 50g of fine actin powder were obtained, which could be stored at -20°C for a few months.

ACTIN

F-actin was prepared from acetone dried powder by the method described by Pardee & Spudich (1982). Normally, 10g of actin powder were stirred in 400ml of 10mM tris, 0.5mM ATP, 0.2mM $CaCl_2$, 1mM DTT, pH 8, 0°C for 30min. The mixture was filtered several times, and the supernatant was then exposed to a set of polymerisations at high ionic strength and de-polymerisations at low ionic strength for purification. Non-polymerised material and other impurities were removed by a cycle of high speed centrifugations. The first extract was filtered through

cheesecloth and solids were kept as a source for purifying troponin/tropomyosin and troponin C. The filtrate was then spun at 70 000 x g and 4°C for 1 hour in a MSE 60 centrifuge and the supernatant was then polymerised by adding 100mM KCl and 2mM $MgCl_2$. After an hour at room temperature, F-actin was collected by a 3 hour spin at 70 000 x g and 4°C. The pellets were re-suspended in 100ml of 10mM tris, 0.5mM ATP, 0.2mM $CaCl_2$, 1mM DTT, using a glass homogeniser. Frothing was avoided. F-actin was de-polymerised by dialysis overnight against 50 volumes of the same buffer at 4°C. G-actin was spun at 70 000 x g and 4°C for 1 hour to remove any polymerised actin. A second polymerisation was performed by the addition of 100mM KCl and 2mM $MgCl_2$. After an hour at room temperature the polymerised actin was collected by centrifugation at 70 000 x g and 4°C for 3 hours. The pellets were collected and homogenised in about 10ml of experimental buffer. The solution was then dialysed against a minimum of 250ml re-suspension buffer. The high viscosity of actin made it necessary to spin the actin in a bench centrifuge for a few minutes to remove air-bubbles. Actin concentrations were assayed in a 1 : 50 dilution of the stock with experimental buffer. Care was taken not to introduce air-bubbles into the solution when mixing. Absorbance of the solution was scanned from 260 to 400nm and corrected at 280nm for light scattering artefacts by extrapolating a sloping baseline from 360 to 380nm. The actin concentration was calculated using $E^{1\%}_{280} = 11.04\ cm^{-1}$ (West et al., 1967) and 42kDa Mtw. (Elzinga et al., 1973). Yields from 10g acetone powder varied between 150-200mg of purified

actin. Actin was either used in this form or further treated with a pyrene label for fluorescence measurements. Purity of actin was normally assessed by SDS-page polyacrylamide gels (Fig. 2.1a) and showed little variation between preparations. Actin solutions were kept at $4^{o}C$ and were never older than 10 days.

PURIFICATION OF TROPONIN/TROPOMYOSIN

The residue from the actin extraction of the acetone powder were further treated to co-purify troponin and tropomyosin. The method by Potter (1982) was basically followed with modifications. All buffer used, contained DTT to maintain the reduced state of TnC, which is thought to be essential for its functioning (Lehrer, 1975).

Tropomyosin/troponin (Tm/Tn) was extracted for 5 hours at room temperature with 1M KCl, 25mM tris, 0.1mM $CaCl_2$, 0.1mM DTT, pH 8.0 at a 10ml/g dry actin powder ratio and then the homogenate was left at $4^{o}C$ overnight. The suspension was filtered through cheesecloth and centrifugated at 12 000 x g for 30min at $4^{o}C$. The solids were discarded and the supernatant, which contains (Tn/Tm) was taken to 40% saturation. The addition of the $(NH_4)_2SO_4$ took 20-30min, and the solution was then left for 15min before centrifugation at 12 000 x g for 30min at $4^{o}C$. The pellet was discarded. The supernatant was then taken to 55% saturation with ammonium sulphate, and after leaving it for 15min, spun at 12 000 x g for 15min at $4^{o}C$. The precipitate was re-dissolved in 1M KCl, 25mM tris, 0.1mM $CaCl_2$, 0.1mM DTT, pH 8 with the aid of a hand homogenizer. The protein concentration was determined by measuring absorbance at 280nm ($E^{1\%}_{280}$ of $3.8cm^{-1}$, Hartshorne &

Figure 2.1a SDS-Polyacrylamide Gel of actin

Figure 2.1b SDS-Polyacrylamide Gel of fractions obtained from Mono Q Ion Exchange

Fractions obtained from the Mono Q ion exchange column as described in figure 2.2 were subjected to SDS-PAGE and Coomassie Blue stained.

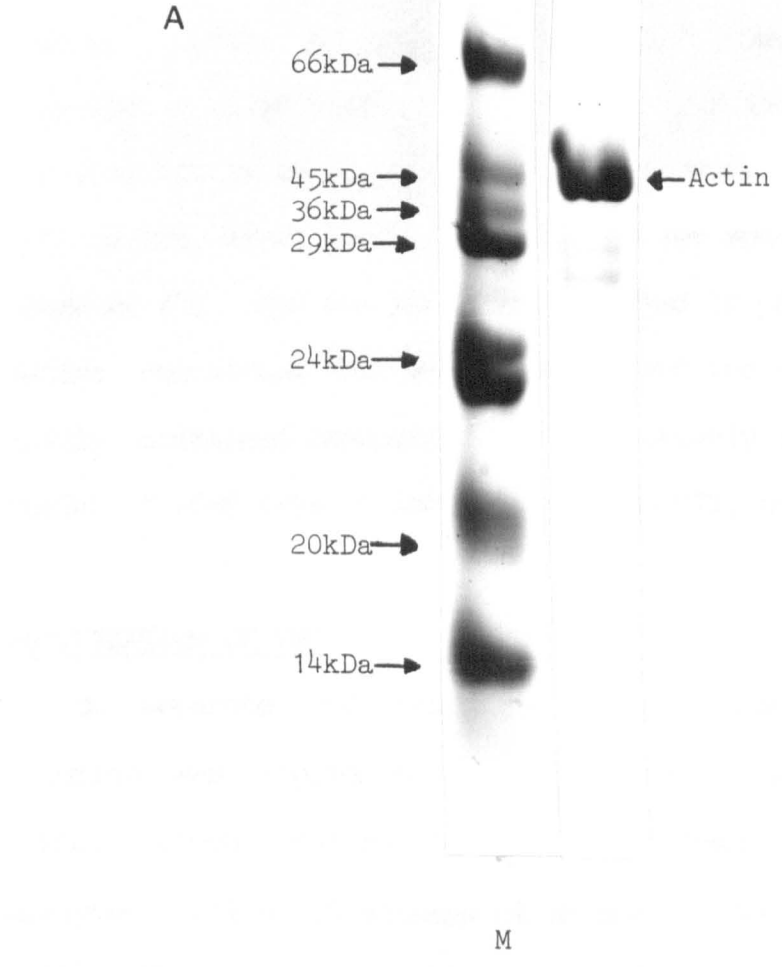
A
66kDa
45kDa
36kDa
29kDa
24kDa
20kDa
14kDa
Actin
M

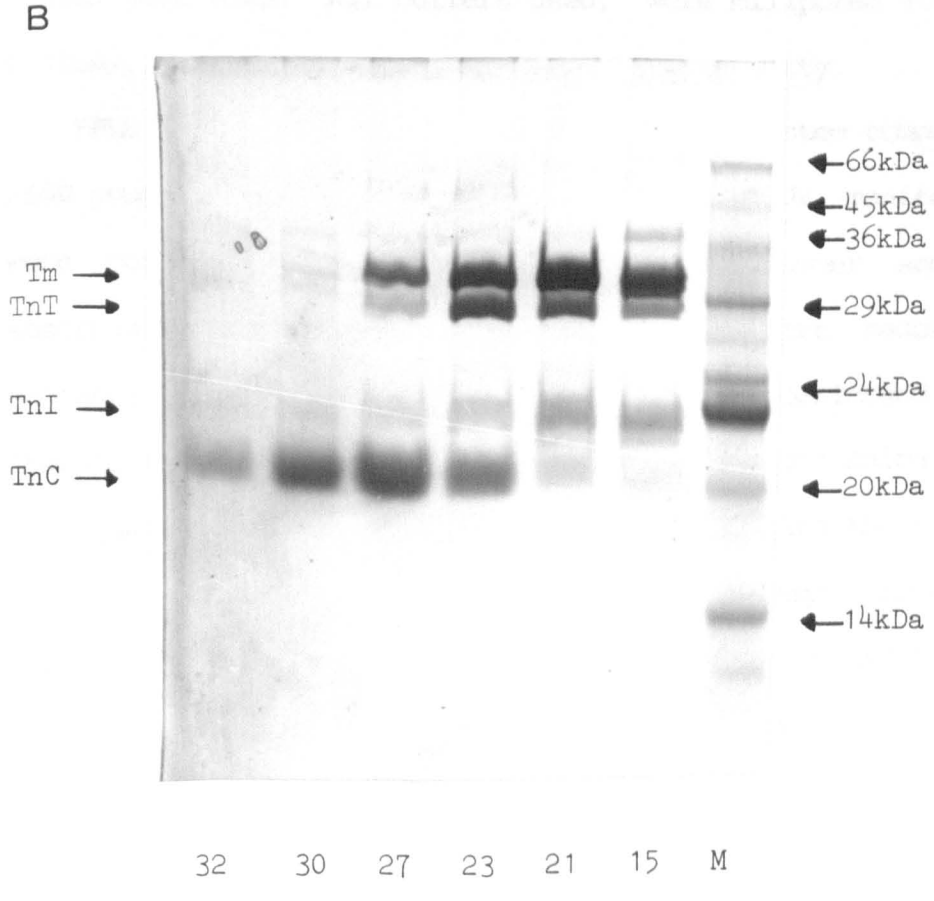
B
Tm
TnT
TnI
TnC
66kDa
45kDa
36kDa
29kDa
24kDa
20kDa
14kDa
32
30
27
23
21
15
M

Mueller (1969); Mwt 150kDa, Greaser & Gergely (1971)) and adjusted to about 1mg/ml. This solution was then stirred rapidly, and with the pH being continuously monitored, adjusted to pH 4.6 with 1M HCl. After 30min, the solution was spun at 12 000 x g for 20min at $4^{o}C$, and the pH was re-adjusted to pH 7.0 with KOH. The pellet containing (Tm) was discarded and the supernatant, which mainly contained troponin, was exhaustively dialyzed against a buffer of 25mM tris, 0.1mM $CaCl_2$, 0.1mM DTT, pH 7 at $4^{o}C$.

PURIFICATION OF TNC

To separate TnC from the troponin complex, the protein solution was applied to a Fast Protein Liquid Chromatography (FPLC) column. Before loading the column, the solution was dialyzed against 10 volumes of 6M urea, 50mM tris, 1mM EDTA, 0.1mM DTT, pH 8 overnight and then filtered through a sieve of 0.25mm pore size. All buffers used, were milipored (filter size 0.22um). The chemicals were of high grade quality.

FPLC was performed on a Pharmacia FPLC system comprising 2 x P500 pumps, FRAC100 fraction collector, UV1/UV monitor. These were controlled by a LCC 500 gradient programmer and the UV absorbance was recorded on a Pharmacia chart recorder. Ion exchange chromatography on the FPLC was performed using a Pharmacia Mono Q (1ml) column. This is a strong anion exhanger with quarternary amine side chains. Before using the column, it was necessary to equilibrate it with 10 column volumes of a buffer containing 6M urea, 50mM tris, 1mM EDTA, 0.1mM DTT, pH 8.

Results, using the Mono Q column, were very reproducible. The

concentration of salt required to elute specific proteins was highly dependent upon the gradient used and results shown here indicate only little variation. Figure 2.2 shows one run on the Mono Q, using a TnC solution. For each run approx 7mg of protein is loaded on to the column and washed with 5 column volumes (5ml) buffer. The column was then eluted with a 0.5M KCl gradient. The peak of TnC at 280nm absorbance is also shown for each run and illustrates the same concentration of KCl required to elute it. Fig. 2.1b shows the fractions obtained from the Mono Q ion exchange on a SDS-Polyacrylamide Gel, identifying sample number 30 as pure TnC. The protein concentration was determined, using $E^{1\%}_{280}$ of $1.41cm^{-1}$ (Horwitz et al., 1979) and Mwt. of 18kDa (Collins et al., 1977; Zot & Potter, 1987b). Yields could be variable depending on the quality of the acetone dried actin powder, but between 15-20mg of purified TnC was obtained from 10g of powder.

LABELLING TROPONIN C WITH DANSYLAZIRIDINE (DANZ)

TnC was labelled by the method of Johnson et al. (1978). The solution containing TnC from the FPLC Mono Q column was exhaustively dialyzed against 25mM tris at pH 8 and then equilibrated against the incubation buffer (10mM potassium phosphate, 90mM KCl, 2mM EGTA, pH 7, 20°C) overnight. A stock solution of 0.01M dansylaziridine in absolute ethanol was used to label 2mg/ml solutions of TnC. The labelling was conducted in 1.5M excess of DANZ to protein concentration under saturating Ca^{2+} conditions (2.5mM Ca^{2+} in the above EGTA buffer solution). These reaction solutions of TnC and DANZ were incubated for 24

Figure 2.2 Elution profile of troponin C from Mono Q Ion Exchange Column

One run of TnC (7mg protein) was loaded onto a 1ml Mono Q FPLC ion exchange column and run at a flow rate of 1ml/min. After washing, the column was eluted with a KCl gradient, shown in the figure by the dotted line. The 280nm absorbance was continuously monitored. TnC was eluted in fraction number 30.

Buffer: 6M urea, 50mM tris, 1mM EDTA, 0.1mM DTT, pH 8, 20^{o}C.

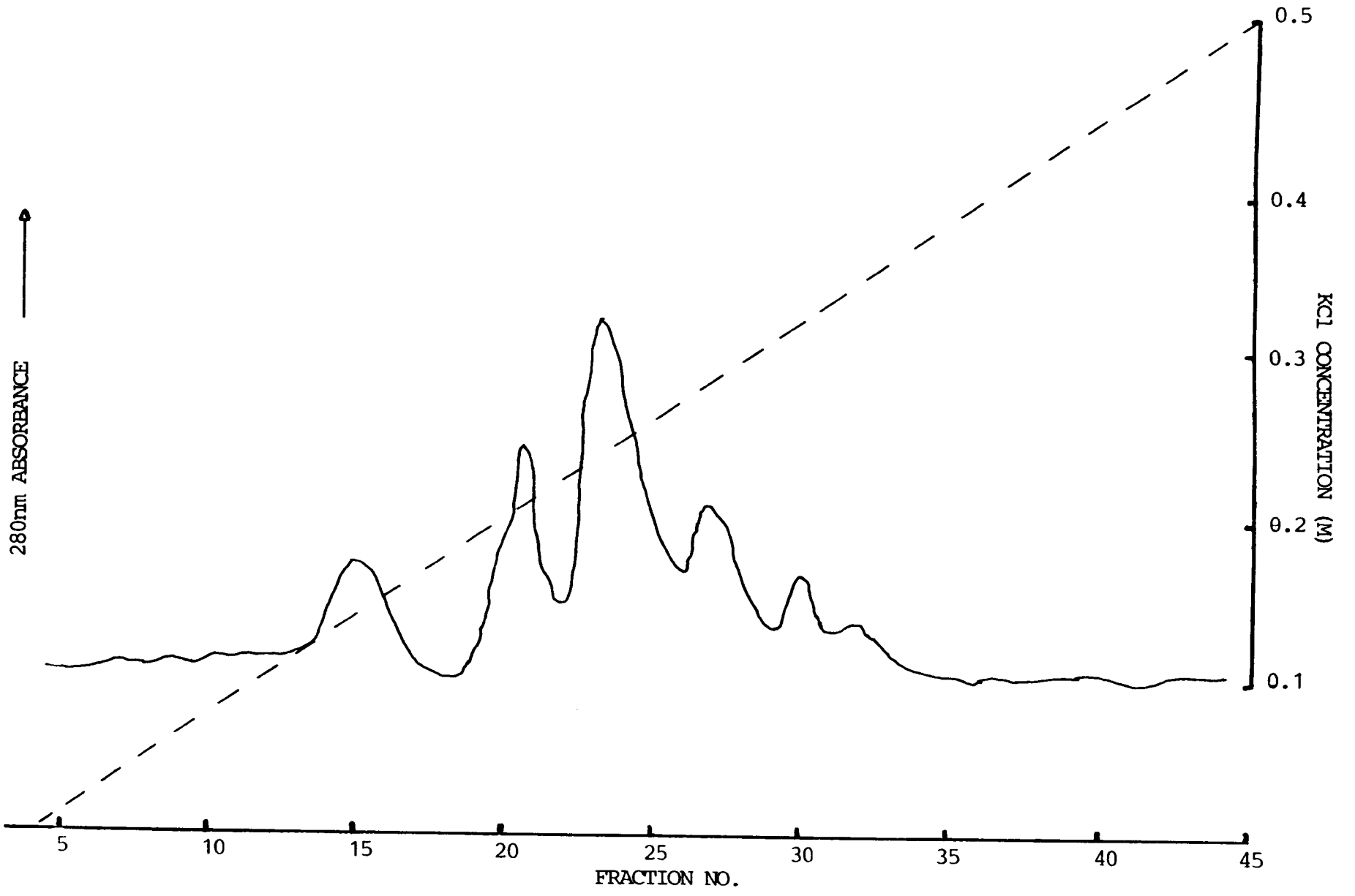
280nm ABSORBANCE
0.5
0.4
0.3
0.2
0.1
KCl CONCENTRATION (M)
5
10
15
20
25
30
35
40
45
FRACTION NO.

hours at ambient temperature and then dialyzed exhaustively against 10mM phosphate, 90mM KCl and 2mM EGTA buffer at pH 7.0. An extinction coefficient for DANZ in ethanol of 4500 M^{-1} at 340nm was used. The amount of label incorporated into the protein was calculated using an extinction coefficient of 3980 M^{-1} for dansyl fluorophore (Lin, 1978). The absorbance spectra of TnC_{DANZ} (260-550nm) with an absorbance maximum for DANZ at 340nm and for TnC at 280nm is given in fig. 2.3.

ACTIN LABELLED WITH N-(1-PYRENE)IODOACETAMIDE

Actin was covalently labelled at Cys 374 with N-(1-pyrene)iodoacetamide essentially by the method of Kouyama & Mihashi (1981) and Cooper et al. (1983), but with some modification (Criddle et al., 1985). The label was introduced to gain further information about the acto-S1 interaction.

Actin was labelled as F-actin before the final 3 hour spin of the unlabelled preparation. After the polymerisation of actin for 1 hour the solution was assayed, and the concentration determined as described above. The solution was then diluted to 1mg/ml with a buffer containing 100mM KCl and 2mM $MgCl_2$. From the stock solution of pyrene iodoacetamide, kept in DMF at -20°C, 0.9mg was added per 100mg of actin. Labelling was conducted in 1.5M excess of pyrene label to protein concentration. The label was added to a beaker containing the stirring actin solution. The reaction was allowed to proceed at room temperature in a dark environment for 18 hours. After incubation, the solution was spun at 5 000 x g for 1 hour to remove unreacted label and denatured

Figure 2.3 Absorbance spectrum of dansylaziridine (DANZ) labelled TnC

Spectrum of TnC with 33% label incorporation. Label concentration: 35uM; TnC concentration: 116uM. Experimental buffer: 90mM KCl, 10mM potassium phosphate, 2mM EGTA, pH 7, 20^{o}C. Absorbance at 280nm = TnC; absorbance at 340nm = DANZ.

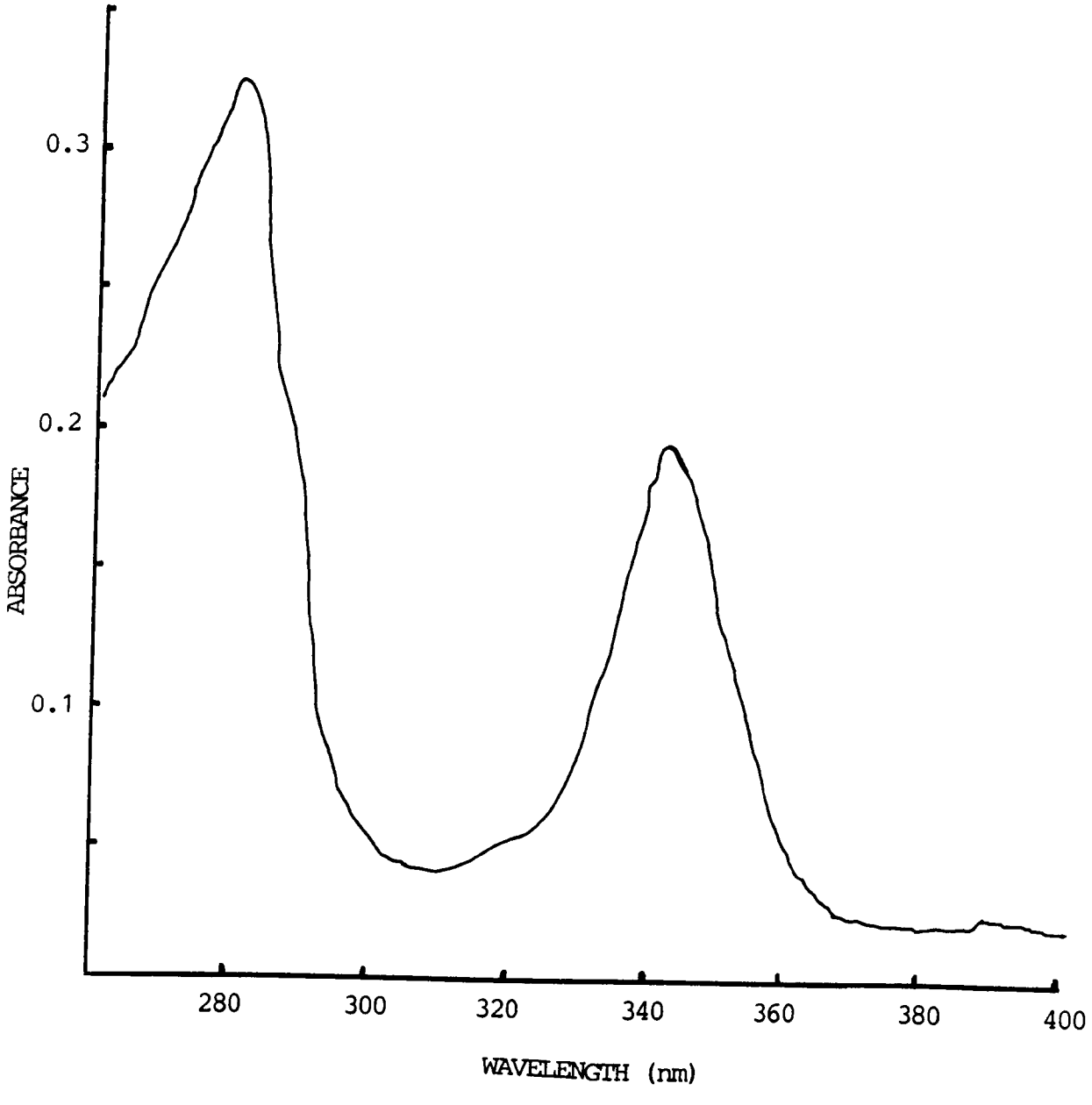
0.3
0.2
0.1
ABSORBANCE
280
300
320
340
360
380
400
WAVELENGTH (nm)

protein. Labelled F-actin was collected by centrifugation at 70 000 x g and 4°C for 3 hours. The pellets were resuspended in 10ml of experimental buffer, carefully homogenised and dialysed overnight at 4°C against the experimental buffer. Lumps of heterogeneous material, occasionally found in the preparation, were removed by passing through glass wool.

Calculation of actin concentration was made difficult by the absorption of pyrene label at 280nm. The concentration of pyrene in the labelled actin solution was calculated from the absorbance at 344nm, where actin absorption is negligibly, using $E = 2.2 \times 10^4\ M^{-1}cm^{-1}$ (Kouyama & Mihashi, 1981). To obtain the absorbance for pyrene at 280nm, the concentration of pyrene was multiplied by its extinction coefficient of $2.33 \times 10^4\ M^{-1}\ cm^{-1}$ at 280nm (Criddle, 1985). Pyrene concentration was deducted from the total absorbance at 280nm, and actin concentration was determined using $E^{1\%}_{280} = 11.04\ cm^{-1}$ (West et al., 1967) and 42kDa Mwt. (Elzinga et al., 1973). Label incorporation was normally between 90% and 100% although over and underlabelling occurred. Reasons for this were assumed to be, impurity between batches of N-(1-pyrene)iodoacetamide or the labelling of a second site on actin.

ABSORBANCE MEASUREMENTS

Absorbance measurements were carried out in a Pye-Unicam SP-8 100 UV spectrophotometer. Matched 3ml or 1ml quartz cuvettes of 1cm path length were used for protein assay. Protein dilutions were normally made up in the cuvette with experimental buffer.

SDS-POLYACRYLAMIDE GEL ELECTROPHORESIS

Polyacrylamide gel electrophoresis was performed according to Laemmli (1970) on a BioRad protean dual slab gel supplied by Hoefer Scientific Instruments. Protein separation gels (12%) were made up in 25mM tris, 50mM sodium acetate, 0.5mM EDTA, 0.2% SDS, 0.5% acrylamide and 0.5% bisacryalamide (electrophoresis grade chemicals). Samples were prepared by boiling for 4min in a sample buffer containing 10% glycerol, 10% SDS, 5% (v/v) mercaptoethanol, 2mg/ml bromophenol blue. Samples were run between 20-200ug protein not exceeding 150ul. Normally 4-5 hours were allowed for each gel to run at 60mA. Molecular weight protein weight markers were: alpha-lactalbumin (14kDa), trypsin inhibitor (20kDa), trypsinogen (24kDa), carbonic anhydrase (29kDa), glyceraldehyde-3-phosphate dehydrogenase (36kDa), egg albumin (45kDa) and bovine albumin (66kDa), unless otherwise stated.

After electrophoresis, the gels were stained with 0.25% (w/v) Coomassie R250 in destain mixture (20% (v/v) methanol, 7.5% (v/v) acetic acid) for 1 hour at 65 ^{o}C and destained in the above solvent mixture containing no Coomassie R250. Finally, they were washed in double distilled water and photographed.

FLUORESCENCE AND LIGHT SCATTERING MEASUREMENTS

Fluorescence and light scattering measurements were carried out on a Perkin Elmer LS-5B luminescence spectrophotometer. The cell holder was thermostatically temperature controlled by a LKB 2219 water bath with a temperature control within 0.1^{o}C.

Normally, a 3ml four sided quartz cuvette of 1cm path length was used for equilibrium measurements, but for some experiments also a 800ul four sided quartz cuvette was employed. Additions of proteins or reagents were, either carefully stirred by hand so as not to cause formation of air bubbles or continuously stirred, using a Rank Bros 100 magnetic stirrer and a Spinbar F37150 flea. Magnetic stirring was only possible in a 3ml cuvette. Pyrene-actin fluorescence was recorded by exciting at 365nm and emitting at 407nm. TnC_{Danz} was excited at 340nm and emission was monitored at 510nm. Kinetic data were collected on a Perkin-Elmer R-100A chart recorder. The recorder output was digitized and transferred to a Hewlett Packard computer 300 for analysis.

TITRATOR

A purpose built titrator was used for continuous titrations. Solutions at 4.1ul per minute were dispensed from a 1ml Hamilton syringe via a plasic tube into the quartz cell placed in the luminescence spectrophotometer. Mixing of the solution, titrated into the 3ml cuvette, was ensured through continuous stirring by a magnetic flea. Simultaneous recording of changes in fluorescence were collected on an EPSON PCAX2 computer and later transferred to the Hewlett Packard computer 300 for analysis.

STOPPED FLOW SPECTROPHOTOMETER

The principle of this method is to mix two reactant solutions by rapid flow, to stop the flow and to observe the change continuously in an observation cell. The application and

limitation of the flow method are discussed in detail by Gutfreund (1972).

All experiments were carried out on an SF-4 stopped-flow spectrophotometer supplied by Hi-tech Scientific Ltd., Salisbury. A schematic diagram of the flow unit is shown in fig. 2.4. The unit consists of two 2ml Hamilton drive syringes, which can be filled from reservoirs. The syringes are driven simultaneously by compressed air from a pressure driven ram mounted upon the base unit. At 3 bar normal operating pressure, the dead time of this apparatus was measured to be 1.5msec (Millar, 1984). The solutions were rapidly mixed in a quartz observation/reaction cell immersed in a thermostated tank containing 50% ethylene glycol. The cell was set in fluorescence/light scattering mode with 2mm or 10mm path length. Light was transmitted to the cell via a quartz fibre optic light guide. Emitted light from the reaction/observation cell was sent via a silvered quartz rod to the photomultiplier. The flow was stopped, using another 2ml Hamilton syringe. A micro switch was pressed by the stopping syringe to give a trigger pulse. The thermostated tank was mounted in a dewar flask, which accepted liquid nitrogen for low temperature experiments. Temperature was regulated by an internal heater and thermocouple, which maintained the temperature within $0.1^{o}C$.

OPTICS AND DATA COLLECTION

A purpose built stabilized power supply was the energy source for the 100W high pressure mercury lamp (Wotan HBO) or Xenon

Figure 2.4 Stopped flow apparatus from Hi-tech Scientific

The schematic diagram shows the flow module and the two different arrangements of the mixing/observation cell to give a 2mm or 10mm path length for fluorescence of transmission (from the instruction manual supplied by Hi-Tech Scientific, Salisbury, UK).

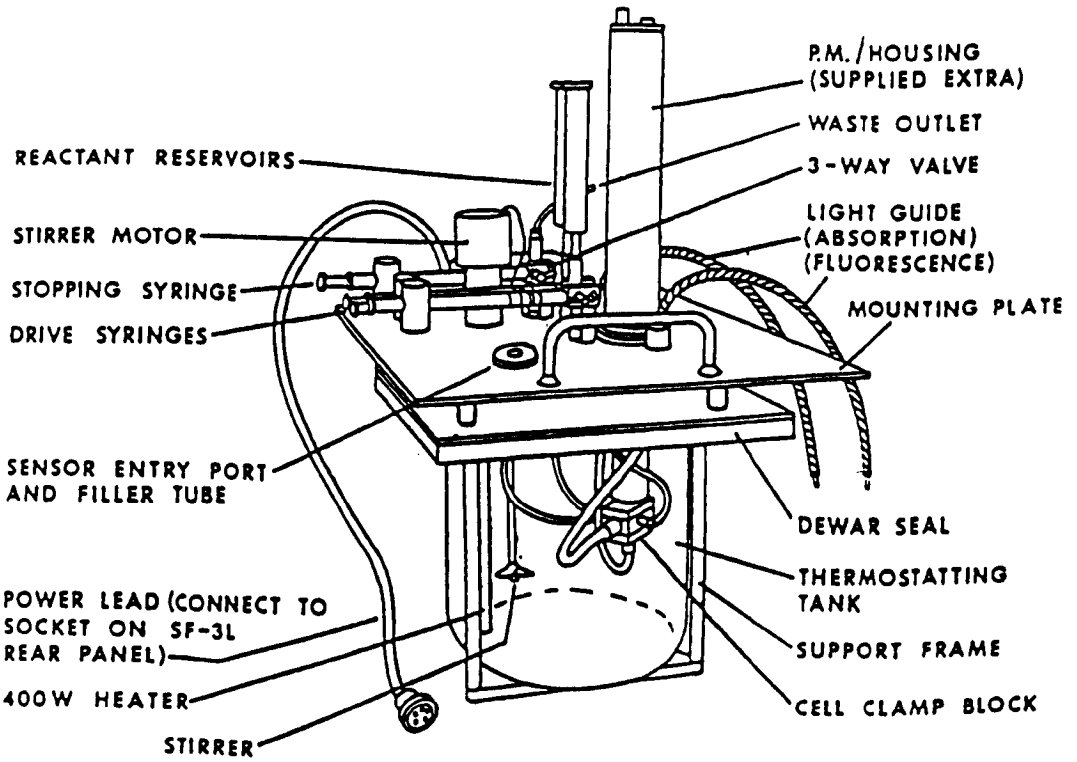

MIXING CELL DETAILS SHOWING
LIGHT GUIDE ARRANGEMENT

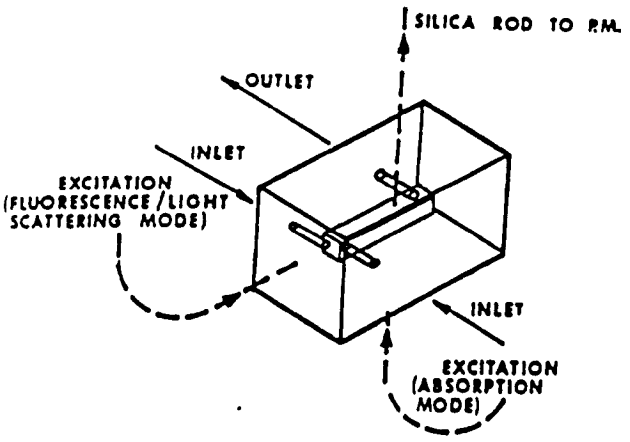

CELL POSITIONED FOR 2mm PATH LENGTH

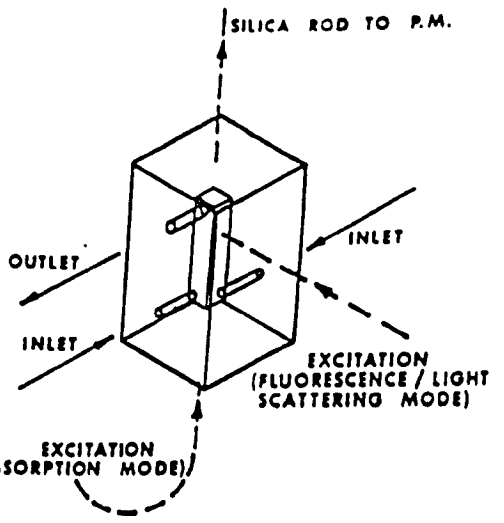

CELL POSITIONED FOR 10mm PATH LENGTH

lamp. The housing of the lamp in the stopped flow and pressure jump apparatus was water cooled. Light was monochromated with a band pass width of 5nm by a Baush & Lomb monochromator. Light scattering measurements of native actin were followed at 365nm and pyrene labelled actin at 410nm and 430nm. Fluorescence measurements on pyrene labelled actin and dansylaziridine labelled TnC were carried out, using exciting light at 365nm and 340nm, respectively. Light was passed through a Schott UG 11 filter for experiments at wavelengths less than 400nm to cut out higher order reflections. Absorbance spectrophotometry of arsenazo III was performed at 655nm excitation wavelength.

Emitted light was detected at 90^{o} for fluorimetry or at 180^{o} for absorbance spectrophotometry, using a photomultiplier driven by an EMI PM28B power supply. For pyrene and dansylaziridine fluorescence a KV 393 glass laminate filter was placed in front of the photomultiplier. The signal was electronically filtered by an unity gain amplifier. The time constant was normally (t_c approx 5%) of the half time of the observed reaction for acto.S1 and calcium.TnC by all kinetic methods used, except for acto.S1 experiments by pressure jump (t_c approx 1%).

High tension power to drive the photomultiplier was adjusted so that the output was between -1V and -5V depending on the reaction being followed. The signal was then offset to zero volt, using the backing off on the unity gain amplifier.

Transient recorders were triggered by a five volt pulse, opening the microswitch on the stopping block of the stopped flow machine, by a quartz pressure transducer in the pressure jump apparatus or internal pulse in the temperature jump machine. The

pulse was supplied by a purpose built power source. Voltage output from the photomuliplier was then digitizied by an analog converter (1401) supplied by Cambridge Electronic Devices, before being transferred to a Hewlett Packard 300 computer for analysis. Transients from temperature jump experiments were recorded on a Nicolet 3091 digital oscilloscope before being transferred to a HP 300 computer. A 10% pre-trigger was used for data collection.

Data was normally stored on double density disks and analysed either as single or averaged traces. Hard copies of the data were obtained, using a Hewlett Packard Quiet Jet Plus printer or Hewlett Packard 7070A plotter.

PRESSURE JUMP APPARATUS

The principle of the pressure jump method is that a reaction mixture at equilibrium is suddenly exposed to a large pressure change. The rapid shift in equilibrium concentrations of the reaction mixture, due to the pressure perturbation, is then followed spectrophotometrically. The application and limitation of the relaxation method are discussed in detail by Gutfreund (1972).

For pressure changes of 100 atmospheres or less, the magnitude of molar volume changes in aqueous solution are known to be sufficiently small to be interpreted by the equation;

$$\Delta K/K = -\Delta V^{\circ} \times \Delta P / R \times T$$

where (K = equlibrium constant; V° = standard volume change; P

= pressure; R = gas constant and T = absolute temperature) the equilibrium constants and thermodynamics can be calculated. Chemical relaxation times can thus be related to rate constants and to the equilibrium concentrations of chemical species in solution. The use of this technique on an acto.S1 system is described by Geeves & Gutfreund (1982), Coates et al. (1985) and Geeves & Halsall (1986).

The schematic representation of the pressure jump apparatus in fig. 2.5 is based on a design by Davis & Gutfreund (1976). The observation cell (A), holding approx 1ml of solution, can be filled via two ports. Pressure is exerted to the observation cell via a teflon membrane from the hydraulic chamber (B). This chamber is filled with oil via a hydraulic pressure line (G), and pressure is applied using a Merlin hand pump. The observation cell filling and emptying ports (H+I) are mounted at 30^{o} angle, enabling air free filling of the cell. Air bubbles, present in the system, can distort or even break the membrane and can interfere with signal detection when in the 1cm light path.

Release of pressure can be achieved in different ways: a) via a manually operated tap in the hydraulic pressure line within 10msec; b) via a mechanical trigger mechanism in less than 200usec; or c) via a bursting disk mechanism within 25usec. For experiments, using the acto.S1 system, the mechanical release was used. This method allowed consecutive collection of traces after the pressure release (200usec). Traces were averaged to increase the signal to noise ratio. Faster release time was not used for reasons of easy repetition of experiments. Pressure release was nearly linear in all cases. Temperature regulation was achieved

Figure 2.5 The pressure jump apparatus

The diagram shows the cell and trigger mechanism taken from Davis & Gutfreund (1976). (Courtesy of Prof. H. Gutfreund)

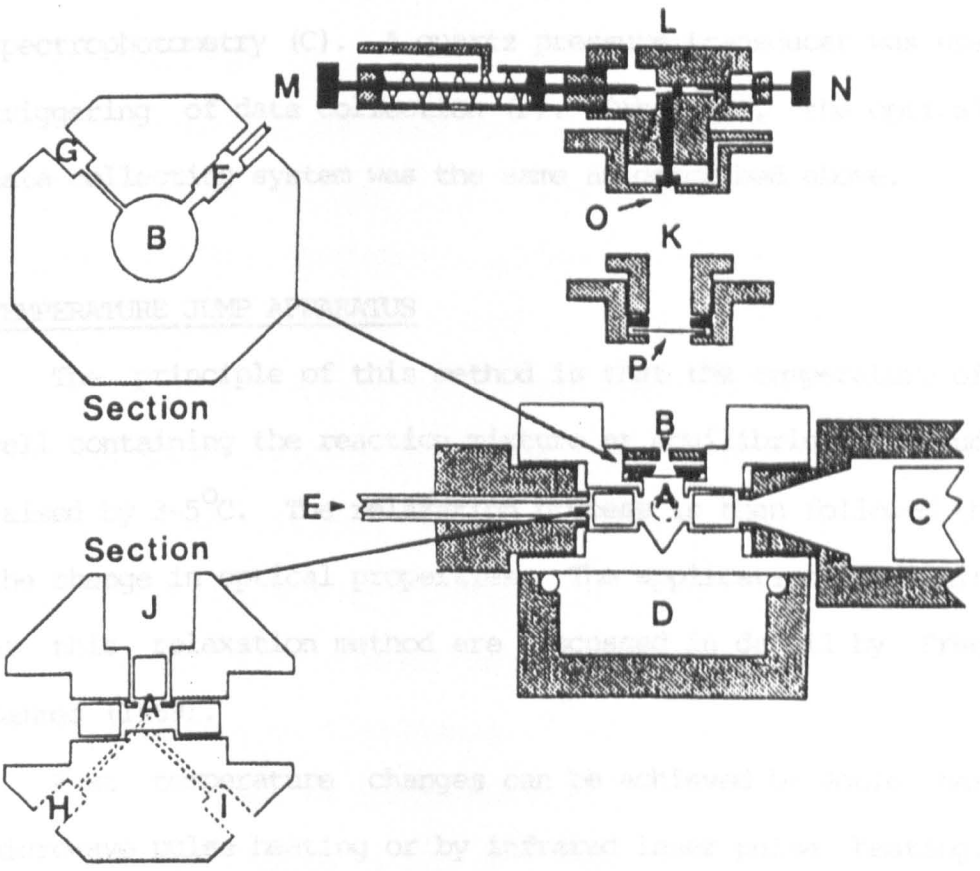

Schematic representation of the pressure-jump apparatus. The instrument is composed of the following components: A, observation cell; B, hydraulic chamber; C, absorbancy photomultiplier; D, thermostatted base; E, quartz fibre optic from light source; F, quartz pressure transducer for the triggering of data collection; G, hydraulic pressure line; H and I, observation cell filling and emptying ports; J, fluorescence emission window; K, bursting disc pressure-release valve; L, mechanical pressure-release valve; M, trigger mechanism; N, reset mechanism; O, valve seat; P, phosphorbronze bursting disc.

by connecting a Grant flow water bath to the base (D) of the apparatus.

Light was introduced via a quartz light guide (E) and detected at 90° for fluorimetry (J) or at 180° for absorbance spectrophotometry (C). A quartz pressure transducer was used for triggering of data collection (F). Otherwise, the optical and data collecting system was the same as described above.

TEMPERATURE JUMP APPARATUS

The principle of this method is that the temperature of the cell containing the reaction mixture at equilibrium, is suddenly raised by 3-5°C. The relaxation process is then followed through the change in optical properties. The application and limitation of this relaxation method are discussed in detail by French & Hammes (1969).

Fast temperature changes can be achieved by Joule heating, microwave pulse heating or by infrared laser pulse heating. The time resolution of the apparatus is determined by the heating method employed. The temperature after the jump is held for not longer than a few seconds (1-5sec) because of convection and thermal conduction. This places an effective limit on the slowness of reactions that can be studied by this method.

For a solution, containing substances at chemical equilibria, rapid temperature perturbation alters the concentration of the chemical species. The magnitude of the concentration change is dictated by the laws of thermodynamics;

Figure 2.6a The temperature jump apparatus

The diagram illustrates the principle of the temperature jump apparatus of the Joule heating type. Temperature jump system (inside the broken line): (H) high tension power supply (0-50kV); (C) capacitor (0.01uF); (G) spark gap; (OG) observation cell.

Detection system: (L) light source; (M) monochromator; (PM) photomultiplier; (AMP) amplifier; (OS) oscilloscope (taken from Hiromi, 1979).

Figure 2.6b Cell of the temperature jump apparatus

Cell used: (A) brass; (B) plexiglass; (C) + (E) electrodes; (D) observation windows; (F) O ring.

(1) + (8) electrodes; (4) sample solution; (5) window for excitation beam; (6) observation window (conical lenses) for fluorescence measurements (taken from Hiromi, 1979).

A

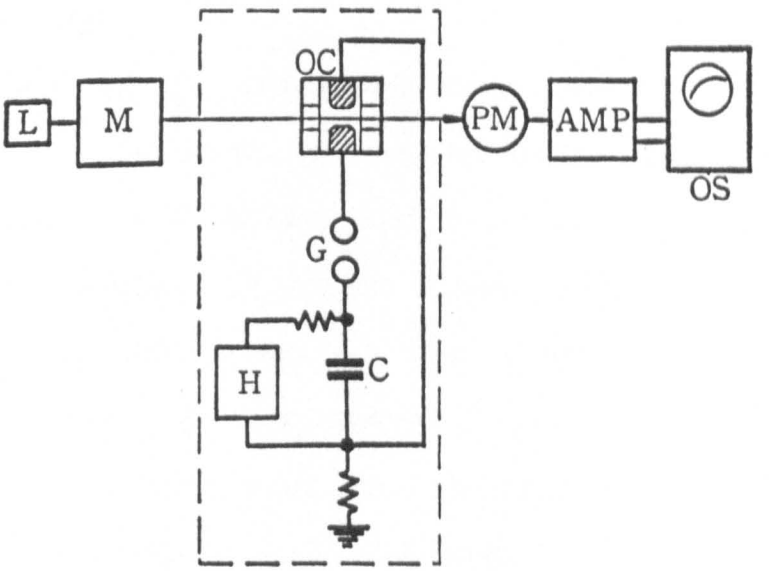

B

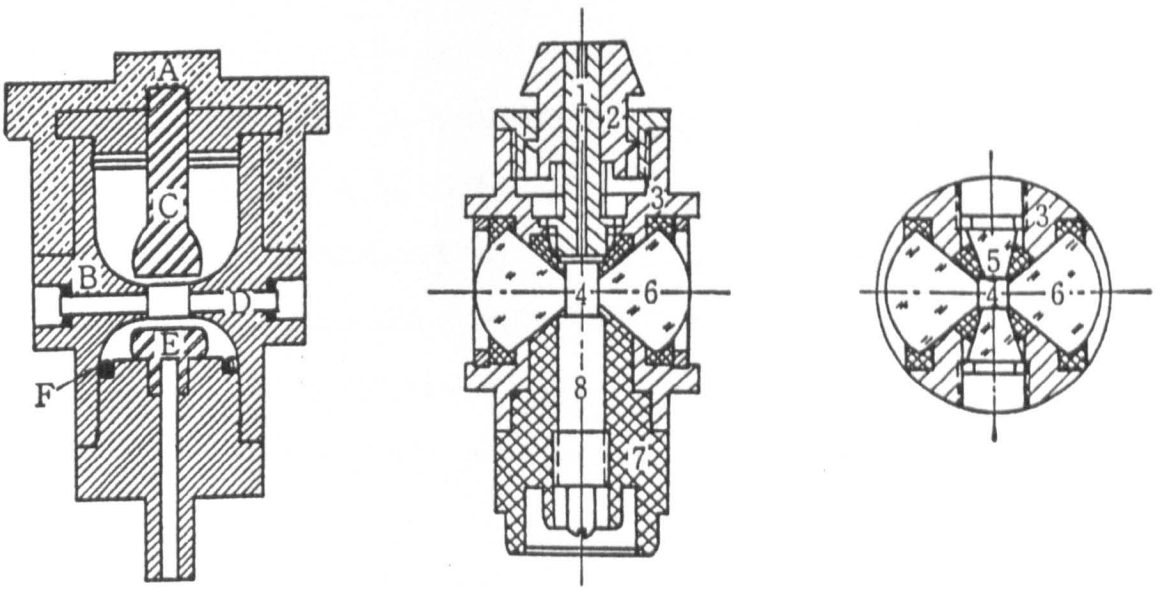

With discharge of 25kV from the 0.01uF capacitor a $5^{o}C$ temperature change was achieved within a few usec. Complete temperature equilibration after each flash was measured to be within 2sec.

CHAPTER 3 THE EFFECT OF IONIC STRENGTH, SOLVENTS, TEMPERATURE AND MONOVALENT ANIONS ON THE INTERACTION OF ACTIN TO MYOSIN SUBFRAGMENT 1 (S1)

INTRODUCTION

Coates et al. (1985) have shown, using pressure relaxation method that the association between myosin subfragment 1 (S1) and actin occurs in a two-step binding preceded by the formation of a collision complex. In the first step S1 binds to actin to form a weakly "attached" state and then isomerizes to a "rigor-like" complex. This transition between the two states is believed to be closely associated with force generation in muscle (Geeves et al., 1984). In their study, Coates et al. (1985) also showed that temperature, ionic strength and organic solvent had a significant influence on the individual steps of the reaction.

It is possible that S1 binds to actin at two distinct sites and that S1 can bind at one site to give an "attached" state and binding at both sites is required to give the "rigor-like" state. Previously, Mornet et al. (1981a) had investigated the topography of an acto.S1 rigor complex by cross-linking technique and results showed that the myosin head S1 enters into a "van der Waal" contact with two neighbouring actin monomers. Structural evidence that myosin heads may interact with two sites on F-actin was produced by Amos et al. (1982). The apparent existence of two independent sites of contact between S1 and F-actin in the rigor state suggested to these authors that the interaction during an active stroke might involve different S1 binding configurations.

In their X-ray diffraction work, Huxley & Kress (1985) also favoured two classes of cross-bridge attachment. During initial tension development most cross-bridges bind to actin in the weakly attached state, producing no tension and then, when fully active, the cross-bridges move into the strongly attached state, producing tension.

The purpose of this chapter is firstly to examine the effects of anions, temperature, ionic strength and organic solvents on acto.S1 in more detail, and secondly to use the differential effect of these parameters to stabilize acto.S1 in the weakly "attached" state, which would allow for structural studies of the two states. Results from steady state titrations, stopped flow and pressure jump experiments of acto.S1 will be presented.

RESULTS

Equilibrium binding measurements

The high sensitivity of the pyrene fluorescence allowed the association constant of S1 for pyr-actin to be measured directly by fluorescence titrations. Fluorescence quenching was linear with S1 concentration until a stoichiometry of 1:1 with actin was reached at approx 70-80% quenching (Kouyama & Mihashi, 1981; Criddle et al., 1985). Fig. 3.1 shows the hyperbolic dependence of pyrene fluorescence with respect to total S1 concentration. The data obtained from the steady state titration were corrected for dilution effects upon addition of S1 and analysed by a non-linear least square fitting routine to the following equation as described by Geeves & Jeffries (1988);

Figure 3.1 Fluorescence titration of myosin subfragment 1 (S1) against pyrene labelled actin

The fluorescence titration was performed by adding S1 into a fluorescence cuvette containing 3ml of 0.5uM pyr-actin, 0.1M KCl, 5mM $MgCl_2$, 20mM cacodylate, pH 7, 20°C. The data were analysed as described in the text and the solid line is the best fit. (K_{ass} = 11 x 10^6; fluorescence quench = 73%).

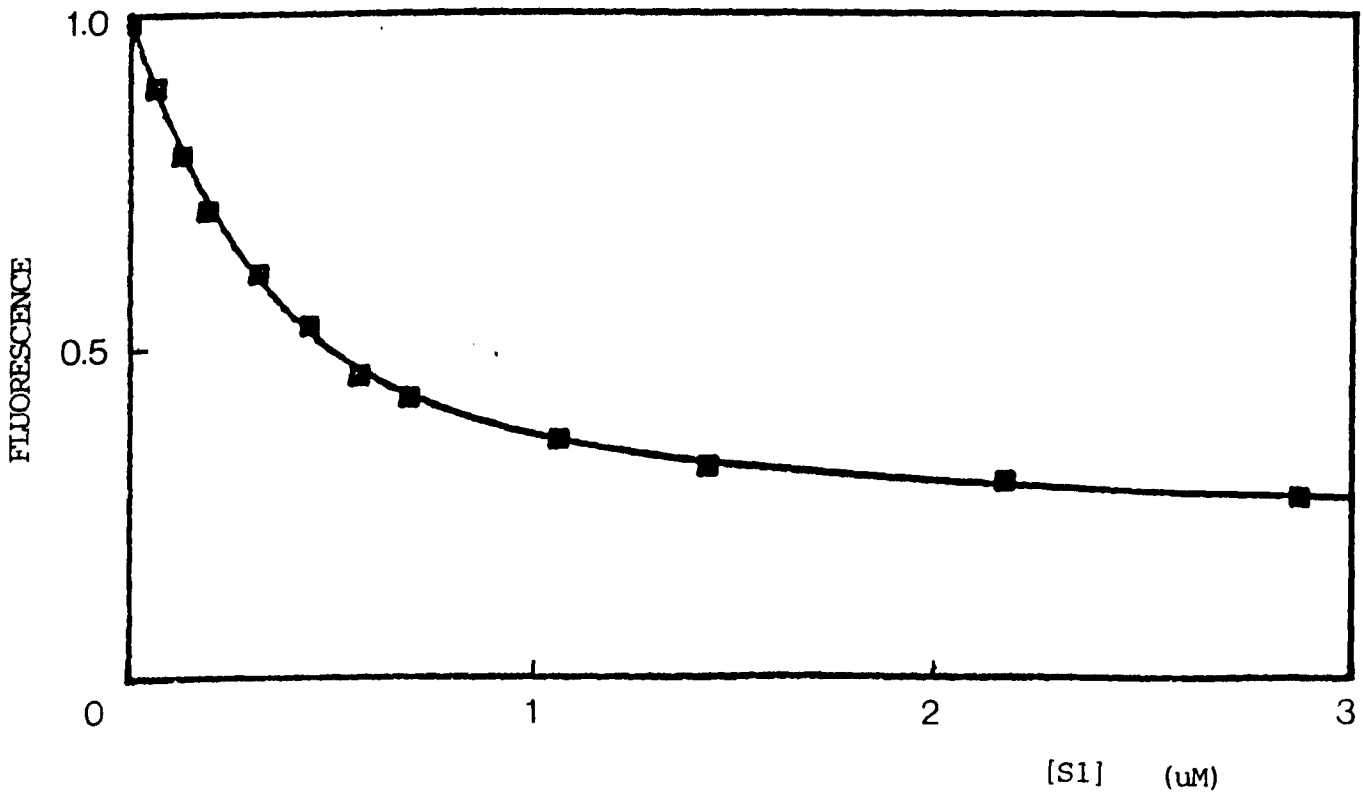
1.0
0.5
0
FLUORESCENCE
1
2
3
[S1] (uM)

$$[A]_o \alpha^2 - \alpha([A]_o + [M]_o + K_d) + [M]_o = 0$$

where $[A]_o$ is the starting concentration of actin, $[M]_o$ is the total concentration of S1 added, K_d is the dissociation constant and α is the fractional saturation of actin by S1. α is defined in terms of the fluorescence signal, F as;

$$\alpha = (F_o - F) / (F_o - F_\infty)$$

where F_o and F_∞ are the fluorescence signals for zero and infinite S1 concentrations, respectively.

The fitted line gives a K_d of 0.09uM (K_{ass} = 11 x 10^6 M^{-1}) (table 3.1), which is in agreement with measurements by Criddle et al. (1985) and Geeves & Halsall (1986). For the determination of the binding constant, actin concentrations similar to the reciprocal binding constant were used. Values shown are averages of experiments, which give a value for the reciprocal binding constant within 2 fold of the calculated total actin concentration.

It has previously been reported that chloride can bind to proteins specifically and inhibit protein-protein interactions (Giles, 1987), therefore, titrations in the presence of different monovalent anions were performed. Results in table 3.1 indicate that other anions at 0.1M concentrations compared with chloride had only a small effect on the association constant, decreasing it slightly. An increase in salt concentration from

Table 3.1 Association constants for the interaction of pyr-actin with S1 in the presence of different monovalent anions as determined by fluorescence titration

Buffer conditions: 20mM imidazole, 5mM Mg-acetate, pH 7, 20°C. (*) Magnesium acetate was replaced by $MgCl_2$. Actin concentrations were near the reciprocal binding constant. Numbers in brackets are standard deviation and the number of observations, respectively.

Potassium Salt	Concentration (M)	Association Constant $M^{-1} \times 10^6$	Concentration (M)	Association Constant $M^{-1} \times 10^6$
chloride*	0.1	11(+/-7.7;7)	0.5	0.2(+/- 0.1,3)
acetate	0.1	9.1(+/-4.0;8)	0.5	1.1(+/-0.7;3)
proprionate	0.1	4.9(+/-1.4;4)	0.5	2.7(+/-0.6;3)
bicarbonate	0.1	5.7(+/-4.5;3)	0.5	0.08-0.09(-;2)
bromide	0.1	2.4-2.9(-;2)	0.5	0.16-0.17(-;2)

0.1M to 0.5M, however, reduced the association constant for chloride, bicarbonate and bromide significantly and less so for acetate and proprionate.

The effect of organic solvents in the presence of different monovalent anions on the acto.S1 interaction was also examined. 40% ethylene glycol in 0.1M chloride reduced the association constant by a factor of 5, and in 0.1M acetate showed only a small decrease in K_{ass}. An increase in chloride concentration to 0.3M demonstrated an insignificant change in K_{ass} to that observed at 0.1M (table 3.2).

Dimethylsulphoxide (DMSO) 20% in 0.1M chloride reduced K_{ass} by a factor of 2. DMSO in excess of 20% resulted in depolymerization/denaturation of F-actin.

Pressure relaxation measurements

The effect of a 100atm pressure perturbation on the fluorescence of a pyrene-actin and S1 solution in 0.5M acetate is shown in fig. 3.2. Two distinct relaxations are apparent: one, which is complete within the pressure release time of the apparatus (200usec.) and the other, which could be fitted by a single exponential. Coates et al. (1985) described the rate of the faster relaxation ($1/\tau_1$) as;

$$1/\tau_1 = k_{+2} + k_{-2}$$

and the rate of the slower relaxation ($1/\tau_2$) as;

Table 3.2 Equilibrium constants for the interaction of pyr-actin with S1

Association constants were obtained by fluorescence titration. Values for K_oK_1 were determined by pressure jump experiment and values for K_2 was calculated from the equation; $K_{ass} = K_oK_1 \times (1 + K_2)$. Volume changes were estimated as described in the text. Numbers in bracket are the standard deviation and the number of observations, respectively. Buffer conditions as in table 3.1.

Potassium salt	K_{ass} (M^{-1})	K_0K_1 (M^{-1})	K_2	Volume change (cm^3/mol)
0.1M chloride	$11x10^6$	$7x10^4$	160	71(+/-37;6)
0.5M chloride	$0.3x10^6$	$0.7x10^4$	42	33(+/-1.5;5)
0.1M acetate	$9.1x10^6$	$7x10^4$	130	47(+/-18;6)
0.5M acetate	$1.1x10^6$	$4.6x10^4$	25	20(+/-1.7;7)
20% DMSO 0.1M chloride	$5.0x10^6$	$8x10^4$	62	48(+/-10;8)
40% Et.Gly 0.1M acetate	$6.6x10^6$	$18.4x10^4$	36	23(+/-12;6)
40% Et.Gly 0.1M chloride	$2.0x10^6$	$10x10^4$	20	34(+/-11;6)
40% Et.Gly 0.3M chloride	$1.1x10^6$	$8x10^4$	14	48(+/-17;6)

Figure 3.2 Pressure induced relaxations of a solution of pyrene labelled acto.S1

Pressure induced changes in the fluorescence of a solution of pyrene labelled acto.S1. The arrow indicates the time of pressure release, the pressure release in each case being a decrease from 10.1MPa (100atm) to 101kPa (1atm). Each trace represents the average for five relaxations on the same solution, and the best fit single exponential to the slow phase is superimposed. (i) 5uM pyr-actin, 10uM S1; $1/\tau_2 = 2.5\ s^{-1}$; ratio of the amplitudes (amp.1/amp.2) = 0.28; (ii) 5uM pyr-actin, 25uM S1; $1/\tau_2 = 9.2\ s^{-1}$; (amp.1/amp.2) = 0.91. Reaction conditions: 0.5M acetate, 20mM imidazole, pH 7, 20°C.

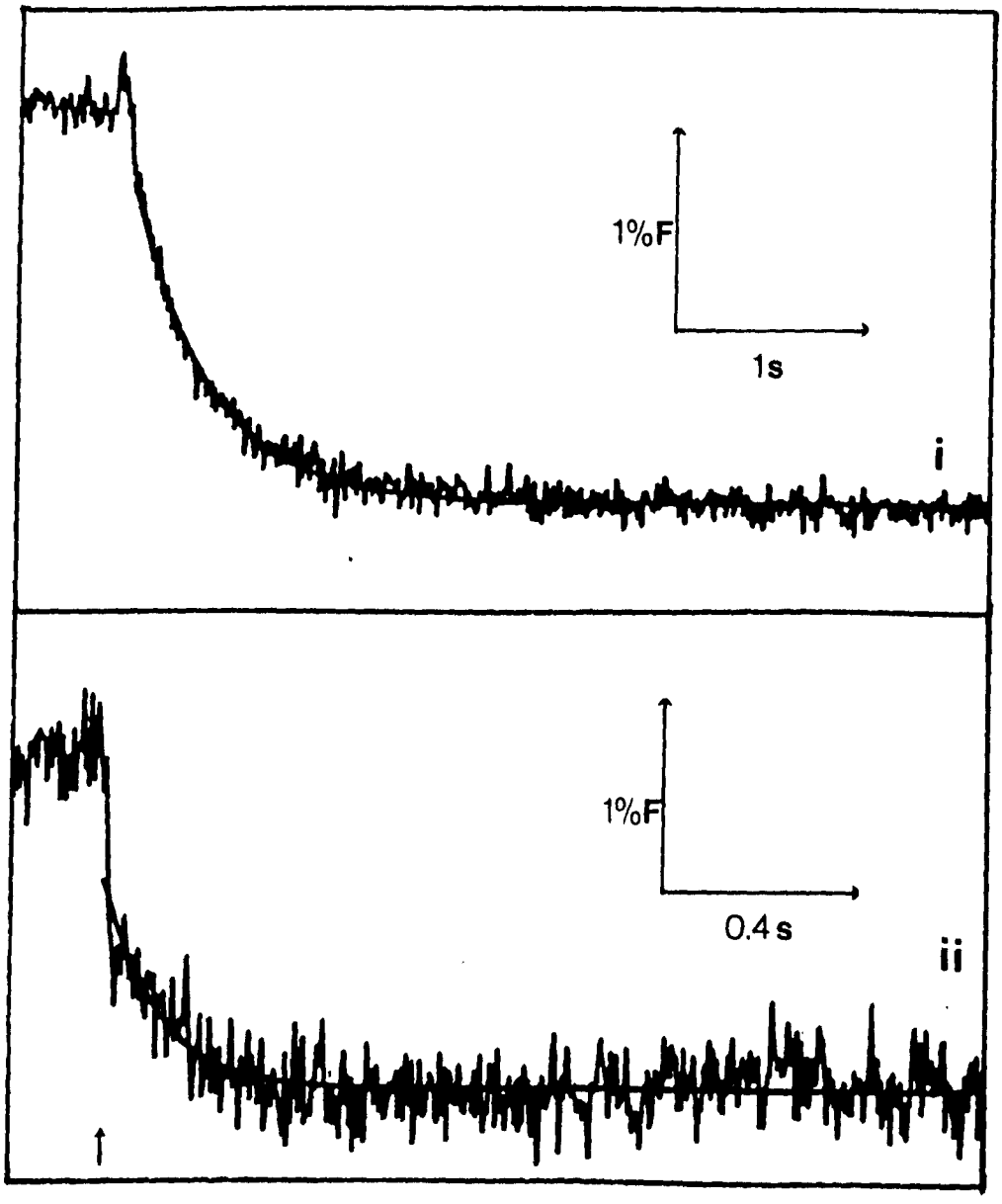
1%F
1s
i
1%F
0.4 s
ii

$$1/\tau_2 = \frac{K_o \times k_{+1} \times ([\bar{A}] + [\bar{S1}])}{K_o \times ([\bar{A}] + [\bar{S1}]) + 1} + \frac{k_{-1}}{1 + K_2}$$

(Bars denote equilibrium free protein concentration, which were calculated, using the binding constants obtained from fluorescence titrations). As the second relaxation rate is linearly dependent on free protein concentration then $K_o \times ([\bar{A}] + [\bar{S1}]) << 1$. The gradient of a plot of $1/\tau_2$ versus free protein concentration, as shown in fig. 3.3a, is then equal to $K_o k_{+1}$. The intercept of this plot was poorly defined, indicating $k_{-1}/(1 + K_2)$ is small. The association rates ($K_o k_{+1}$), which were relatively insensitive to the value of the binding constant used, agreed with association rate constants obtained, using stopped flow methods. Average values for the association rates from pressure relaxations measurements are shown in table 3.3.

The relative magnitudes of $K_o K_1$ and K_2 can be determined by the size of the fast (a_1) and slow (a_2) relaxation amplitude. Fig.3.3b shows that the relative amplitude of the fast phase increases with free protein concentration. The ratio of the two amplitudes is defined by the following equation;

$$\frac{(a_1)}{(a_2)} = \frac{1}{K_2} + K_o K_1 \times \frac{(1 + K_2)}{K_2} ([\bar{A}] + [\bar{S1}])$$

The plots are shown in fig 3.3b and are linearly dependent on free protein concentration. The intercept ($1/K_2$) was poorly defined by these data as it is small. Therefore, $(1 + K_2)/K_2$ equals approx 1; so the gradient of these plots defines $K_o K_1$. The

Figure 3.3 The dependence of pressure induced relaxations of pyrene acto.S1 on free protein concentration

(a) Plot of the reciprocal relaxation time of the slow phase of the relaxation against the free concentration of pyr-actin and S1. The line represents the best fit to the data giving a value of 0.4 s^{-1} for the intercept and a gradient of 3.2 x 10^5 $M^{-1}s^{-1}$.

(b) Plot of the ratio of the observed amplitudes (amp.1/amp.2) against the concentration of free pyr-actin and S1. The line represents the best-fit line to the data and gives a gradient of 4.6 x 10^4 M^{-1} and an intercept of 0.1, which is not significantly different from zero.

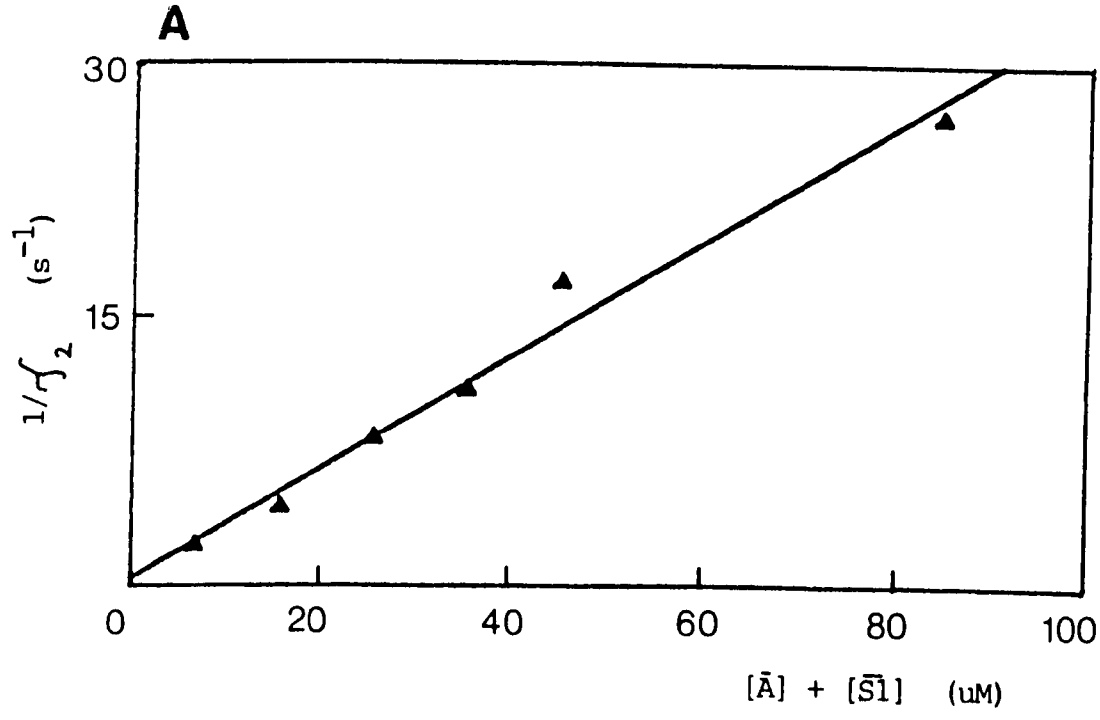
A
30
15
0
20
40
60
80
100
$1/\tau_2$ (s^{-1})
[Ā] + [S̄1] (uM)

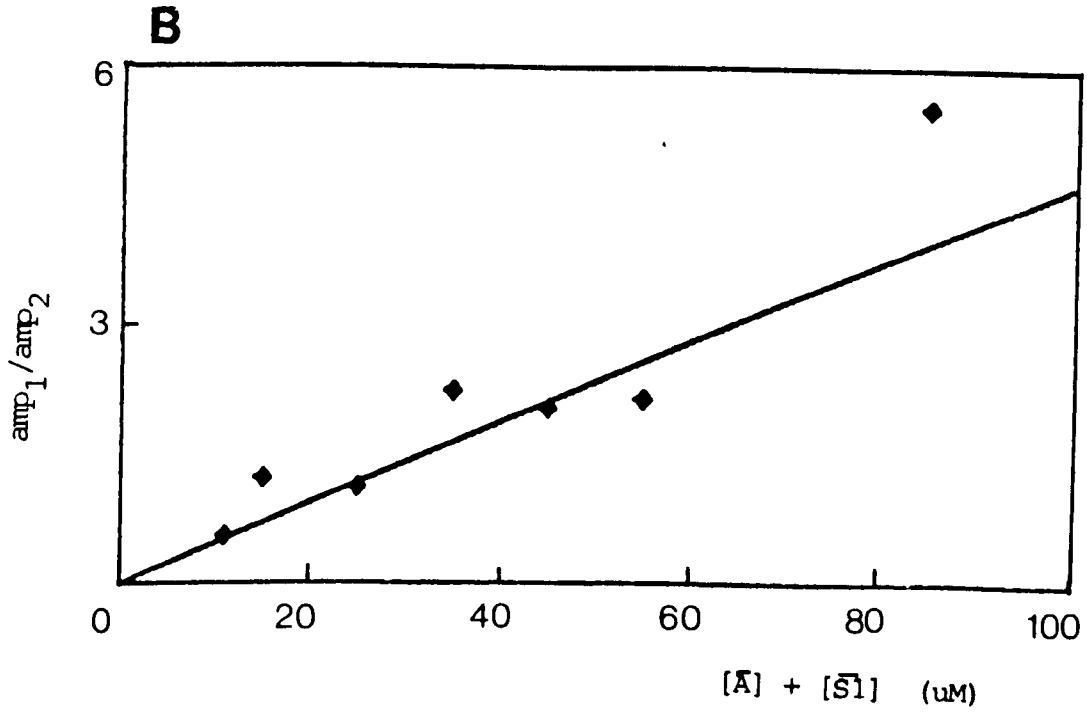
B
6
3
0
20
40
60
80
100
amp_1/amp_2
[Ā] + [S̄1] (uM)

Table 3.3 Rate constants for the interaction of pyr-actin with S1

Association rate constants were obtained from pressure jump and stopped flow experiments. Dissociation rate constants were determined by stopped flow displacement experiments. (*) k_{-1} was calculated from the ratio $K_o k_{+1}/K_o K_1$; n.m. = not measured. Buffer conditions as in table 3.1.

Method	$K_o k_{+1}$		$\frac{k_{-1}}{1 + K_2}$	k_{-1}^*
	P-Jump	Stopped-flow		
	$(M^{-1} \times s^{-1})$		(s^{-1})	(s^{-1})
Potassium salt				
0.1M chloride	12.8×10^5	12.6×10^5	.21	18
0.5M chloride	2.3×10^5	1.77×10^5	.85	33
0.1M acetate	9.6×10^5	10×10^5	.16	14
0.5M acetate	3.2×10^5	4.61×10^5	.33	7
20% DMSO 0.1M chloride	3.2×10^5	n.m.	.06	4
40% Et.Gly 0.1M acetate	3.75×10^5	n.m.	n.m.	2
40% Et.Gly 0.1M chloride	2.4×10^5	n.m.	.1	2.4
40% Et.Gly 0.3M chloride	1.1×10^5	n.m.	.1	1.4

overall binding constant was then used to calculate K_2, using the relationship $K_{ass} = K_oK_1 \times (1 + K_2)$. The results from such analysis are shown in table 3.2.

Data from these experiments gave a better understanding of the effects of the different parameters used and enabled determination of the equilibrium constants of each step.

The difference in K_{ass} observed between acetate and chloride at 0.1M is reflected in a change in K_2. The increase in chloride and acetate from 0.1M to 0.5M decreased K_2 by a factor of 4-5. The value for K_oK_1 remained the same for acetate by this increase and showed for chloride a decrease by a factor 10. These results can be interpreted as an ionic strength effect on K_2 and a specific chloride effect on K_oK_1. Similar results are also expected for bromide and bicarbonate (table 3.1).

The presence of organic solvents in 0.1M chloride or 0.1M acetate shows no effect on K_oK_1, but significantly affects K_2. A decrease by a factor 2-8 in K_2 can be noted. Using these organic solvents an increase in chloride to 0.3M shows no effect on K_oK_1 or K_2 (table 3.2).

Stopped flow measurements

The association rate constant was also obtained by stopped flow methods, which showed good agreement with the slow phase of pressure relaxation measurements.

Pyr-actin was mixed with an excess of S1 in the stopped flow spectrophotometer under pseudo-first order conditions. The fluorescence decay could be described by a single exponential at all concentrations of S1 used. Fig. 3.4 shows typical results for

Figure 3.4 The rate of association of S1 with pyrene actin

The trace represents the average of five consecutive measurements in the stopped flow apparatus. Best fit to a single exponential is shown superimposed. The arrow indicates the time of flow stopping. Buffer conditions: 0.5M acetate, 5mM Mg-acetate, 20 mM imidazole, pH 7, 20°C. Protein concentration: 5uM pyrene-actin and 7.5uM S1. The observed rate (k_{obs}) = 2.5 s^{-1}. The fluorescence signal decreases. The size bar is relative to the final fluorescence value.

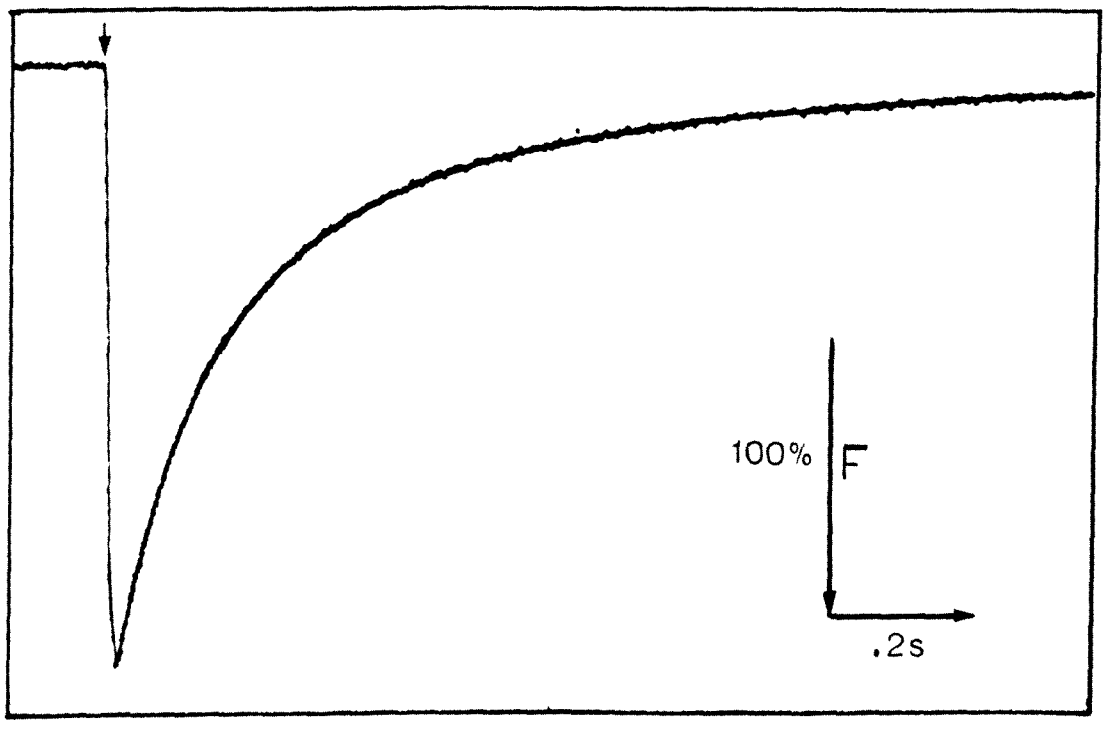
100%
F
.2s

fluorescence transients with least squares best fit exponential superimposed. The observed rate of the fluorescence decay was linear with respect to total S1 concentration $[S1]_o$. Assuming scheme I describes these results over this concentration range, the observed rate of fluorescence decay is described by the following equation (Geeves & Halsall, 1986);

$$\text{(scheme I)} \qquad k_{obs} = \frac{K_o k_{+1} [S1]_o}{K_o [S1]_o + 1} + \frac{k_{-1}}{(1 + K_2)}$$

As the observed rate is linear with respect to $[S1]_o$, $[S1]_o \times K_o << 1$ and $k_{+o} + k_{-o} >> k_{+1}$, k_{-1} and $k_{+2} + k_{-2} >> k_{+1}$, k_{-1} then the gradient of fig. 3.4 will give the value $K_o k_{+1}$. The least squares best fit is shown superimposed. The intercept of this plot, which is a measure of the "off" rate, was too small to be significant indicating $k_{-1}/(1+K_2)$ is small. This rate was, therefore, estimated by displacing the labelled actin with a small excess of S1 by the addition of a 5 fold excess of unlabelled actin as described by Criddle et al. (1985) (fig. 3.5). The observed rate corresponds to $k_{-1}/(1+K_2)$ and was unaffected by increasing the concentration of native actin used in the experiment.

The kinetic data obtained from stopped flow experiments are presented in table 3.3. The data are in agreement with the known effect of ionic strength on the rate of association of actin and S1 (Finlayson, 1969; White & Taylor, 1976; Criddle et al., 1985). Similar rate constants were obtained for chloride and acetate at 0.1M and 0.5M concentrations, respectively. An increase in salt

Figure 3.5 Stopped flow displacement of pyr-actin from pyr-acto.S1 by addition of excess native actin

Change in fluorescence on mixing 2uM pyr-actin and 2.1uM S1 with 10uM actin. The trace is a single reaction in the stopped flow apparatus and the computer-drawn best-fit exponential is superimposed + slope, k_{obs} = 0.33 s^{-1}. Buffer: 0.5M acetate, 5mM Mg-acetate, 20mM cacodylate, pH 7, 20°C. Fluorescence signal is increasing. The size bar is relative to the maximum signal.

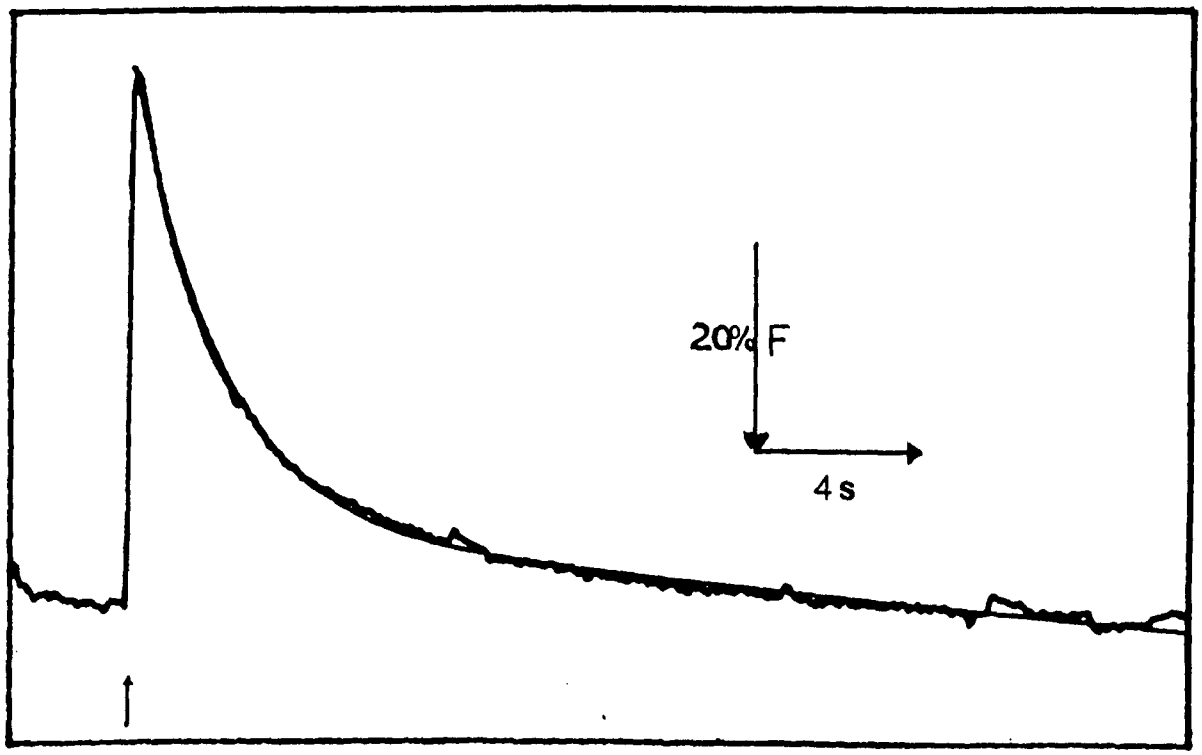
20% F
4 s

concentration or the addition of organic solvents reduced the rates by a factor of 3-4. As the equilibrium constant (K_oK_1) did not change by these treatments (except for 0.5M chloride) these changes must, therefore, be reflected in k_{-1}. Increasing chloride from 0.1M to 0.5M reduced (K_oK_1) by a factor of 10 and as K_ok_{+1} was decreased by a factor of 4-5, the attached state is destabilized by an increase in k_{-1}. The independently measured "off" rate ($k_{-1}/1 + K_2$) shows also a larger value for chloride than for acetate at 0.5M or for 0.1M and 0.3M salt concentration in the presence of organic solvents, which reflects an overall weakening of the acto.S1 complex (table 3.3).

Temperature effect on equilibrium and rate constants

The effect of temperature on the two step binding of actin to S1 has previously been reported by Coates et al., (1985) for 0.1M chloride. It was noted that K_{ass} was reduced by a factor of 10 when the temperature was lowered from 20°C to 2°C. This change was reflected in a significant drop in the rate of association and in a smaller decrease in the equilibrium constant K_oK_1. The results of an experiment carried out in 0.1M acetate over the same temperature range are presented in table 3.4.

The equilibrium constant K_{ass} is only reduced by a factor 2 over the temperature range studied here and the decrease in K_oK_1 is reflected in an increase in K_2. Most noticable is the large reduction of the association rate, which has been observed previously (Marston, 1982; Geeves & Gutfreund, 1982; Criddle et al., 1985) and a smaller reduction in the equilibrium constant K_oK_1.

Table 3.4 The rate and equilibrium constants for the interaction of pyr-actin with S1 at different temperatures

Association constants (K_{ass}) were obtained by fluorescence titration. Values for K_oK_1 were determined by pressure jump experiments and values for $K_{ass} = K_oK_1 \times (1 + K_2)$. Rate constants were established from stopped flow experiments. Volume changes of the pressure sensitive step K_2 were calculated as described in the text. Numbers in bracket are the standard deviation and the number of observations, respectively. Buffer conditions as in table 3.1.

0.1M Potassium acetate	K_{ass} (M^{-1})	K_oK_1 (M^{-1})	K_2	K_ok_{+1} ($M^{-1}s^{-1}$)	Volume change (cm^3/mol)
at 20.0°C	9.1×10^6	7×10^4	130	9.6×10^5	47(+/-18;6)
at 12.5°C	7.0×10^6	5×10^4	140	7.1×10^5	49(+/-17;7)
at 8.2°C	6.0×10^6	3.5×10^4	171	4.5×10^5	76(+/-12;5)
at 4.0°C	5.0×10^6	2.7×10^4	185	2.1×10^5	91(+/-10;6)
at 2.0°C	4.0×10^6	2×10^4	200	1.5×10^5	110(+/-37;6)

The effect of temperature on the rate and equilibrium constant is shown in fig. 3.6 and the thermodynamic data calculated from the Arrhenius and van't Hoff plot are shown in (table 3.5). Both plots indicate a discontinuity around 10°C and a sharp difference in entropy below and above the breakpoint, which could be due to the change in environment or due to a conformational change. Millar & Geeves (1983) also observed a breakpoint around that temperature for ATP-induced dissociation of acto.S1. These workers interpreted their findings with a conformational change in either protein.

From the thermodynamic data in table 3.5 it can be seen that ΔG^{+} (the free energy difference between the two states) for the reaction remains relatively constant under all conditions, and that the change in ΔH^{+} is due to a large change in ΔS^{+}. This indicates some change in order of the system is occuring at a critical temperature (T_m).

Volume changes

Geeves & Gutfreund (1982) and Coates et al. (1985) noted in their pressure relaxation studies a substantial volume change when perturbing the acto.S1 complex. From this, these authors suggested a substantial rearrangement of the hydration sphere around the proteins and possible conformational change. Using the calculated values for K_2 and the known signal amplitudes, V^{o} is calculated by the following equation;

$$\Delta K/K = -\Delta P \times V^{o} / R \times T$$

Figure 3.6 Arrhenius and Van't Hoff plot

(A) Arrhenius plot of the variation of the rate of association ($K_o k_{+1}$) of acto.S1 with temperature.

(B) Van't Hoff plot of the variation of the equilibrium constant ($K_o K_1$) of acto.S1 with temperature.

Buffer: 0.1M acetate, 5mM Mg-acetate, pH 7.

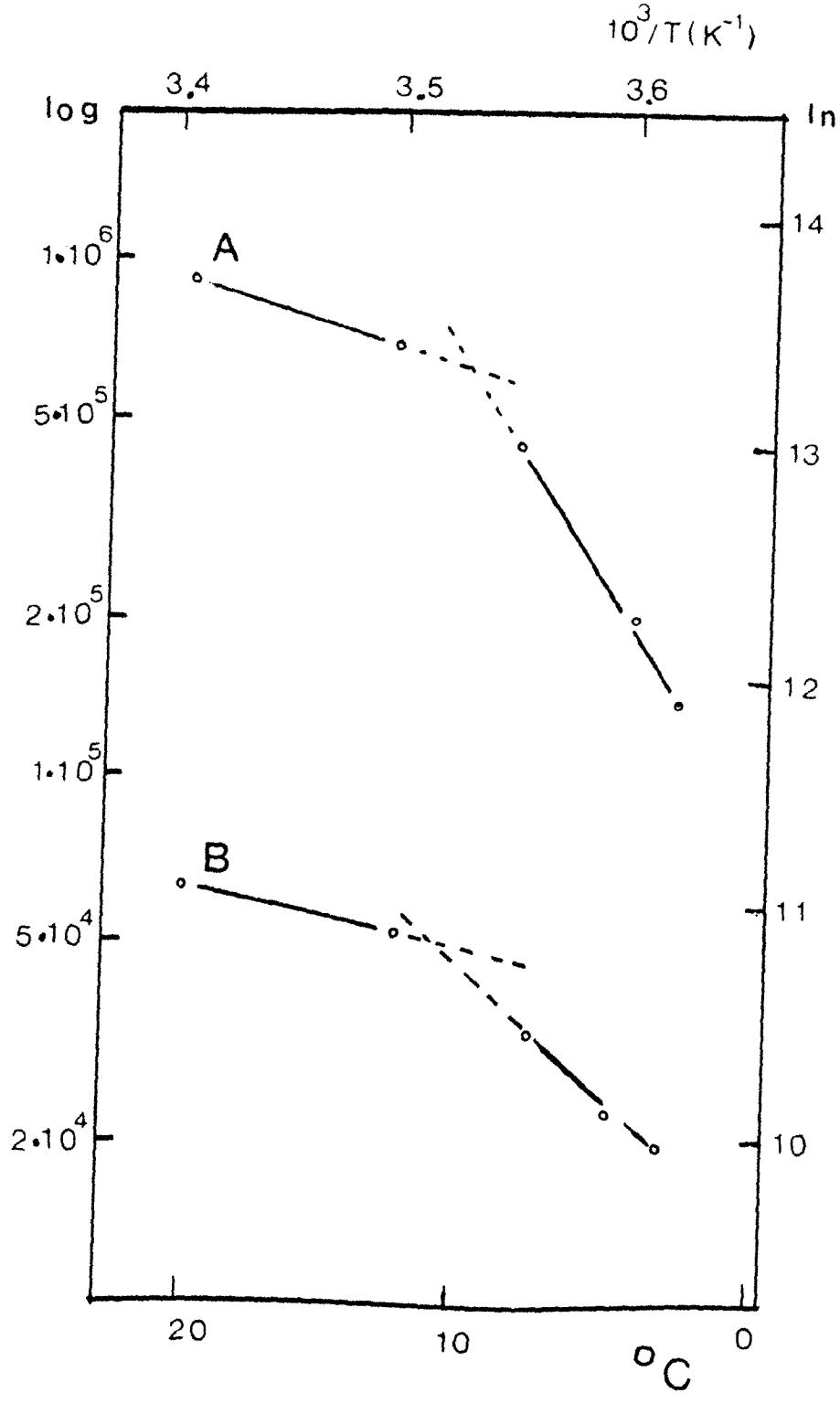
$10^3/T(K^{-1})$
3.4
3.5
3.6
log
ln
$1 \cdot 10^6$
$5 \cdot 10^5$
$2 \cdot 10^5$
$1 \cdot 10^5$
$5 \cdot 10^4$
$2 \cdot 10^4$
14
13
12
11
10
A
B
20
10
0
°C

Table 3.5 Thermodynamic data for the equilibrium and rate of association of acto.S1

The thermodynamic data were calculated using the following equations;

(1) $\ln k = \ln A - (E_a / R \times T)$ (Arrhenius equation)

(2) $\Delta H^+ = E_a - R \times T$

(3) $\Delta G^+ = \Delta H^+ - T\Delta S^+$

(4) $\Delta S^+ = \Delta H^+/T + R \times \ln (k/(k_B \times T / h))$

(5) $\log \frac{K_2}{K_1} = \frac{\Delta H^\circ \times (T_2 - T_1)}{2.303 \times R \times T_1 \times T_2}$ (Van't Hoff equation)

(6) $\Delta G^\circ = - R \times T \times \ln K$

(7) $\Delta G^\circ = \Delta H^\circ - T\Delta S^\circ$

With the following values for the constants: R (gas constant) = 8.31 $JK^{-1}mol^{-1}$, k_B (Boltzmann constant) = 1.38×10^{-23} JK^{-1}, h (Planck constant) = 6.62×10^{-34} J and T (absolute temperature).

Van't Hoff Plot

K_oK_1	ΔH^o	ΔG^o	ΔS^o
	(kJ/mol)	(kJ/mol)	(J/mol/K)
2°C	58.2	-22.4	294
20°C	31.1	-27.2	198

Arrhenius Plot

K_ok_{+1}	ΔH^+	ΔG^+	ΔS^+
	(kJ/mol)	(kJ/mol)	(J/mol/K)
2°C	112.2	39.9	263
20°C	24.8	38.1	-45

Results in table 3.2 indicate that increases in ionic strength or the addition of organic solvents tend to reduce the volume changes by approx a factor of 2. Volume changes for temperatures ranging from 2°C to 20°C in 0.1M acetate show a 2 fold increase with decreasing temperature (table 3.4).

DISCUSSION

The effect of ionic strength

Increased ionic strength or the addition of organic solvent has very little effect upon the equilibrium constant (K_oK_1) for the attached state but produces a marked reduction on the isomerization (K_2). This is similar to the effect of binding nucleotide or nucleotide analogues to the ATPase site where K_2 is markedly reduced with little effect upon K_oK_1 (Geeves et al., 1984; Geeves & Jeffries, 1988). In the case of nucleotide this effect is believed to be the result of a nucleotide conformational change in S1, which is communicated from the nucleotide binding site to the actin binding site, which are separated by some 4nm. As ionic strength and the two organic solvents will have a different influence on electrostatic interactions, hydrogen bonding and hydrophobic interactions, it seems unlikely that both treatments could bind to the nucleotide site and induce a similar conformational change. A more reasonable explanation is that these effectors stabilize the protein conformation.

Warren & Cheatum (1966) investigated the structure and activity of myosin and noticed that the environmental changes, as

those induced by addition of monovalent anions to the medium, can "push" the protein across a phase transition boundary with the resultant formation of a different structure. At concentrations above 0.3M salt, the activity and structure was increasingly affected, following the Hofmeister series (Hofmeister, 1888): $CH_3COO^- < Cl^- < NO_3^- < Br^-$ (Warren et al., 1966). Stafford (1985) examined the effect of different anions on the stability of myosin and reported that chloride destabilized and acetate stabilized the entire macromolecule. These results support the observations of acto.S1 in this chapter that chloride has a destabilizing effect compared to acetate.

The effect of solvents

Although an increase in ionic strength or the presence of organic solvents have a similar effect on the equilibrium constant K_2, their influence on the hydrophobic and electrostatic interaction will be different. The general effect of ethylene glycol on biological systems has been well characterized, and it has been considered to be an inert solvent for proteins (Tanford et al., 1962). Kay & Brahms (1963) showed that the conformation of HMM in the presence of up to 67% ethylene glycol is slightly modified. Tregear et al. (1984) reported a shift in the S1 structure in the presence of 40% ethylene glycol towards the weak binding conformation with actin and a stabilization in that conformation. It seems, therefore, unlikely that increases in ionic strength and organic solvent induce similar conformational changes.

There have been few detailed studies of the effects of

solvent on protein-protein interactions and studies which have isolated individual events are still rarer. Much of the literature has been concerned with the influence of ions and organic solvents on protein folding, which is influenced at high salt concentrations and organic solvents by changes in water structure (Eagland, 1975; Giles, 1987).

The effect of pressure

Analysis of the amplitudes of the pressure relaxation indicates that the reaction involves a volume change of approx $100cm^3/mol^{-1}$ (0.1M KCl), which is indicative of a protein conformational change (Coates et al., 1985).

Generally, protein association involves mutual penetration of hydration layers to form a hydrophobically associated species followed by other intermolecular interactions. This hydrophobic association is the result of the tendency of water to form a more ordered structure in the vicinity of nonpolar hydrocarbon groups (Ross & Subramanian, 1981).

Volume changes are usually the result of a reduction of bulk water surrounding the proteins as this has a larger volume than the ordered structure of water.

The high concentration of ions or the presence of organic solvent concentrations may have some effect on the order of free water surrounding the protein and, thereby, reduce the perturbable volume. This effect then reduces the free energy difference (principally Δ S) between bulk water and the water of the protein hydration shell. This smaller free energy difference may result in a lower binding energy for the protein-protein

interaction. Although K_2 is not sufficiently well defined for ΔV to be calculated with any meaningful precision, but the data do suggest that ΔV is reduced by a factor of two at 0.5M ionic strength and in the presence of organic solvents (table 3.2).

A decrease in temperature from 20°C to 2°C is associated with an increase in volume change in the mass of water by a factor of 2 (table 3.4), which reflects a change from an ordered to a randomized water structure. This can be explained by the enhancement of solvent structure by the dissolution of nonpolar groups (usually hydrocarbons) in water, which is greatest at low temperature. The tendency for hydrophobic association is increased because of this and the amount of bulk water released becomes larger; bulk water having a larger volume that the ordered water associated with the hydration shell (Kauzmann, 1959).

The effect of temperature

For most protein-protein interactions a linear Arrhenius plot is a common feature. However, a non-linear plot, as observed in the association reaction ($K_o k_{+1}$) of actin and S1, can reveal important mechanistic information and such plots are good evidence for a structural or phase change in the proteins involved at a certain critical temperature (Londesborough, 1980). Discontinuous Arrhenius plots have been reported for ATP-induced disscociation of acto.S1 (Millar & Geeves, 1983) and for ATP binding to S1 (Biosca et al., 1983).

Although the calculation of thermodynamic parameters is an easy task, their interpretation is not. There is some evidence

for a conformation change from the breakpoint in the plots, which is reflected also in the large entropy change. However, another most likely source of such large entropy increase seems to be displacement of water from the surface area of the two proteins, which come in close contact during association. As charged and hydrophobic side-chains groups are involved in the acto.S1 interaction (Kodama, 1985), the surface charge, which can be inferred from the ionic strength dependence of the binding constant, becomes important. It is concluded that the release of water molecules from aliphatic chains of acto.S1 could, therefore, also account for a change in entropy (Highsmith, 1977; Borejdo, 1983).

The effect of the different conditions on the two-step binding

From the results shown here only a few general statements about the nature of the reactions in the two-step binding can be made. The equilibrium constant K_oK_1 appears to be unaffected by ionic strength or by the presence of the two organic solvents, but is influenced by temperature. Chloride concentrations above 0.1M destabilize the attached state by increasing the rate of dissociation. There is a general ionic strength and organic solvent effect and a specific temperature effect on the rate of formation of the attached state. It is known that the formation of the attached state is a complex reaction and, therefore, an effect on the formation of the collision complex cannot be distinguished from an effect of the rate of the transition to the attached state.

The isomerization step K_2 is affected by ionic strength, and

the effect appears to be relatively independent of the nature of the anion used. A similar effect is produced by organic solvents. Temperature has only a marginal influence on K_2.

CONCLUSIONS

The data presented here show how different conditions can be used to occupy preferentially one of the two acto.S1 states. Ionic strength and organic solvent can be used to reduce the "rigor-like" state without reducing the occupancy of the "attached" state. However, it was not possible to find conditions which would allow the acto.S1 complex to be mainly in the "attached" [A-M] state. Under all conditions more than 90% of the acto.S1 complex was in the "rigor-like" [AM] state.

However, recent experiments performed in the presence of ADP at different ionic strength and also in the presence of solvent showed that the effects of solvent and ionic stength on K_oK_1 are maintained under these conditions (Geeves & Jeffries, 1988). It was demonstrated that the value for K_2 could be reduced to 10 (0.1M KCl, 20^oC) and even further in the presence of ethylene glycol. This suggested, that it may be possible to use both solvent and ADP to trap a stable [A-MD] state for structural analysis.

The following chapter examines the effect of ADP in the presence of different anions at different ionic strength in order to find conditions where K_2 could even be further reduced.

CHAPTER 4 THE EFFECT OF DIFFERENT ANIONS AND IONIC STRENGTH ON THE ISOMERIZATION STEP OF ACTO.S1 IN THE PRESENCE OF ADP

INTRODUCTION

Studies in chapter 3 have shown that the fluorescence of pyrene labelled actin monitors the isomerization step of the acto.S1 binding complex in the absence of nucleotide. The equilibrium of this step was demonstrated to be sensitive to different experimental conditions, however, varying conditions produced < 5% of the acto.S1 complex in the weakly "attached" state.

Investigations by Geeves et al. (1986) have shown that the fluorescence of the pyrene group monitors this step also in the presence of nucleotide. This allowed Geeves & Jeffries (1988) to characterize the two binding states in the presence of different nucleotides, nucleotide analogues and under different solvent conditions. It was demonstrated in their extensive study that these treatments can be used to reduce the "rigor-like" binding of the acto.S1 complex.

The aim of the experiments reported in this chapter is to examine the influence of ADP and different anions at different ionic strength on the isomerization step. Since both parameters have influence on the equilibrium constant (K_2) of this step, it may, therefore, be possible to use these conditions to weaken the "rigor-like" state further, which would allow for most of the acto.S1 complex to exists in a stable [A-MD] state. In establishing this, it would then allow for structural studies to

be to carried out.

Equilibrium binding studies with ADP

The binding of unlabelled actin to S1.ADP has been measured by sedimentation (Greene & Eisenberg, 1980) by stopped flow (Marston, 1982; Trybus & Taylor, 1980; Siemankowski & White, 1984) and by pressure relaxation study (Geeves & Gutfreund, 1982). A binding constant (K_d) of approx 2uM in 0.1M KCl at pH 7-8 and 20°C was measured by all the different techniques. Geeves (1989) confirmed this value with pyr-actin, demonstrating that the fluorescent label showed no significant effect on the affinity of actin for S1.ADP.

Studies of the isomerization step

The difference observed in the fluorescence signal quench of pyr-actin at saturating [S1] in the presence and absence of ADP was the basis of the investigation by Geeves & Jeffries (1988). Taking previous evidence for an isomerization step, produced by Coates et al. (1985) and later by Geeves et al. (1986) into account, the following approach was adopted. If, under saturating S1 concentration upon addition of nucleotide no dissociation of the acto.S1 complex occurs (i.e. no change in light scattering) then any change in fluorescence signal must report a transition in the acto.S1 complex. As the fluorescence signal specifically monitors the isomerization, this fluorescence change represents a shift from the "rigor-like" to the "attached" state. The equilibrium constant for this step was calculated by dividing the ratio of the low by that from the high

fluorescence state

$$\frac{(F_A - F_D)/(F_A - F_{AS})}{(F_{AS} - F_D)/(F_A - F_{AS})} = K_2$$

F_A = fluorescence of actin; F_D = fluorescence in the presence of saturating [ADP]; F_{AS} = acto.S1 fluorescence.

Geeves & Jeffries (1988) reported that organic solvent and increasing KCl concentration in the presence of ADP had a marked influence on the isomerization step, leaving the association constant to form the weakly bound state virtually uneffected by these treatments. An equilibrium constant (K_2 approx 2.5) was obtained for acto.S1 in 0.3M KCl and in 0.1M KCl with addition of 40% ethylene glycol, suggesting less than 30% of the acto.S1 complex in the "attached" state.

RESULTS

Titrations

Pyr-actin was used in all experiments and titrations were performed and analysed essentially as described in chapter 3. Fluorescence quenching of pyr-actin by S1 was approx 70% and actin concentrations were used near their binding constants. Some reassociation of actin with S1, which appeared during experiments was believed to be due to contaminating ATP in the ADP. This effect was eliminated by preincubation of ADP, Ap_5A and a small amount of S1.

The association constants of acto.S1 in 0.1M chloride and in

the presence of 1mM ADP are in agreement with measurements carried out by Geeves (1989) (table 4.1). An increase in salt concentration to 0.3M reduced the association constant by a factor 10; a similar decrease was observed in the absence of nucleotide. However, using acetate and proprionate at the same ionic strength in the presence of ADP showed only a reduction of K_{ass} by a factor of 4.

Measurements of the isomerization step

Fluorescence and light scattering signals were obtained by excitation at 365nm or 413nm, respectively. The emission wavelength was set at 407nm or 420nm, respectively with a 2.5nm slit width each. Fluorescence and light scattering readings were taken from a stable pyr-actin signal before excess of S1 was added. At 0.1M salt concentration, 50uM S1 and at 0.3M salt concentration, 100uM S1 were added. Homogeneity of the solution in the cuvette was achieved by careful mixing. Introduction of air bubbles was avoided because of interference with the light scattering signal. Measurements were taken after each addition when the signal had stabilized.

Results of an experiment adding 5uM pyr-actin, 50uM S1 and 1mM ADP to a solution containing 0.1M proprionate, 20mM cacodylate, 5mM $MgCl_2$, pH 7 at 20°C is shown in fig. 4.1a. The small transient decrease in light scattering signal on addition of ADP was caused by contaminating ATP. No change in light scattering upon addition of ADP indicated that no dissociation of the acto.S1 complex had occurred, therefore, acto.S1 must either exist in the "attached" or "rigor-like"

Table 4.1 The effect of different anions and ionic strength on the equilibrium constants for pyr-actin.S1 interaction in the absence/presence of ADP

Equilibrium constants in the absence of ADP were taken from chapter 3 for comparison. Buffer conditions as in table 3.2.

The values for K_{ass} and K_2 in the presence of ADP were obtained by fluorescence titration and the value for K_oK_1 was calculated from the relationship $K_{ass} = K_oK_1 \times (1 + K_2)$.

Buffer: 20mM cacodylate, pH 7, 20°C. In addition chloride buffer contained 2mM $MgCl_2$, all other contained 2mM Mg-acetate.

* from Geeves & Halsall (1986).

\+ determined in separate experiments.

Titration and Pressure jump data taken from chapter 3 / table 3.2+1	K_{ass} (M^{-1})	K_oK_1 (M^{-1})	K_2
0.1M chloride	$11x10^6$	$7x10^4$	160
0.1M acetate	$9.1x10^6$	$7x10^4$	130
0.1M proprionate	$4.9x10^6$	$7x10^4$	70
0.3M chloride*	$1x10^6$	$1.3x10^4$	74
0.3M acetate+	$5x10^6$	$7x10^4$	74
0.3M proprionate+	$4.2x10^6$	$7x10^4$	60
0.5M chloride	$0.3x10^6$	$0.7x10^4$	42
Titration and K_2 measurement			
0.1M chloride + 1mM ADP	$4.7x10^5$	$3.6x10^4$	13
0.1M acetate + 1mM ADP	$7.3x10^5$	$2.7x10^4$	27
0.1M proprionate + 1mM ADP	$1.2x10^6$	$7x10^4$	17
0.3M chloride + 1mM ADP	$4.7x10^4$	$1.3x10^4$	2.6
0.3M acetate + 1mM ADP	$1.6x10^5$	$1.4x10^4$	11
0.3M proprionate + 1mM ADP	$4.0x10^5$	$2.5x10^4$	15
0.5M chloride + 1mM ADP	--not measurable--		1.6

Figure 4.1 The effect of ADP on the equilibrium constant K_2

Light scattering and fluorescence changes upon addition of ADP to acto.S1. The same solution was used to monitor optical signal.

	Excitation (wavelength)	Emission (wavelength)
(A) Light scattering	413nm	420nm
(B) Fluorescence	365nm	407nm

Experimental conditions: 3ml quartz cuvette containing 0.1M proprionate, 20mM cacodylate, 2mM Mg-acetate, pH 7, 20°C. pyr-actin = 5uM; S1 = 50uM; ADP = 1mM. Slit width of the Perkin Elmer LS-5B luminescence spectrophotometer = 2.5nm (excitation/emission); chart recorder speed of the Perkin-Elmer R-100A = 2cm/min. The value for K_2 was calculated as described in the text; K_2 = 17.

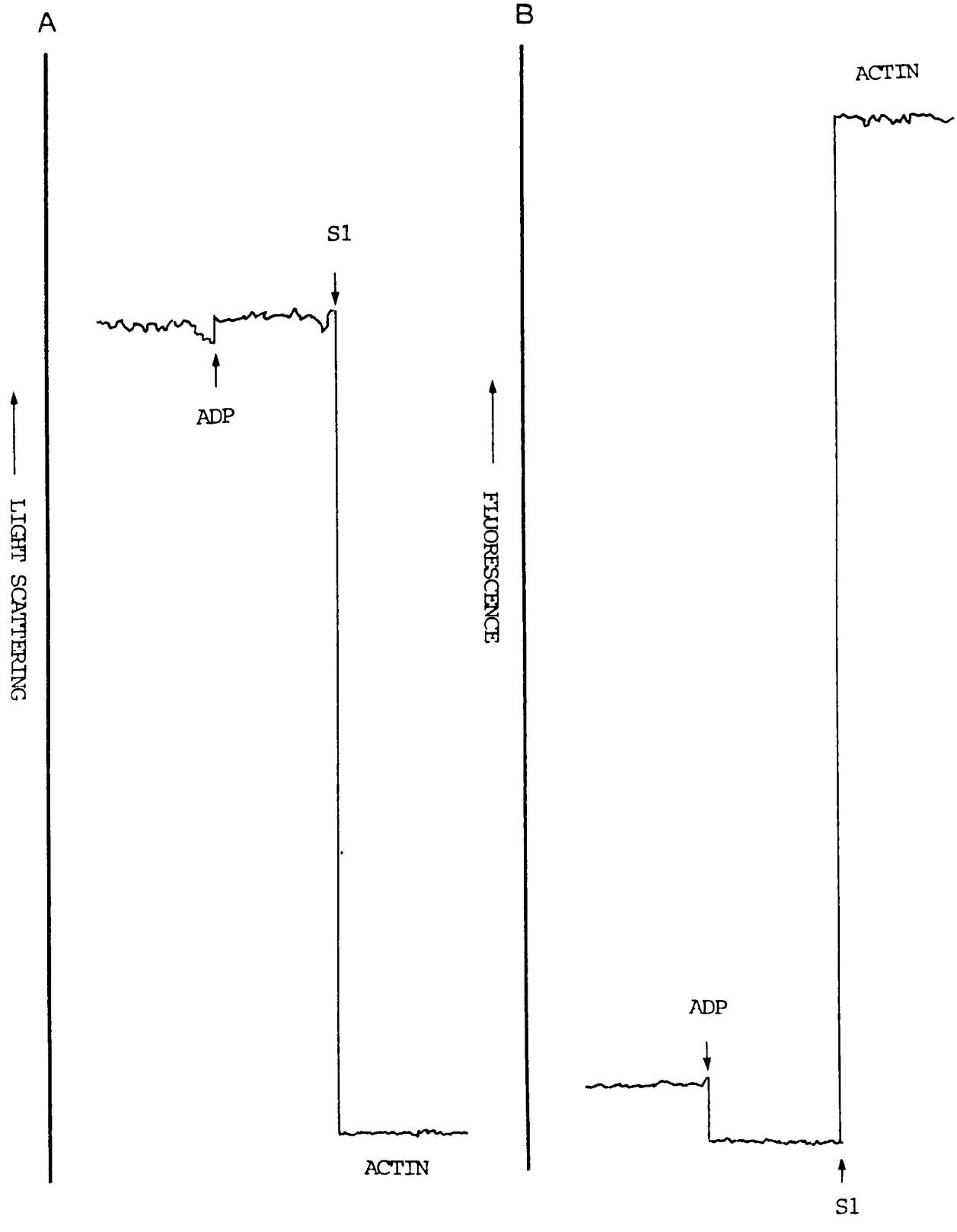
A
B
S1
ADP
ACTIN
LIGHT SCATTERING
FLUORESCENCE
ACTIN
ADP
S1
30s

state. The initial fluorescence increase in fig. 4.1b due to contaminating ATP did not return to the level observed for acto.S1 alone. This implied that a proportion of acto.S1 present existed in the high fluorescent "attached" state.

Only monovalent anions were used in an attempt to find conditions, where K_2 could be further reduced. Equilibrium constants for the isomerization step obtained by this method are listed in table 4.1. For comparison, values for K_{ass}, K_oK_1 and K_2 in the absence of ADP from chapter 3 are included.

The equilibrium constant of acto.S1 in chloride and in the presence of ADP is similar as reported by Geeves & Jeffries (1988). A reduction in K_2 by a factor of 5 was observed when the salt concentration was increased from 0.1M to 0.3M. These results indicate an ionic strength (chapter 3) and an ADP effect on K_2. An equilibrium constant of approx 2.6 would allow less than 30% of the acto.S1 in the intermediate state [A-MD]. At 0.5M this value was further reduced to approx 1.6, estimating a binding constant of about 80uM. The high protein concentration, however, could place an effective limit on an attempt to carry out structural studies.

Results for acto.S1 in acetate and proprionate in the presence of ADP showed that K_2 was not substantially affected when increasing the concentration from 0.1M to 0.3M. For proprionate, no change in the equilibrium constant was observed and for acetate, the value for K_2 was reduced by approx half by these treatments, allowing less than 10% of the acto-S1 complex to be in the [A-MD] state.

There is a noticable but constant decrease in K_2 by a factor

of 5 when comparing acetate and proprionate in 0.1M and 0.3M in the presence and absence of ADP. This change is larger in 0.1M KCl (approx 10 fold) and significantly increased in 0.3M and 0.5M (approx 30 fold), suggesting some chloride effect on K_2.

A reasonable explanation for the differences observed is, that the binding of ADP to the S1 nucleotide binding site is affected by the anions used. To gain further information of the influence of anions on the protein-protein and protein-nucleotide binding, transient kinetic measurements of ADP.S1 for actin and ADP for acto.S1 were carried out.

Stopped flow measurements

It has been shown that ADP binds to acto.S1 rapidly and reversibly and competes with ATP when dissociating acto.S1. In a typical stopped flow displacement experiment, 5uM acto.S1 were mixed with 50uM ATP in the presence of increasing concentrations of ADP (fig. 4.2a). The dissociation was monitored by change of fluorescence signal and was fitted by a single exponential. The rate of dissociation for this reaction was calculated, using the following equation (White, 1977);

$$k_{obs} = k_o/(1 + [ADP]/K_d)$$

where k_o is the observed rate constant in the absence of ADP and K_d is the dissociation constant of ADP for acto.S1. A plot of observed rate constants against ADP concentration in 0.1M proprionate is shown in fig.4.2b.

The data obtained, using this method and those obtained by

Figure 4.2 Rate of dissociation of acto.S1 in the presence of ADP

(A) 5uM acto.S1 was mixed with 50uM ATP in the presence of 31uM ADP in 0.1M proprionate, 20mM cacodylate, 5mM $MgCl_2$, pH 7, 20°C. Dissociation was monitored by fluorescence. (k_{obs} =108 s^{-1}).

(B) A plot of observed rate constants as a function of ADP concentration. The fit to the equation $k_{obs} = k_o/(1 + [ADP]/K_d)$ gave a K_d of approx 85uM.

K_d = dissociation constant of ADP for acto.S1

k_o = observed rate constant in the absence of ADP

A

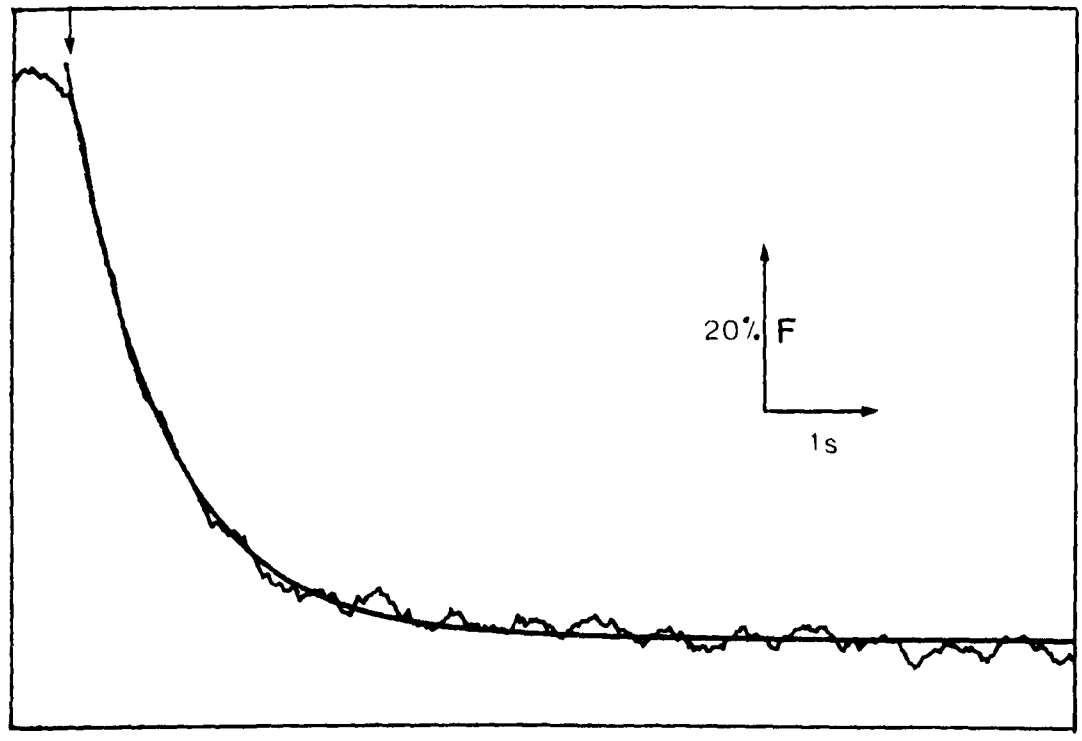

B

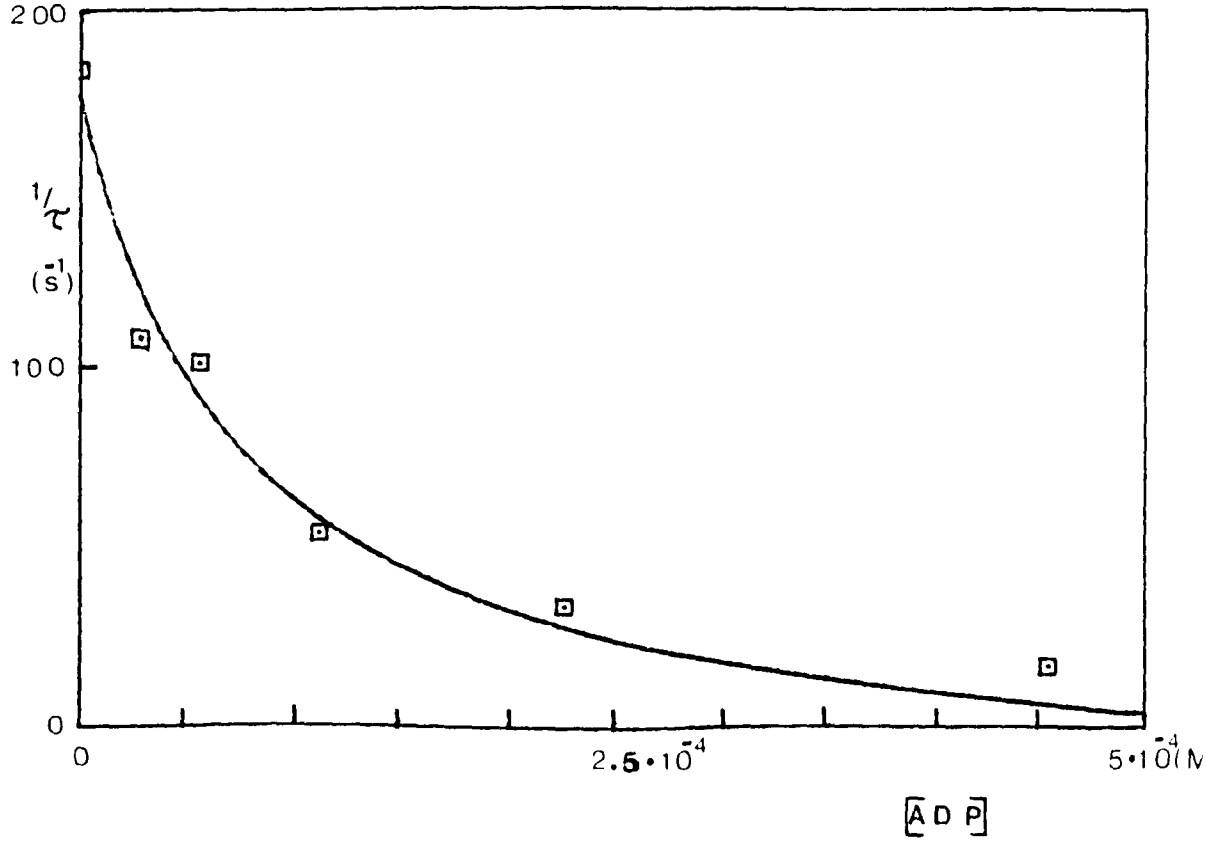

fluorescence titration of pyr-actin against S1 in the presence and absence of ADP, table 4.1, were analysed in terms of the equilibrium (Scheme I);

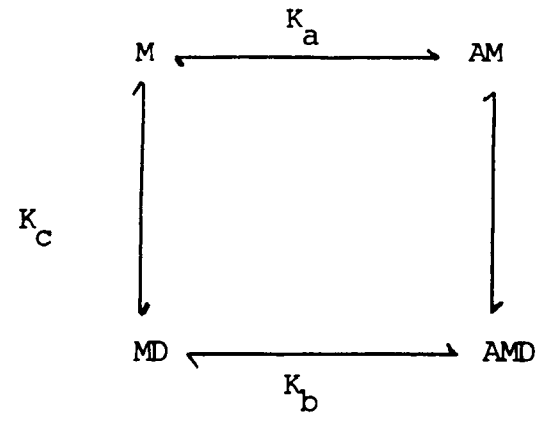

(Scheme I)

(The overall binding constant of both actin and ADP binding to S1, which is given by the product of the two individual binding constants, must be the same irrespective of the order, in which the two bind (i.e. $K_a \times K_d = K_c \times K_b$).

The results listed in table 4.2 indicate the same dissociation constant of ADP for acto.S1 in 0.1M KCl and in 0.1M acetate (approx 200uM) and approx 85uM in 0.1M proprionate. White (1977) had estimated a value of 200uM (0.1M KCl, 5mM $MgCl_2$, 10mM tris, pH 8.0, 20^{o}C). An analysis of the different values did not provide a conclusive answer.

Increasing the concentration from 0.1M to 0.3M had the same effect on the dissociation constant of ADP for acto.S1, (K_d) in KCl and acetate (approx 330uM) and in propionate (approx 140uM). The differences observed could not be assigned to any binding step specifically and, therefore, the analysis of these equilibria are believed more complex than this simple approach.

Table 4.2 Equilibrium constants for the formation of a ternary complex between actin, S1 and ADP

The equilibrium constants for K_a were obtained from pressure jump studies. Values for K_b and K_d were determined by fluorescence titration and stopped flow measurements, respectively. K_c was calculated from the relationship;

$$K_a \times K_d = K_c \times K_b.$$

Buffer conditions: for pressure jump as in table 3.2

for fluorescence titration as in table 4.1

for stopped flow as in table 3.3

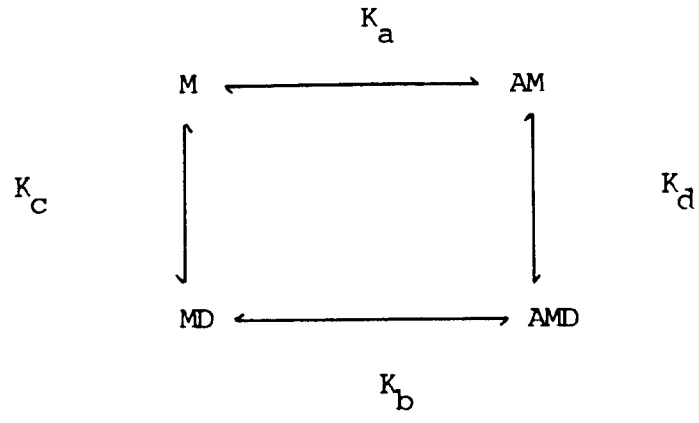

Potassium salt	K_a (M^{-1})	K_b (M^{-1})	K_c (M^{-1})	K_d (M^{-1})
0.1M chloride	11×10^6	4.7×10^5	1.1×10^5	5050
0.1M acetate	9×10^6	7.3×10^5	0.7×10^5	5200
0.1M proprionate	4.9×10^6	12×10^5	0.5×10^5	11700
0.3M chloride	1×10^6	0.47×10^5	0.6×10^5	3030
0.3M acetate	5×10^6	1.6×10^5	0.9×10^5	2930
0.3M proprionate	4.2×10^6	4×10^5	0.7×10^5	7040

DISCUSSION

Generally, the protein structure and stability is the net result of several differing and perhaps competing interactions, such as protein-protein, protein-solvent, protein-electrolyte and electrolyte-solvent interactions. These effects may be divided into two classes; the first may be due to the "direct interaction" of the ions with specific charged groups on the macromolecule, and the second where the ions affect the macromolecule through their modification of the solvent environment of the macromolecule. The two effects outlined may be taken to represent extremes of behaviour, but it should be possible, however, to discuss an observed effect as being a combination with one or other of the types of interaction predominating.

The manner, in which the ions modify the aqueous environment of the macromolecule is markedly dependent upon the structure and constituents of the ions. Von Hippel & Wong (1962) reported the effect of various ions on the formation and stability of a fibrous protein (collagen) to be in the order CH_3COO^- < Cl^- < Br^-. A similar series was described for a globular protein (ribonuclease) in aqueous solution (von Hippel & Schleich, 1969b). Warren et al. (1966) and Stafford (1985) found that these anions in the above order disrupt the organized structure of myosin and the ATPase activity.

To what extent ions specifically affect the structure and, therefore, the activity of enzymes and what kind of structural

modifications are induced, remain unanswered questions to date. The effect of ions are probably mediated, at least partly, through modifications in the structure of water in the vicinity of the proteins (Low, 1985). A clear understanding of these effects unfortunately remains dependent on the still unknown equilibrium structure of that vicinal water and of all thermodynamical changes induced during the interaction of ions-water-proteins.

CHAPTER 5 BINDING STUDIES OF ACTIN TO S1 BY SLOW TEMPERATURE JUMP

INTRODUCTION

Investigations in chapter 3 have shown that the rate of association of actin to S1 has a very high temperature dependence, and the thermodynamic data of the reaction suggested a conformational change in the proteins. These observations have given the incentive to look at the binding of acto.S1 by the temperature jump method.

Temperature jump perturbation technique for studying chemical and biochemical systems is an established method (Eigen & DeMaeyer, 1963). The standard methods use electrical discharge or laser flash to increase the temperature in a few microseconds and subsequent chemical relaxation of the system to the new equilibrium can be followed between 10^{-6} and 10^{-1} sec (Czerlinski et al., 1964; Czerlinski, 1966). However, since the temperature after the jump is held for not longer than few seconds because of convection and thermal conduction, it prevents observations of longer relaxation times. Slower relaxations have been investigated by switching circulating fluids of two thermostated baths. A device described by Pohl (1968) could equilibrate a spectrophotometer cell within a few seconds. More recently, Nakatani (1985) designed a machine, which pushed a solution at an initial temperature (T_1) through a heat exchanger before entering an observation chamber thermostated at a second temperature (T_2).

In this chapter a simple modification of a stopped flow

machine for the use of a temperature jump apparatus is described. This device is capable of temperature jumps larger than 10°C in less than 150msec and suitable of measuring acto.S1 binding reactions. The use of this apparatus to monitor protein-protein interactions other than acto.S1 is envisaged.

MATERIALS AND METHODS

The apparatus

The temperature jump apparatus is basically the stopped flow spectrophotometer SF4 from Hi-Tech Scientific Ltd., Salisbury, with little modification. A schematic representation of the equipment is shown in fig. 5.1.

The sample solution is held in a single syringe at room temperature (T_1). A driving mechanism operated by compressed air pushes the sample via a delay line into the observation cell. The tubing and the cell are immersed in a thermostated tank containing 50% ethylene glycol. Temperature regulation is provided by an internal heater and thermocouple and is maintained to 0.1°C. For low temperature jumps the base unit is filled with liquid nitrogen. The delay line is designed to allow the solution to equilibrate to the new temperature (T_2) by the time it arrives at the cell. Absorbance and fluorescence observations are allowed along a 2mm or 10mm light path in the quartz cell. The solution from the cell is collected in a second syringe. A microswitch is triggered by a front stop, which initiated signal detection. The optical and detection system are discussed in chapter 2.

Figure 5.1 Diagrammatic representation of the slow temperature jump machine

The instrument is composed of the following components: (A) pressure driving ram with syringe. (B) tubing immersed in thermostated tank. (C) quartz observation cell. (D) stopping syringe. Components below the dotted line are thermostated (T_2) and those above are at ambient temperature (T_1).

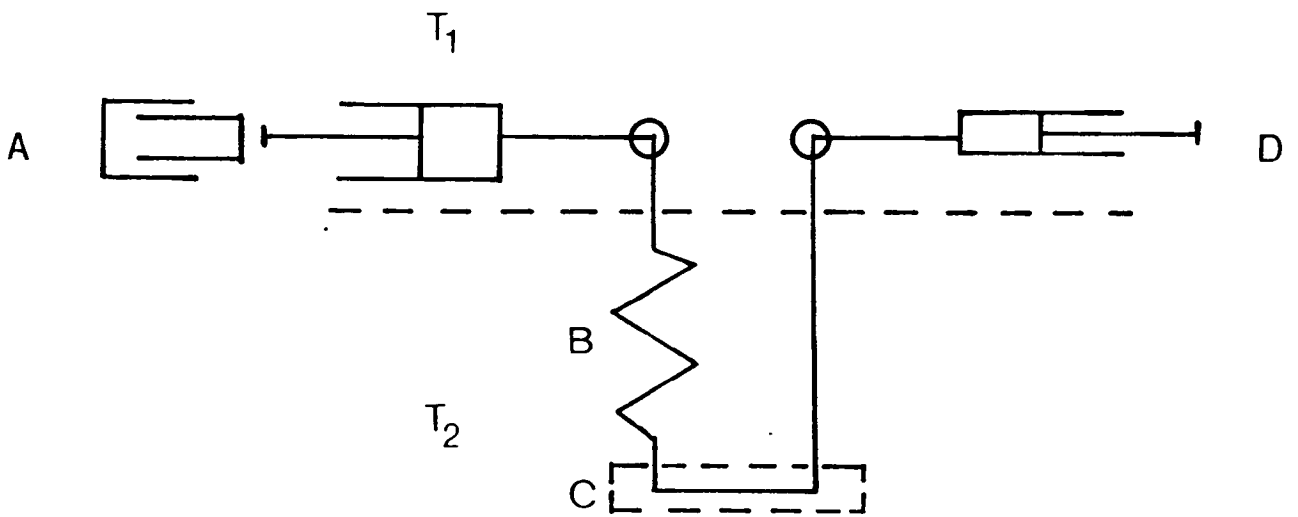
T1
A
D
B
T2
C

Indicator

Reactions involving the uptake or release of protons can be traced by using a pH indicator in weakly buffered or unbuffered solution. The small change in pH of the reaction mixture caused by proton transfer is then followed through the absorbance change of the indicator. This approach has been widely used to calibrate fast temperature systems with proton transfer occurring in the usec range. As a test of this temperature jump apparatus 25uM Phenol red in 0.1M Tris/HCL, pH 8.2 at 570nm is used (Gutfreund, 1972).

RESULTS

Testing the apparatus with Phenol red

Before using the apparatus as a temperature jump machine it was necessary to demonstrate that optical changes detected were comparable with absorbance changes obtained by other methods. This was investigated using 25uM Phenol red in 0.1M Tris/HCl at pH 8.2 as a temperature sensitive indicator in the observation chamber. Absorbance changes over the temperature range $5^{o}C$ - $33^{o}C$ were recorded. A plot of absorbance readings against temperature (^{o}C) with a gradient of -0.011 (absorbance units/^{o}C) for 10mm optical path is shown in fig. 5.2. The same result was obtained in a standard Pye-Unicam SP8-200 UV/VIS spectrophotometer.

Having established that the apparatus is measuring temperature induced optical changes in a chemical system, consideration had to be given to the length, internal diameter

Figure 5.2 Plot of absorbance changes of Phenol red with temperature in the slow temperature apparatus

Temperature dependence of the absorbance of 25uM Phenol red in the observation chamber. Conditions: 0.1M tris/HCl, pH 8.2 at 570nm. Gradient = 0.011 (absorbance units/^{o}C).

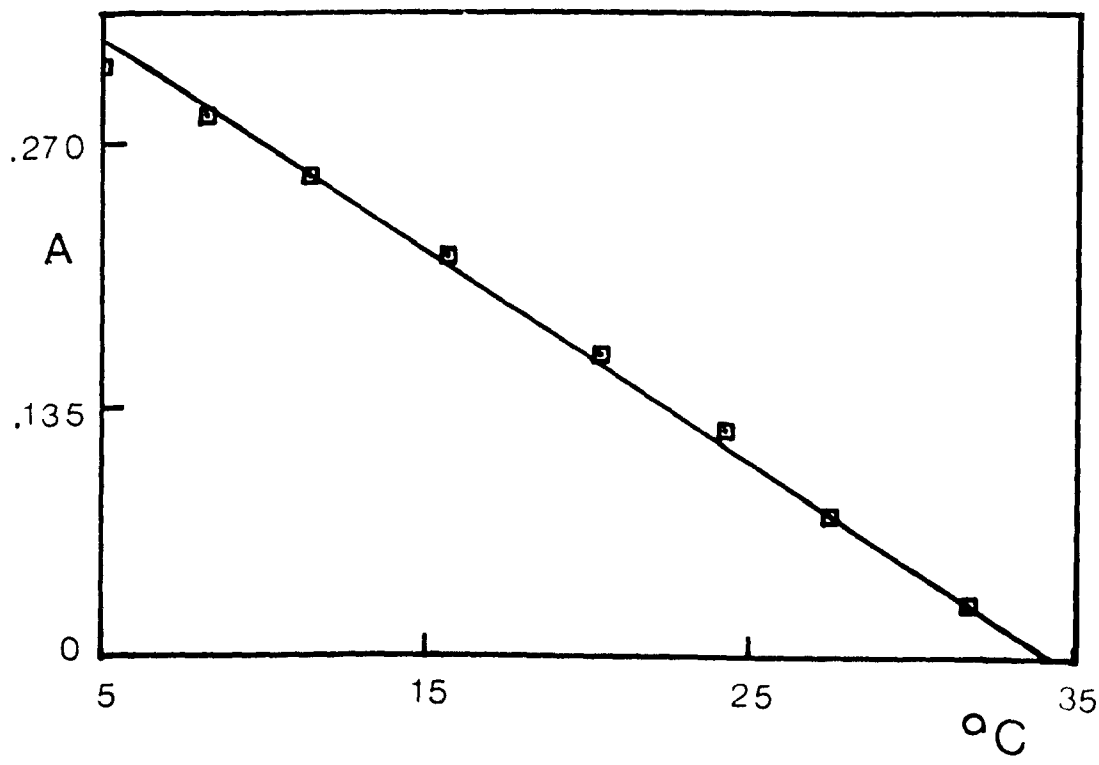
.270
A
.135
0
5
15
25
35
°C

and material of the tube and to the speed, at which the sample travels through the tube to achieve maximum speed of heat exchange with minimum sample volume.

To test heating or cooling of the solution travelling from the sample syringe to the observation chamber, a 15°C difference in temperature was set up between (T_1) and (T_2). If no temperature change occurred during the push, then 0.165 (absorbance units) absorbance change should be observed. Any transient absorbance change will, therefore, show the efficiency of the temperature equilibration. Using a combination of teflon delay tubing (ID = 1.5mm) and stainless steel tubing (ID = 0.73mm) an absorbance change of approx 0.07 (absorbance units) was observed, indicating a 42% temperature equilibration during the push (fig. 5.3a.i). Replacing the teflon tubing with stainless steel tubing an absorbance change of approx < 0.01 (absorbance units) was detected, suggesting that more than 95% temperature equilibration had taken place by the time the solution arrived at the observation cell (fig. 5.3b.i).

To establish the minimum volume required for the solution to arrive from the sample syringe in the observation cell, the following procedure was adopted: the delay tube and observation cell were filled with distilled water and increments of 50ul Phenol red were pushed into the system. A change in absorbance indicated the arrival of the indicator in the cell. A minimum volume of 200ul was needed, but a total of 300ul was routinely used to ensure complete washout of the old solution.

Before undertaking a temperature jump experiment, another

Figure 5.3 Plot of absorbance changes after temperature jump with recorded time of push

Change in absorbance units following a 15°C temperature jump from 20°C to 5°C of 25uM Phenol red in 0.1M tris/HCl, pH 8.2, 570nm. (i) represents an average of 3 relaxations. (ii) recorded voltage output from a linear movement transducer attached to the driving syringe.

(A) Delay tube 10cm of 1.5mm (ID) teflon and 13cm of 0.73mm (ID) stainless steel tubing. Driving pressure 1.5 bar, pushing time 280msec., absorbance change approx 0.07 (absorbance units).

(B) Delay tube teflon replaced with 10cm of 0.18mm (ID) stainless steel tubing. Driving pressure 1.5 bar, pushing time 230msec., absorbance change approx<0.01 (absorbance units).

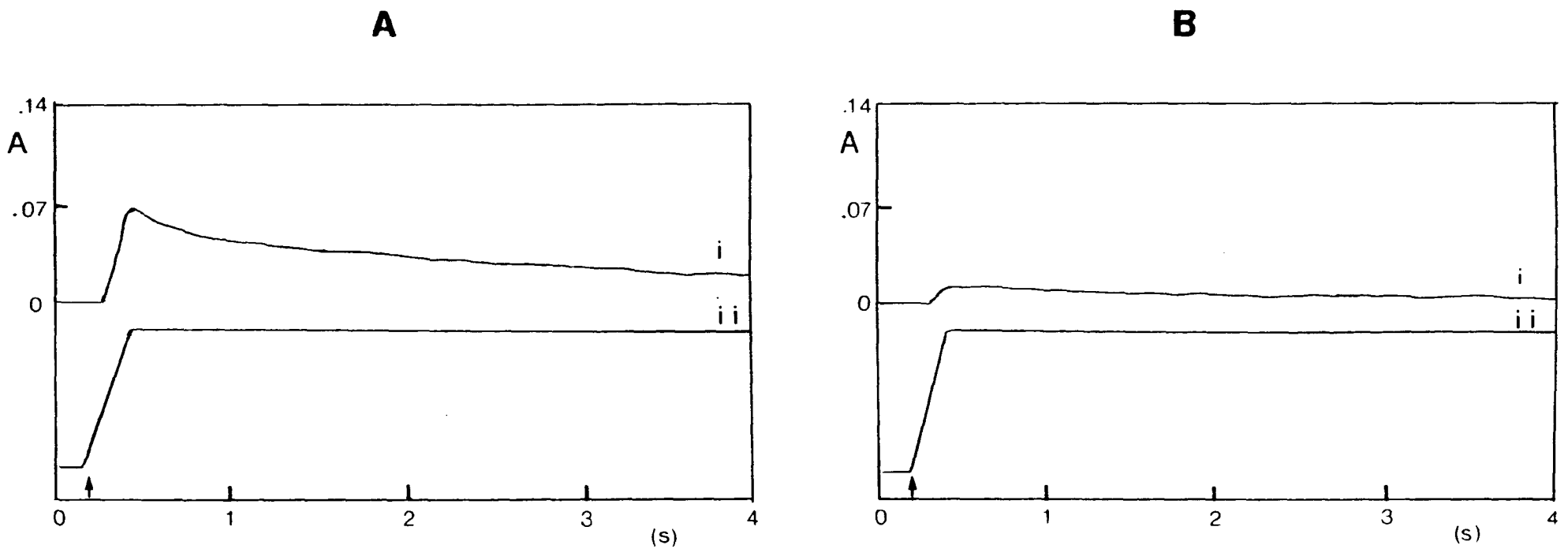
A
.14
A
.07
0
i
i i
0
1
2
3
4
(s)
B
.14
A
.07
0
i
i i
0
1
2
3
4
(s)

piece of information that was necessary, was, how soon the solution arrived from the sample syringe in to the observation cell. To investigate this, a linear potentiometer was attached to the syringe drive arm. The movement of the drive arm was monitored simultaneously with absorbance changes of the solution (fig. 5.3a+bii). The travel time measured by this method was < 150msec at 3 bar. This is an overestimate of the dead time of the system as the connectors between the sample syringe and tubing and tubing and cell hold a large volume.

Slow temperature jump studies of acto.S1

Having shown that the apparatus can be used as a temperature jump machine, it was now possible to carry out studies on an acto.S1 system. The apparatus was loaded with 5uM pyr-actin and 5uM S1 in 0.3M KCl, 20mM cacodylate, 5mM $MgCl_2$ at pH 7. Three pushes of 300ul were carried out so as to fill both the tubing and cell and, therefore, eliminate dilution. The solution was left for 10min to equilibrate to the preset temperature. A volume of 300ul of acto.S1 was then pushed from 20°C to 5°C. The resulting fluorescence change is shown in fig. 5.4a. The solution arrived within 150msec in the cell, and the increase in fluorescence followed the dissociation of acto.S1 as the binding is weakened at lower temperature. The observed reciprocal relaxation time was 0.64 s^{-1} and a plot of $1/\tau$ as a function of ($[\bar{A}] + [\bar{S1}]$) is shown in fig. 5.4b. The equilibrium concentration of free proteins was calculated from the dissociation constant (K_d = 1.66uM), which was obtained, using the same proteins in a separate fluorescence titration experiment as described in

Figure 5.4 Temperature induced relaxation of a solution of pyr-actin and S1

(A) Temperature induced changes in the fluorescence of a 0.3ml solution of 5uM pyr-actin.S1 at 3 bar. The arrow indicates the end of the push of the solution. The trace is an average of 3 traces and the computer-drawn best-fit exponential is superimposed, k_{obs} = 0.64 (s^{-1}).

(B) Plot of the observed rates (s^{-1}) against the concentration of free pyr-actin and S1. The line represents the best-fit line to the data and gives a gradient of 1 x 10^5 $M^{-1}s^{-1}$ and an intercept of 0.208 (s^{-1}).

Conditions: temperature jump from 20°C to 5°C.

buffer: 0.3M KCl, 20mM cacodylate, 5mM $MgCl_2$, pH 7.

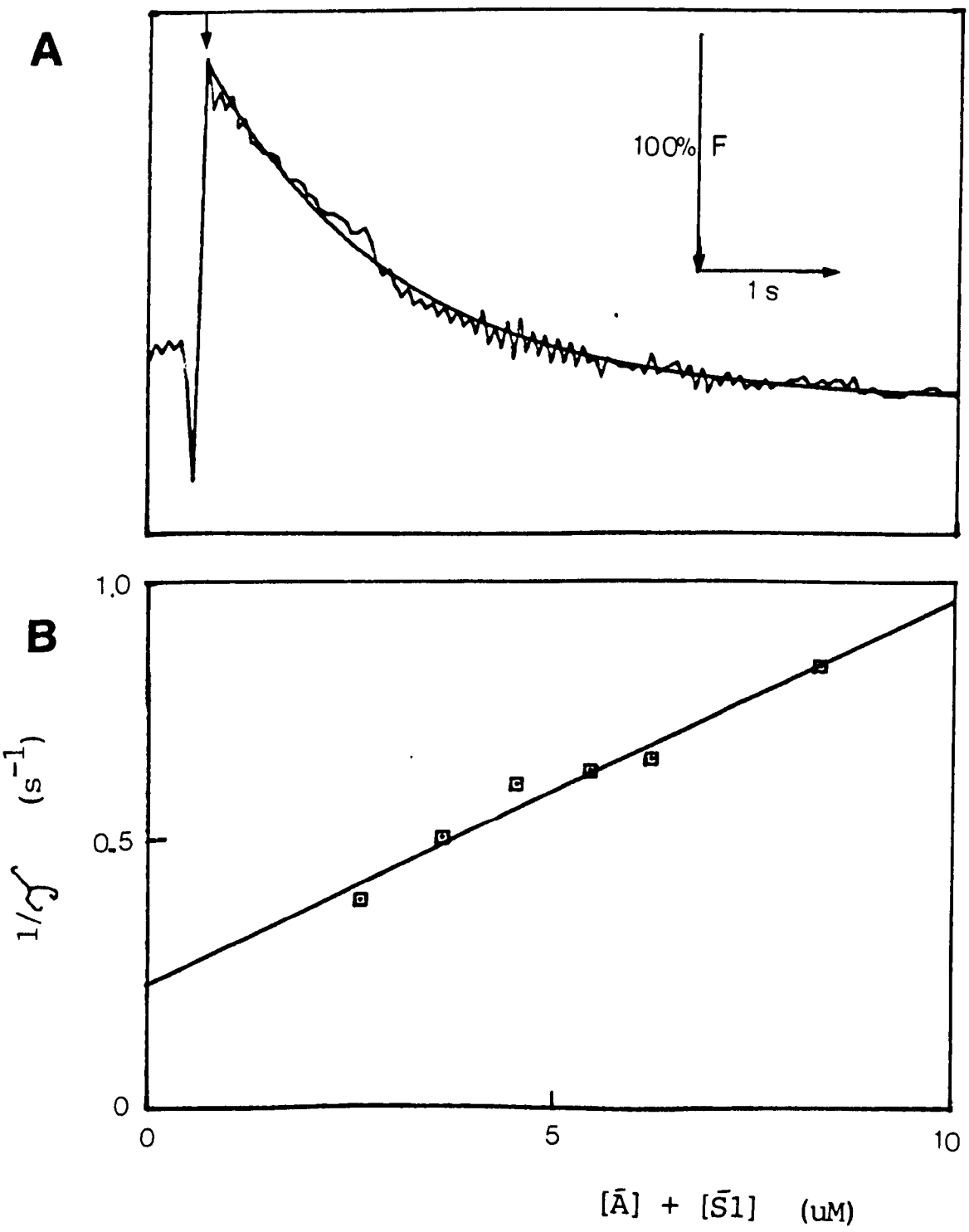
A
100% F
1 s
B
1.0
0.5
0
0
5
10
1/τ (s⁻¹)
[Ā] + [S̄1] (uM)

chapter 3. The data in fig. 5.4b are shown with the best fit straight line superimposed and with a gradient of 1 x 10^5 $M^{-1}s^{-1}$ and an intercept of 0.208 s^{-1}. This data is consistent with the three-step model shown in chapter 3, where step 0 and step 2 are rapid equilibrium steps compared with step 1. The observed rate (k_{obs}) is given by;

$$k_{obs} = \frac{K_o k_{+1} [S1]}{K_o \times [S1] + 1} + \frac{k_{-1}}{1 + K_2}$$

This is linear when K_o x [S1] << 1 and so a plot of [S1] against (k_{obs}) will give a gradient to $K_o k_{+1}$ and an intercept equal to the dissociation rate $k_{-1}/(1 + K_2)$.

The ratio of $k_{-1}/(1 + K_2)$ and $K_o k_{+1}$ = 2.08uM, which is in good agreement with the independently measured K_d of 1.66uM. $K_o k_{+1}$ and $k_{-1}/(1 + K_2)$ were measured in a separate stopped flow experiment under the same experimental conditions and gave 1.2 x 10^5 $M^{-1}s^{-1}$, respectively; again in good agreement with the values obtained here.

DISCUSSION

Temperature jump studies performed in this work have shown that this method can be used to measure acto.S1 binding reactions. The results of acto.S1 binding measured by this method and and pressure jump technique (chapter 3) are in good agreement. As acto.S1 binding is believed to be preceded by a diffusion controlled reaction (Coates et al., 1985), and diffusion controlled reactions show relatively small temperature

dependence (Gutfreund, 1972) the temperature dependence of this reaction must, therefore, be on step 1. This and the sharp breakpoint in the Arrhenius plot (Fig.3.6a) support the idea of a conformational change in step 1.

Finally, the easy conversion and wide availibility of stopped flow equipment in biochemical laboratories can make this apparatus a useful tool measuring kinetics of reversible reactions. The kind of temperature change used in above experiments and the small amounts of material needed, is also appropriate for many other solutions. However, the apparatus is not fully optimised and reductions in both the sample volume and the time resolution may be possible. Using the current equipment relatively large volumes exist in the connectors between the sample syringe and the stainless steel tubing and between the tubing and the observation cell. Customised connectors could eliminate these volumes. Small bore stainless steel tubing is used for the heat exchanger as this material is reasonably inert and readily available for use with high performance liquid chromatography systems. Yet, stainless steel is not the first choice of material for a heat exchanger and a better material may be available depending on the sensitivity of the sample to metals. The addition of independent thermostating of the sample syringe will allow a wider range of temperature jumps to be studied.

Further, advantages of the apparatus are that large temperature jumps (> $10^{o}C$) can be made to both higher and lower temperatures. There is no limit on the repeat rate for the

temperature jumps as a fresh sample can be examined as soon as observation of the preceeding sample is complete. There is no delay while the sample chamber re-equilibrates to the initial temperature as in conventional temperature jump equipment. This allows rapid repeated data collection under conditions where signal averaging is necessary because of low signal to noise ratio. The repeat rate is also an advantage when labile systems are being studies.

CHAPTER 6 THE EFFECT OF HYDROSTATIC PRESSURE ON THE BINDING OF Ca^{2+} TO TROPONIN C

INTRODUCTION

Studies on purified actin and myosin subfragment (S1) presented in chapter 3 have shown that the isomerization step of the acto.S1 complex is pressure-sensitive. This isomerization represents a change from the weakly "attached" to the "rigor-like" complex and has been proposed to be closely related to the force-generating event of the cross-bridge cycle. It has, therefore, been of interest to determine if the pressure-sensitive isomerization identified in solution is also responsible for a pressure-induced change in tension in muscle fibre. Fortune et al. (1989) have investigated the effect of changes in hydrostatic pressure on maximally calcium-activated tension in glycerinated rabbit psoas fibres. These workers reported that steady active tension was depressed by 8% for a 100atm pressure rise. Studies by Brown (1934a;b), and more recently by Geeves & Ranatunga (1990) have shown that tetanic tension in intact muscle fibres is also depressed by 5-8% at high pressure. These findings are consistent with the idea that increased pressure is perturbing force generation in the cross-bridge.

The findings of Fortune et al. (1989) relate a specific pressure sensitive protein isomerization identified in solution to a pressure sensitive transition between two attached states of the active cross-bridge.

In the intact muscle, i.e. no membranes are removed and the

sarcoplasmic reticulum is present, activation is achieved via electrical stimulation. Release of neuro-transmitter depolarises the muscle membrane and a rise in $[Ca^{2+}]$ occurs in the cytoplasm of around 0.1 to 10uM. Relaxation is achieved by accumulation of calcium to the sarcoplasmic reticulum. These isolated twitches are applied via its nerve or directly by a small shock. A single shock causes a twitch contraction. Repeated shocks cause multiple twitches and above a characteristic stimulation frequency these fuse to give a tetanic contraction, which remains steady until stimuli are withheld or fatique sets in.

The work in the single fibre system has been carried out at 30uM free$[Ca^{2+}]$, i.e. enough to be equivalent to a fused tetanus. The effect of pressure on both twitch and tetanic tension has recently been investigated by Geeves & Ranatunga (1990). In the case of a fused tetanus, i.e. equivalent to maximally calcium activated tension in skinned fibre, a depression of tension was reported. However, in the case of twitch tension an increase in observed tension was seen (30-80%). The latter suggests that the muscle is "switched on" to a greater extent per stimulus at high pressure by either more calcium release per stimulus, by a change in calcium affinity or by a change in the inhibitory function of the regulatory proteins. In the case of tetanic tension the muscle is "switched on" fully, therefore, any further calcium release at high pressure causes no change in tension. Therefore, the basis of depression seen in tetanic muscle and skinned muscle at high calcium may have a common mechanism, i.e. a specific effect of pressure on K_2, i.e. transition of AMN to A-MN

in the model of Geeves et al. (1984) (fig. 1.6). The binding of calcium to the thin filament will be investigated in this chapter.

Pressure jump technique is used to evaluate the effect of increased pressure on the calcium affinity to the regulatory proteins in solution. This defines the limits of changes in calcium affinity to the thin filaments in intact muscle fibres and determines whether these changes are sufficient to account for the observed pressure effect on twitch tension.

Troponin C is of particular interest as it plays an important part in the thin filament regulation of muscle contraction (Potter, 1982). Since this protein was first isolated many different techniques (including equilibrium dialysis, ultracentrifugation, sedimentation) have been used to measure its Ca^{2+} binding properties (Fuchs & Briggs, 1968; Hartshorne & Pyun, 1971; Greaser & Gergely, 1973). The majority of studies to date agree on a binding constant for the low-affinity, regulatory sites of approx $3x10^5$ M^{-1} for calcium (20^oC, 0.1M KCl, pH 7) (Potter & Johnson 1982; Zot & Potter, 1987a).

In order to measure changes in calcium concentration at high pressure two optical signals are used. The chromophoric dye, arsenazo III, which is water soluble and capable of measuring a wide range of $[Ca^{2+}]$ (Baylor et al., 1986) and the fluorogenic dye, dansylaziridine, covalently attached at Met 25 of TnC, which does not alter the calcium binding of TnC (Johnson et al., 1978).

The rate of association of calcium to the regulatory sites of TnC is also investigated in this chapter. So far only stopped

flow transient kinetic techniques have been employed to determine exchange rates of Ca^{2+} to the regulatory sites of TnC. Johnson et al. (1979) and Ilo & Kondo (1981) used the fluorescent label dansylaziridine (DANZ) attached to TnC as indicator and Rosenfeld & Taylor (1985a) employed the fluorescent label 4-(N-iodoacetoxyethyl-N-methyl)-7-nitrobenz-2-oxa-1,3-diazole (IANBD) attached to TnI. These investigations showed that Ca^{2+}-binding produces a large fluorescence change within the instrumental dead time. This suggested that Ca^{2+}-binding by TnC occurs very rapidly, which is consistent with the idea that Ca^{2+}-binding to each class of sites on TnC is a diffusion-controlled reaction (Potter & Johnson, 1982). The rate of dissociation of calcium from the Ca^{2+}-specific site of TnC, using stopped flow, was measured at a rate of 230-346 s^{-1} (Johnson et al., 1979; Iio & Kondo, 1981) and from the ratio "off-rate"/"on-rate" the equilibrium binding constant was calculated. This is in agreement with the independently recorded value of approx $3x10^5$ M^{-1} (Potter & Johnson, 1982).

Since the association of calcium to the regulatory proteins is believed to be at the diffusion limited rate (approx 10^8 M^{-1} s^{-1}) (Eigen, 1963), it requires fast reaction kinetics. Pressure jump and temperature jump techniques are used here in an attempt to measure the rate of calcium binding to TnC.

RESULTS

The binding of calcium to arsenazo III

Prior to the determination of changes in the affinity of TnC

to calcium at high pressure, it was necessary to define the binding constant of arsenazo III for calcium under experimental conditions at atmospheric pressure. In establishing this, it would allow the detection of calcium changes with high accuracy and the calculation of changes in affinity of arsenazo III at high pressure precisely. Changes in affinity of TnC for calcium can then be corrected for changes in affinity of arsenazo III at high pressure. In this study the following conditions are used: 0.1M KCl, 1mM $MgCl_2$, 20mM imidazole or 20mM phosphate, pH 7, $20^{o}C$.

The titration described in fig. 6.1a was perfomed at 10uM arsenazo III with increasing free$[Ca^{2+}]$ and changes in absorbance were measured at 655nm. The free$[Ca^{2+}]$ was determined, using Ca/EGTA buffers (chapter 2). The absorptions spectra to fig. 6.1a is given in the inset. The absorbance change recorded at atmospheric pressure of the solution containing 10uM arsenazo III on adding 10uM free$[Ca^{2+}]$ was 0.1 (absorbance units). From the relation of the Lambert-Beers-Law an absorption coefficient at 655nm of 10^4 litre x mol^{-1} x cm^{-1} was determined, which was in agreement with the value reported by Hole (1980).

The secondary plot of free$[Ca^{2+}]/\Delta A_{655nm}$ against free$[Ca^{2+}]$ with the intercept on the ordinate axis indicates a K_d of approx 10uM for arsenazo III to calcium (fig. 6.1b). This value agrees with measurements by Hole (1980), and arsenazo III at 10uM concentration is used in the subsequent studies.

Figure 6.1 Determination of the binding constant of arsenazo III for calcium

(A) The graph of absorbance change at 655nm vs. free[Ca^{2+}]. In the inset the absorption spectra is given and the arrow indicates absorbance at 655nm. The titration was performed in 0.1M KCl, 20mM imidazole, 2.5mM EGTA, 1mM $MgCl_2$, pH 7, 20°C.

(B) The graph of free[Ca^{2+}] / ΔA_{655nm} vs. free[Ca^{2+}]. A secondary plot of the data in (A); K_d approx 10uM. The binding constant (K_d) was determined by the equation;

$$[\text{calcium}]_t = \frac{[\text{calcium}]_t \; [\text{ars.III}]_t}{\Delta A / \varepsilon} - K_d$$

$[\text{calcium}]_t$ = total calcium concentration

$[\text{ars.III}]_t$ = total arsenazo III concentration

A = absorbance; ε = extinction coeff. for arsenazo III

K_d = binding constant

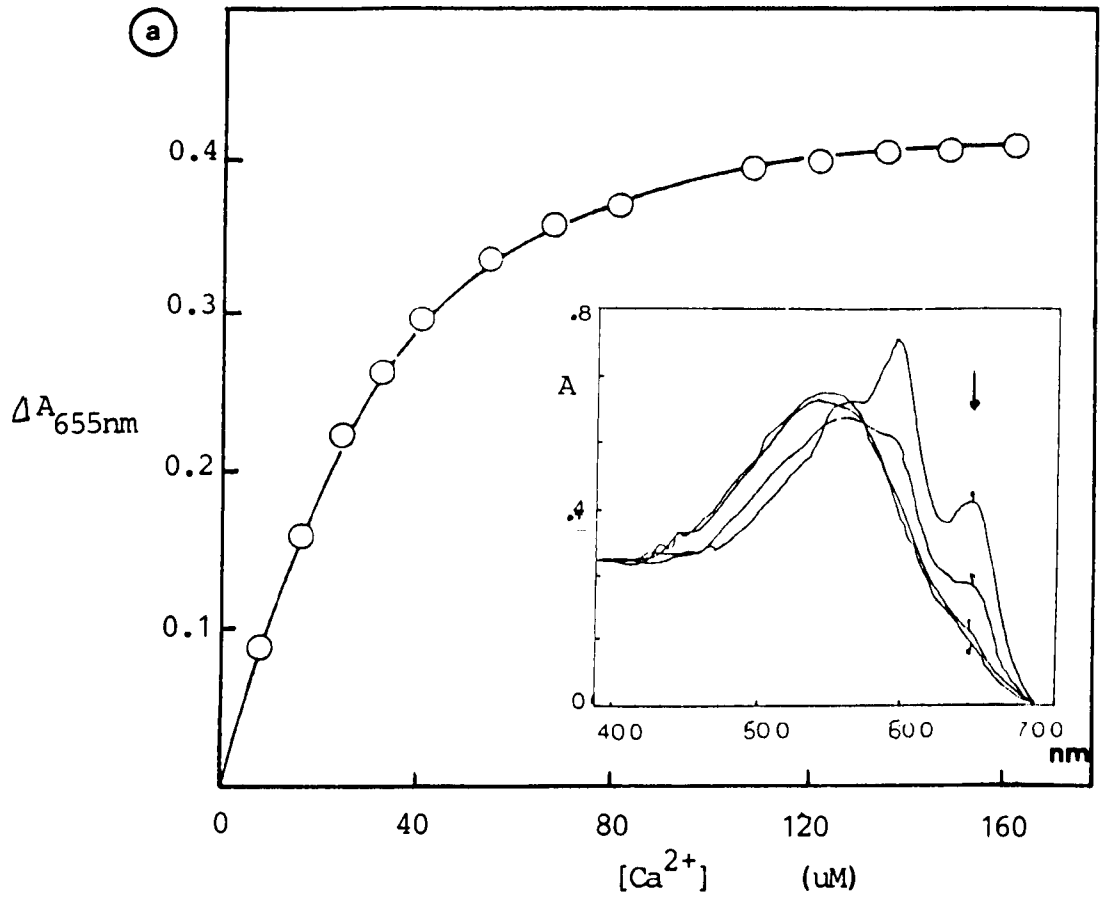
a
0.4
0.3
0.2
0.1
ΔA655nm
.8
A
.4
0
400
500
600
700
nm
0
40
80
120
160
[Ca2+] (uM)

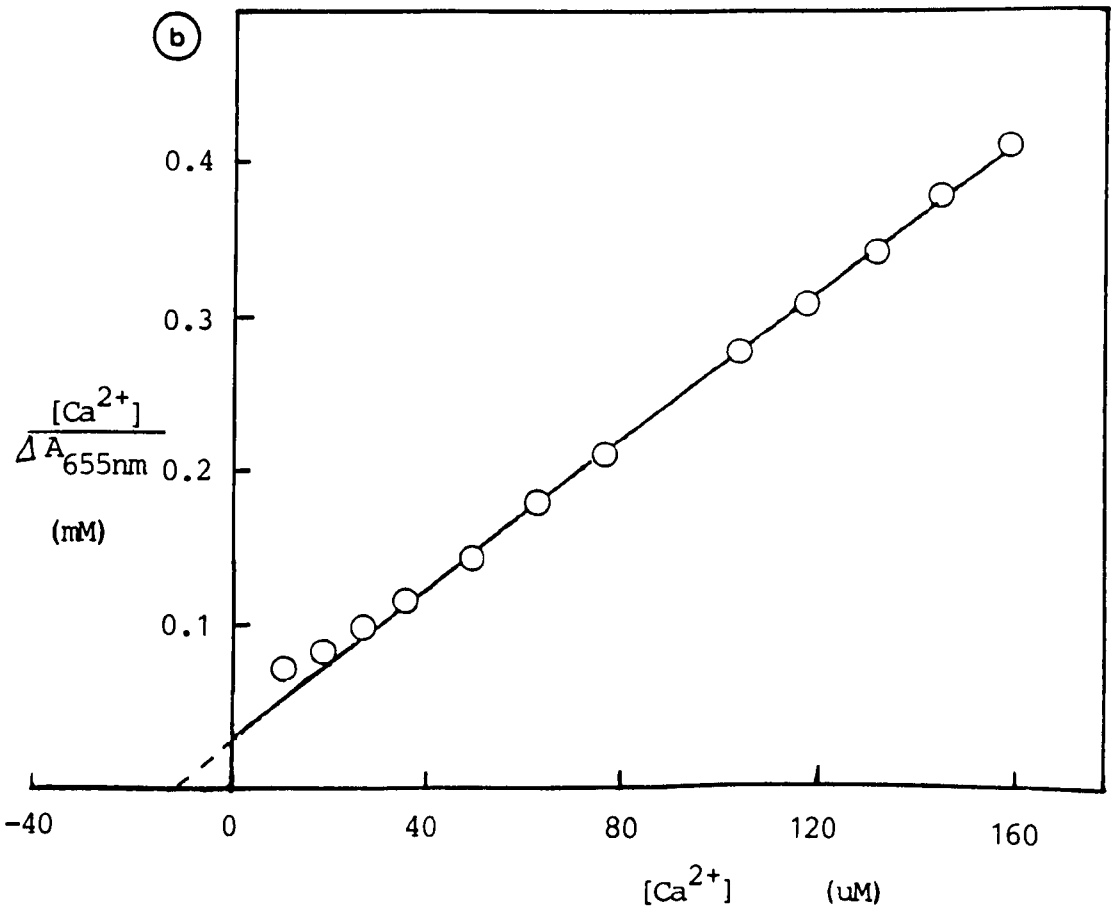
b
0.4
0.3
0.2
0.1
[Ca2+]
ΔA655nm
(mM)
-40
0
40
80
120
160
[Ca2+] (uM)

Effect of 100atm hydrostatic pressure on Ca^{2+}-binding to arsenazo III

Prior to the determination of the effect of high pressure on the affinity of arsenazo III to calcium, the influence of buffer components on transmission changes at 655nm was investigated. Since transmission changes are used to determine free[Ca^{2+}] changes and hence changes in affinity of arsenazo III for calcium, these calculations have to be corrected for transmission changes caused by buffers. A list of different solutions exposed to 100atm pressure with the detected transmission changes at 655nm are shown in table 6.1. An average change in transmission of approx 0.1 (%T) was observed for all solutions. This shows that the effect of pressure on buffer containing 10uM arsenazo III or [EGTA] up to 2.5mM is no different to dist. water or buffer only and, therefore, indicates that pressure has no effect on the optical properties of arsenazo III. Subsequent analysis of calcium binding to arsenazo III has been corrected for this general pressure effect.

In the studies reported here two methods for determining free [Ca^{2+}] have been used when employing arsenazo III. Free[Ca^{2+}] was calculated for buffer solutions in the presence of 2.5mM EGTA, using a computer programme (chapter 2). The absorbance readings for various free[Ca^{2+}] were recorded and were the basis for the calculation of changes in free calcium at high pressure. Free[Ca^{2+}] in the absence of EGTA was determined by direct addition of calcium to the solution by achieving the same OD-change as obtained in the presence of EGTA. Both methods gave the same absorbance and, therefore, the free[Ca^{2+}] agreed to within 1%.

Table 6.1 The effect of 100atm hydrostatic pressure on Ca^{2+}-binding to arsenazo III

Optical density of different buffer solutions containing 10uM arsenazo III at high and low free$[Ca^{2+}]$ was measured at atmospheric pressure. These solution were then exposed to 100atm hydrostatic pressure. Changes in transmission were recorded at 655nm and shifts in free$[Ca^{2+}]$ were calculated, using the relationship;

$$A = \varepsilon \times c \times d \quad \text{(Lambert-Beer-law)}$$

$$A = \log I_o/I$$

$$A = -\log T$$

Buffer: 0.1M KCl, 1mM $MgCl_2$, pH 7, 20°C.

TABLE 6.1

Buffer: +10uM arsenazo III +20mM imidazole no EGTA	ΔT(%) at 655nm	Δfree[Ca^{2+}] (uM)
1uM free[Ca^{2+}]	0	0
10uM free[Ca^{2+}]	0.1(+/-0.02;5)	0.020(+/-0.003;5)
+2.5mM Ca/EGTA		
1uM free[Ca^{2+}]	0	0
10uM free[Ca^{2+}]	0	0
dist. water	0.1(+/-0.02;7)	
buffers only	0.12(+/-0.02;7)	
buffer +(1uM-2.5mM EGTA)	0.1(+/-0.02;2)	
buffer + 10uM arsenazo III	0.1(+/-0.01;6)	
+10uM arsenazo III +20mM phosphate no EGTA		
1uM free[Ca^{2+}]	0.2(+/-0.03;5)	0.025(+/-0.002;5)
10uM free[Ca^{2+}]	0.3(+/-0.02;5)	0.060(+/-0.01;5)
+2.5mM Ca/EGTA		
1uM free[Ca^{2+}]	0	0
10uM free[Ca^{2+}]	0.15(+/-0.02;2)	0.032(+/-0.005;2)

(Standard deviation and number of experiments in brackets.)

Solutions at 1uM and 10uM free[Ca^{2+}] defined as described above were exposed to a 100atm rise in pressure. No change in optical signal was observed at 655nm at 1uM free[Ca^{2+}] in the absence of EGTA and at 10uM free[Ca^{2+}] a transmission change of 0.1 (%T) was recorded in the absence of EGTA (table 6.1).

The change in optical signal allows the change in free[Ca^{2+}] at high pressure to be calculated. Using the equations;

$$A = c \times \varepsilon \times d$$

$$A = -\log I/I_o$$

(c= concentration; ε = absorption coeffient; d= path length; I= intensity of light after the probe; I_o = intensity of light before the probe) a difference in free[Ca^{2+}] of 0.02uM was obtained at high pressure. Since the transmission change has been corrected for the effect of pressure on buffer components, the recorded change at 100atm pressure rise must be due to a change in affinity of arsenazo III to calcium. Using the relationship;

$$K_{ars.III} = \frac{[Ca^{2+}.ars.III]}{[Ca^{2+}]\ [ars.III]}$$

allows the equilibrium constant to be calculated at 10MPa pressure. At atmospheric pressure the equilibrium constant for arsenazo III was determined to be 10^5 M^{-1} and since the free[Ca^{2+}] used in this study was 10uM, the ratio of [Ca^{2+}.arsIII] and free[ars.III] equals 1. At an initial

concentration of 10uM arsenazo III, then 5uM arsenazo III is in the bound form and 5uM arsenazo III in the free form. At high pressure an additional 0.02uM free[Ca^{2+}] is bound and from the above relation the equilibrium constant can be calculated ($K_{ars.III}$ at 100atm = 1.01×10^5 M^{-1}). This indicates an approx 1% change in equilibrium constant at high pressure compared to atmospheric pressure. The associated volume change calculated from the change in equilibrium constant, using the relationship $\Delta K/K = -\Delta P \times \Delta V^{\circ} / RxT$ was approx $-2.4cm^3$/mol. This is a small volume change and is of the magnitude of hydrogen bond transfer from an intrinsic to a water bonded state (Davis & Gutfreund, 1976).

Using EGTA to control the free[Ca^{2+}] level in imidazole buffer showed at high pressure for 1uM and 10uM free[Ca^{2+}] no change in optical signal (table 6.1) and employing phosphate buffer at 1uM free[Ca^{2+}] also no change was observed. However, at 10uM free[Ca^{2+}] a change of 0.15 (%T) was measured. Calculating the change in free[Ca^{2+}] of this concentration at high pressure in the presence and absence of 2.5mM EGTA showed a difference in free[Ca^{2+}] of 0.032uM and 0.060uM, respectively. This allowed the equilibrium constant of EGTA for calcium to be estimated at high pressure. Since EGTA does not absorb light at 655nm any additional change in transmission with EGTA present must be due to changes in calcium binding to EGTA. These differences in free[Ca^{2+}] can, therefore, be subtracted directly and can be used to estimate the change in equilibrium constant at high pressure by the relationship;

$$K_{EGTA} = \frac{[Ca.EGTA]}{[EGTA]\ [Ca^{2+}]}$$

(K_{EGTA} = 2.5×10^7 M^{-1} at atmospheric pressure; deducted difference in free$[Ca^{2+}]$ at 100atm pressure = 0.028uM; total free$[Ca^{2+}]$ = 10uM; [EGTA] = 2.5mM). The change in equilibrium constant for EGTA at high pressure is estimated at approx 0.3% and the volume change calculated from the change in equilibrium constant is < $-1cm^3$/mol. This result shows that Ca/EGTA buffers can be used to control free$[Ca^{2+}]$ levels at high pressure. These were employed in the following experiments.

The effect of 100atm hydrostatic pressure on Ca^{2+}-binding to arsenazo III in the presence of TnC

In the above experiments it has been shown that 100atm hydrostatic pressure changes the equilibrium constant of arsenazo III for calcium by 1%. Since TnC is not absorbing light at 655nm, any additional changes in transmission with TnC present must, therefore, be due to changes in calcium binding to TnC. Transmission changes from these experiments are listed in table 6.2. Data from parallel experiments with and without TnC over a free$[Ca^{2+}]$ range between 1uM and 50uM showed a higher transmission change in the presence of TnC between 0.07-0.1 (%T) at 100atm. Changes in free$[Ca^{2+}]$ were calculated and used to determine the shift in equilibrium constant for TnC at 100atm hydrostatic pressure. Calculations were carried out as described previously. Results showed an approx 1% change in K_{TnC}, using

Table 6.2 The effect of 100atm hydrostatic pressure on Ca^{2+} -binding to arsenazo III in the presence of TnC

Optical density of solutions in different buffer containing 10uM arsenazo III over a free$[Ca^{2+}]$ range of 1uM to 50uM in the presence and absence of TnC were measured at atmospheric pressure. The same solutions were then perturbed by 100atm pressure and the transmission change was recorded at 655nm. The difference in $[Ca^{2+}]$ in the presence and absence of TnC was calculated, using the relationship in table 6.1.

Buffer: 0.1M KCl, 1mM $MgCl_2$, 20mM imidazole, 2.5mM EGTA, pH 7, $20^{o}C$.

TABLE 6.2

	10uM arsenazo III (-Δ T%)	10uM arsenazo III +3uM TnC (-Δ T%)	Diff. (-Δ T%)
1uM free[Ca^{2+}]	0.0	0.1(+/-0.01;3)	0.1
5uM free[Ca^{2+}]	0.05(+/-0.01;3)	0.12(+/-0.01;3)	0.07
10uM free[Ca^{2+}]	0.1(+/-0.01;3)	0.2(+/-0.02;3)	0.1
50uM free[Ca^{2+}]	0.15(+/-0.02;3)	0.25(+/-0.02;3)	0.1

	10uM arsenazo III Δ[Ca^{2+}] (uM)	10uM arsenazo III +3uM TnC Δ[Ca^{2+}] (uM)	Diff. Δ[Ca^{2+}] (uM)
1uM free[Ca^{2+}]	0.0	0.01(+/-0.001)	0.01
5uM free[Ca^{2+}]	0.01(+/-0.001;3)	0.03(+/-0.005;3)	0.02
10uM free[Ca^{2+}]	0.02(+/-0.003;3)	0.04(+/-0.009;3)	0.02
50uM free[Ca^{2+}]	0.24(+/-0.02;3)	0.38(+/-0.04;3)	0.14

(Standard deviation and number of experiments in brackets)

imidazole buffer at high pressure; again this change is small. The volume change calculated as above from the change in equilibrium constant was small (approx $-2.4cm^3/mol$). The implication of this result for calcium binding to the regulatory proteins in muscle fibre will be discussed briefly.

The binding of calcium to TnC_{DANZ}

In the above experiments the change in amplitude due to TnC binding calcium at various free calcium concentrations upon 100atm pressure perturbation was estimated at 0.07-0.1%. This is small, and in order to define this change accurately a more sensitive method was used. Employing the fluorescent dye, dansylaziridine, covalently attached to TnC could allow for more precise measurements. However, prior to the determination of this change at high pressure, it was necessary to ascertain the binding constant of TnC_{DANZ} for calcium at atmospheric pressure. This would then permit changes at high pressure to be monitored precisely.

Troponin C was prepared and labelled with dansylaziridine as described in chapter 2. The equilibrium binding constant of TnC_{DANZ} for calcium was determined by calcium fluorescence titration. Light was excited and emitted at 340nm and 510nm, respectively. Upon Ca^{2+}-binding to the Ca^{2+}-specific regulatory sites of TnC_{DANZ}, the fluorescence of TnC_{DANZ} increased by a factor of 1.7. This is in agreement with previous results published by Johnson et al. (1978). Changes in fluorescence of TnC_{DANZ} as a function of free$[Ca^{2+}]$ are shown in fig. 6.2. The midpoint of the fluorescence change occured at pCa of approx

Figure 6.2 The Ca^{2+}-dependence of TnC_{DANZ} fluorescence

Titration was performed into 3mls of buffer containing 10uM TnC_{DANZ} and 90mM KCl, 20mM cacodylate, 1mM $MgCl_2$, 2.5mM EGTA, pH 7, 20°C. Increase in TnC_{DANZ} fluorescence is shown as a function of free$[Ca^{2+}]$. The trace is fitted by eye. Total fluorescence enhancement is approx 1.7 fold; midpoint of fluoresence increase at pCa approx 5.6, which equals a K_d of TnC for calcium of 2.5uM. The inset shows the fluorescence spectra of TnC_{DANZ} with
(a) $< 10^{-7}$ M^{-1}, (b) 10^{-6} M^{-1}, (c) 10^{-5} M^{-1},
(d) 10^{-3} M^{-1} free$[Ca^{2+}]$.

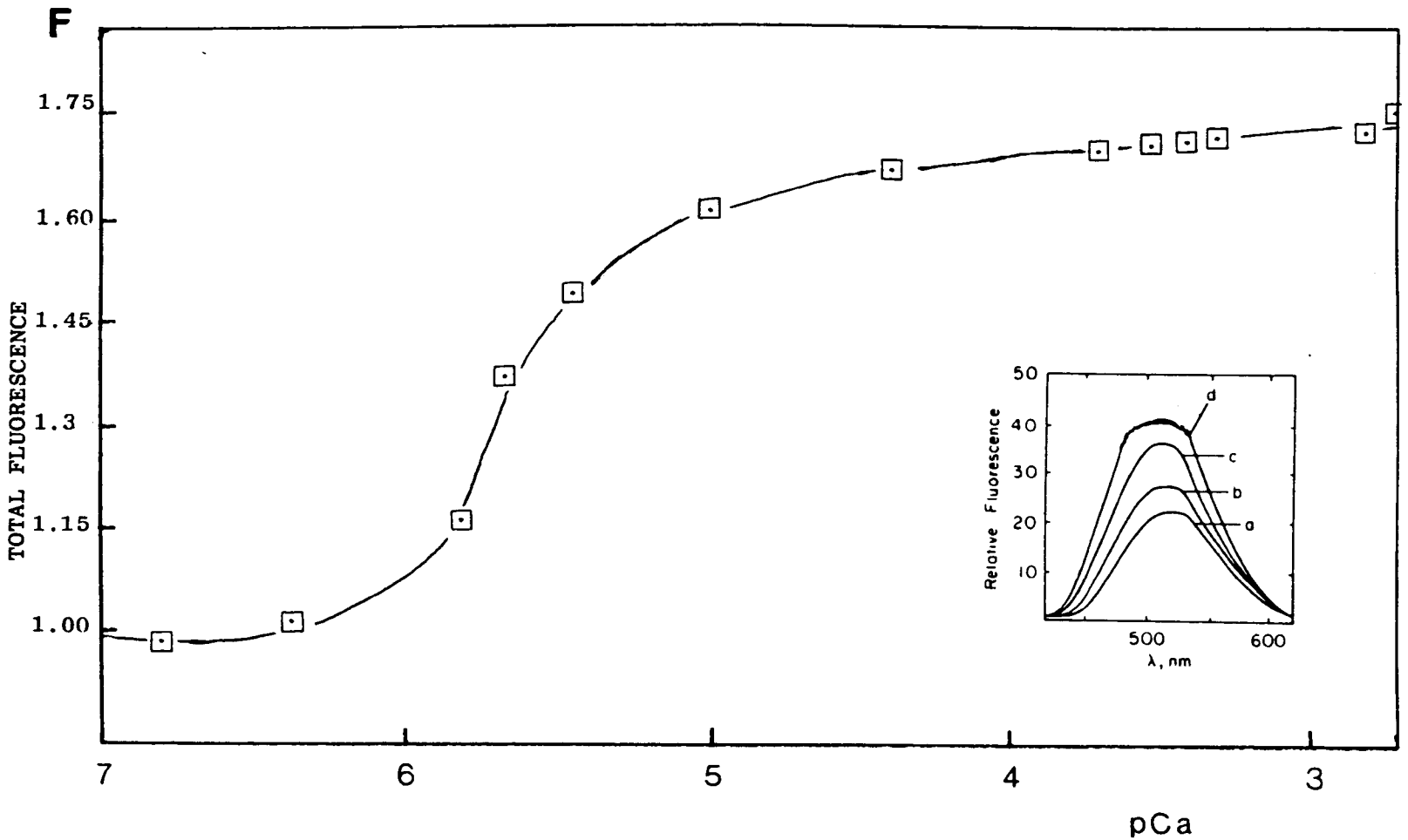
F
1.75
1.60
1.45
1.3
1.15
1.00
TOTAL FLUORESCENCE
7
6
5
4
3
pCa
50
40
30
20
10
Relative Fluorescence
d
c
b
a
500
600
λ, nm

5.6. This indicated a K_{TnC} of approx $4x10^5$ M^{-1} and agrees with the results by Potter & Johnson (1982). The fluorescence spectra of TnC_{DANZ} at several different calcium concentrations is demonstrated in the inset to fig. 6.2. In the following experiments TnC_{DANZ} was used at 3uM concentration.

The effect of 100atm hydrostatic pressure on the Ca^{2+}-binding to TnC_{DANZ}

Results from pressure perturbation experiments of solutions containing TnC_{DANZ} at various free$[Ca^{2+}]$ in imidazole buffer are shown in table 6.3. The measured changes in fluorescence are small (< 1%). The calculated free$[Ca^{2+}]$ changes are similar to the previously observed changes, using arsenazo III (table 6.2). This confirms above results that high pressure has only a small effect on the equilibrium constant.

In order to achieve a larger fluorescence change and subsequent free$[Ca^{2+}]$ change at high pressure, imidazole buffer was replaced with phosphate. Imidazole (pK 7) shows a negligible volume change upon ionisation and is pH-stable upon pressure perturbation; phosphate (pK 7.2) is pressure-sensitive. Results in table 6.3 show an approx 2 fold increase in amplitude when using phosphate buffer. This effect can be assigned to the dissociation of the weak acid (K_2HPO_4/KH_2PO_4) in water, which is reflected in a shift in pK and pH, respectively (Gutfreund, 1972). The calculated changes in equilibrium constant at 100atm pressure by these methods is approx 3% when compared to atmospheric pressure and is negligible.

Table 6.3 The effect of 100atm pressure on the binding of calcium to TnC_{DANZ}

Solutions containing 3uM TnC_{DANZ} in different buffer were perturbed by 100atm pressure. Changes in fluorescence from atmospheric pressure were monitored and free $[Ca^{2+}]$ calculated. Excitation: 340nm; emission: 510nm.

Conditions: 3uM TnC_{DANZ}, 90mM KCl, 1mM $MgCl_2$, 2.5mM EGTA, pH 7, $20^{o}C$.

TABLE 6.3

CONDITIONS:	Δ(%) Fluorescence 20mM imidazole	Δ(%) Fluorescence 20mM phosphate
1uM free[Ca^{2+}]	n.m.	n.m.
5uM free[Ca^{2+}]	< 1.0	2.0(+/-0.2;2)
10uM free[Ca^{2+}]	< 1.0	2.3(+/-0.2;2)
50uM free[Ca^{2+}]	< 1.0	2.2(+/-0.2;2)
	Δ free[Ca^{2+}] (uM) 20mM imidazole	Δ free[Ca^{2+}] (uM) 20mM phosphate
1uM free[Ca^{2+}]	0	0
5uM free[Ca^{2+}]	0.02	0.04(+/-0.005;2)
10uM free[Ca^{2+}]	0.04	0.09(+/-0.01;2)
50uM free[Ca^{2+}]	0.20	0.44(+/-0.05;2)

n.m. = not measurable
(Standard deviation and number of experiments in brackets)

Rate measurements of calcium binding to TnC_{DANZ} by pressure jump method

Above results have shown that the pressure jump method can be used to monitor calcium changes. Analysis of the relaxation transient to evaluate the kinetics of the binding reactions of calcium to TnC_{DANZ}, using imidazole buffer, however, was not possible because of the small fluorescence changes (< 1%) and the high signal to noise ratio. Therefore, in order to obtain a measurable and subsequent better signal to noise ratio, imidazole was replaced with phosphate buffer. Again, the high signal to noise ratio of the traces did not allow for kinetic analysis and averaging ten and more traces did not improve the data.

Previously, Potter et al. (1977) have shown the binding of calcium to the Ca^{2+}-specific site of TnC to be temperature dependent. Thermodynamic calculations have indicated a binding constant of 2.25uM (0.1M KCl, 25°C, pH 7) with tighter binding at lower temperature and weaker binding at higher temperature. Pressure relaxation studies of calcium to TnC_{DANZ} at protein concentrations near the binding constant were performed at 30°C, 20°C and 5°C. The changes in fluorescence at different free$[Ca^{2+}]$ upon 100atm perturbation are shown in fig. 6.3a,b,c. Assuming the reaction was of the form;

equation (1)
$$Ca^{2+} + TnC_{DANZ} \underset{k_{-1}}{\overset{k_{+1}}{\rightleftharpoons}} TnC_{DANZ}.Ca^{2+}$$

the data were then analysed in terms of eq. (1);

Figure 6.3 Pressure induced fluorescence relaxations of $Ca^{2+}.TnC_{DANZ}$

The arrow indicates the time of pressure release from 100atm to 1atm. Traces are computer averaged results of ten consecutive relaxations of the same solution with best fit exponentials superimposed. Reciprocal relaxation times a) at $5^{o}C$ = 1070 s^{-1} b) at $20^{o}C$ = 1320 s^{-1} c) at $30^{o}C$ = 1720 s^{-1}.

Fluorescence signals are increasing, the size bar is relative to the fluorescence at high pressure.

Buffer: 90mM KCl,20mM phosphate, 1mM $MgCl_2$, 2.5mM EGTA, pH 7.

Conditions: a) 1uM TnC_{DANZ} and 4uM free$[Ca^{2+}]$

b) 3uM TnC_{DANZ} and 5uM free$[Ca^{2+}]$

c) 4uM TnC_{DANZ} and 9uM free$[Ca^{2+}]$

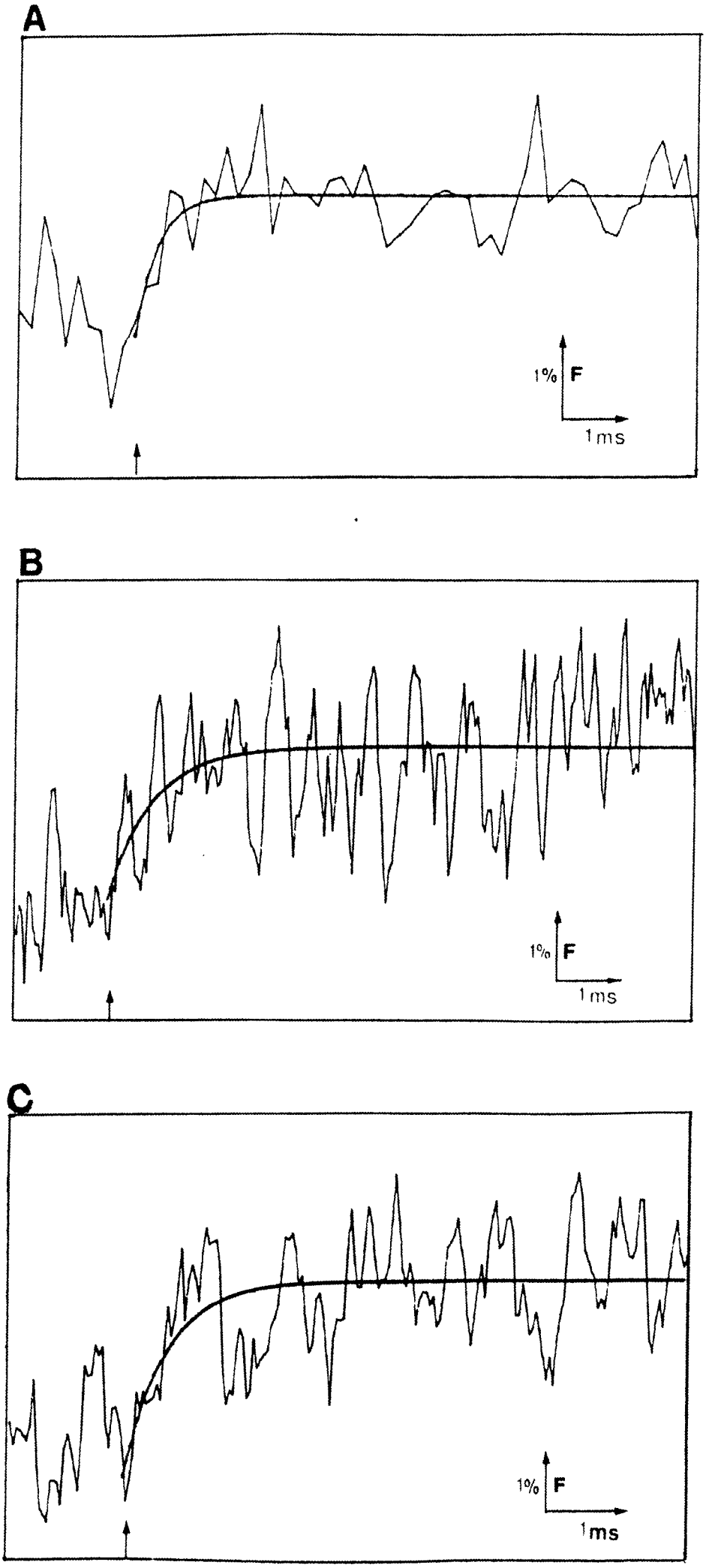
A
1% F
1 ms
B
1% F
1 ms
C
1% F
1 ms

$$1/\tau = k_{+1} \times ([Ca^{2+}] + [TnC]) + k_{-1} \qquad (1)$$

The observed values $1/\tau$ were compared to the calculated values, using the diffusion controlled "on-rate" (k_{+1} approx 10^8 $M^{-1}s^{-1}$) and the measured "off-rate" (k_{-1} approx 340 s^{-1}) (Johnson et al., 1979). Both values are similar (table 6.4). However, it was impossible to perform measurements over a wide range of free$[Ca^{2+}]$ under any temperature condition, which was again due to the high noise to signal level. The rates can, therefore, only be regarded as an estimate of the binding properties.

Rate measurements of calcium binding to TnC_{DANZ} by temperature jump method

Since the rates of calcium binding to TnC_{DANZ} by pressure jump could not be established for a wide range of free$[Ca^{2+}]$ an attempt was made to monitor the binding reaction by temperature jump method. Preliminary static titration experiments of calcium to TnC_{DANZ} at 15°C and 20°C have shown a shift in pCa with weaker binding at higher temperature, also reported by Potter et al. (1977). Solution containing 3uM TnC_{DANZ}, 140mM KCl, 50mM cacodylate, 1mM $MgCl_2$, 2.5mM EGTA, pH 7 at 1uM and 10uM free$[Ca^{2+}]$ were used in temperature jump experiments. These were thermally equilibrated to 15°C in the temperature jump apparatus described in chapter 2. A 5°C temperature jump was effected by discharging the 0.01uF capacitor, which was charged with 25kV, through the sample. The recorded traces, however, were variable for reasons, which are discussed.

Table 6.4 The rate constants for $TnC_{DANZ}.Ca^{2+}$ interaction

Rate constants at 5°C, 20°C and 30°C were obtained from pressure jump studies. The calculated values were based on $k_{+1} = 10^8\ M^{-1}s^{-1}$ and $k_{-1} = 340\ s^{-1}$. Assuming a single step reaction, then $1/\tau = k_{+1}\ ([Ca^{2+}] + [TnC]) + k_{-1}$.

Buffer: 90mM KCl, 20mM phosphate, 2.5mM EGTA, 1mM $MgCl_2$, pH 7.

(T^{o})	TnC_{DANZ}	Free $[Ca^{2+}]$	k_{obs} (s^{-1})	
			measured	calculated
at 30°C	4uM	9uM	1720	1640
at 20°C	3uM	5uM	1320	1140
at 5°C	1uM	4uM	1070	840

DISCUSSION

The experiments in this chapter have shown that increased pressure changes the binding affinity of calcium to TnC in solution by approx 1-3%, depending on buffer conditions. If in a muscle fibre the effect of pressure on TnC is no different to that in solution then results by Geeves & Ranatunga (1990) cannot be explained in terms of a change in affinity of TnC for calcium. It remains a possibility that the augmented twitch tension under pressure is the result of the increased release of calcium from the sarcoplasmic reticulum in the intact fibre or due to a change in the inhibitory function of the regulatory proteins. To substantiate these ideas, however, it is necessary to measure the calcium release in the fibre under pressure and to monitor physiochemical properties in the $(actin)_7$Tn/Tm unit, respectively.

Previously, arsenazo III has been used to measure calcium flux between the sarcoplasmic reticulum and myoplasm in muscle (Baylor et al., 1983). Attempts to measure Ca^{2+} binding to TnC, however, showed that a large fraction of dye molecules are not free in the myoplasmic solution and hence not available to sense calcium activity (Baylor et al., 1985). Therefore, quantitative interpretation of the dye signal was difficult and requires methods for estimating the concentration of bound dye molecules and characterizing their properties. Griffiths et al. (1984) and Ashley et al. (1988) have demonstrated, using TnC_{DANZ} that this modified protein remains free in solution when injected into muscle fibre. However, quantitative measurements of calcium

release from the sarcoplasmic reticulum have not been achieved to date.

The increase in twitch tension upon exposure to 100atm hydrostatic pressure in intact muscle could be the direct effect of pressure on the regulatory proteins of the thin filament. In their cooperative binding model of myosin to regulated actin, Geeves & Halsall (1987), proposed that troponin/tropomyosin (Tn/Tm) controls the acto.S1 interaction by inhibiting the isomerization step identified by Coates et al. (1985). From work by (Geeves & Halsall, 1987) and (Haselgrove, 1972; Greene & Eisenberg, 1980a), the $(actin)_7$Tn/Tm unit is thought to exist in a dynamic equilibrium between an open and a closed state. S1 can bind to either state but only the open form allows the isomerization step to take place. The effect of pressure on this equilibrium could account for a shift in the inhibitory function of the $(actin)_7$Tn/Tm unit. Measurements of excimer fluorescence of pyrenyliodoacetamide labelled Tm would allow for the determination of the equilibrium constant (K_T) Ishii & Lehrer (1990).

It has also been shown in this study that the effect of high pressure on the binding of calcium to TnC and EGTA is negligible. This allows pressure perturbation experiments to be carried out on skinned muscle fibres at low $[Ca^{2+}]$, using EGTA buffers to maintain $[Ca^{2+}]$ and the idea of pressure perturbing the $[A_7]^{on}/[A_7]^{off}$ state to be tested. Using these conditions, an increase in tension must, therefore, be the result of the effect of pressure on the inhibitory function of the regulatory proteins.

The evaluation of the rate binding properties of TnC to calcium could not be achieved by pressure jump and temperature jump method, using arsenazo III and dansylaziridine. The determination of the association reaction would have been important for a clearer understanding of the molecular mechanism, by which muscle contraction is regulated. Its value could have given an answer to the differences over the rate of calcium binding to TnC. Results from low-temperature stopped flow studies have suggested that calcium binding to the low affinity calcium specific sites of TnC is not a simple diffusion-limited process (Rosenfeld & Taylor, 1985b). Similarly, Griffiths et al. (1984) and Ashley et al. (1988) have reported that the fluorescence change of TnC_{DANZ} injected into muscle fibres is slower than would have been predicted for a diffusion-controlled rate of association for Ca^{2+} to the Ca^{2+}-specific site.

The low fluorescence label incorporation (30%) in troponin C was not sufficient to keep the signal to noise ratio at an acceptable level for adequate signal detection and subsequent analysis. Further, the shift of only approx 0.1% free$[Ca^{2+}]$ from the TnC.calcium solutions by 100atm pressure rise imposed a limit on the pressure jump method for measuring binding reactions.

Reasons for not accomplishing binding measurements by temperature change have been reported by Kao & Tsien (1988). They indicated that the break-up of the label and/or protein due to sudden temperature increase may account for this. Another possible reason has been suggested by Rosenfeld & Taylor (1985a). These workers have proposed, contrary to Potter et al. (1977),

that the overall equilibrium constant of Ca^{2+} for TnC does not change with changes in temperature, which would make temperature jump experiments impossible to perform.

The observations by steady state titration in this work showed a change in K_d with temperature and, therefore, support the results by Potter et al. (1977). The reason for obtaining ambiguous results from temperature jumps is probably due to the break-up of the fluorescent label or photobleaching since a loss of sample fluoresence was observed after temperature jumps.

GENERAL DISCUSSION

INTRODUCTION

One aim of muscle biochemistry has been to describe the mechanics of muscle contraction in terms of the kinetics and energetics of the actomyosin interaction. The known energetics of many intermediates in the contractile cycle have been used to construct a biochemically explicit model of the cross-bridge cycle (Eisenberg et al., 1980). Although the mechanism of contraction is not yet understood at molecular level, there has been considerable progress towards this aim in recent years. Studies by Eisenberg & Greene (1980) and Geeves et al. (1984) have suggested a model, in which a myosin head binds weakly to an actin filament, a conformational change in the protein complex occurs, translating the actin filament by 5nm to 10nm, ending in a tight complex between actin and myosin, with myosin forming an acute angle with actin. However, a number of important questions remain unanswered and one of fundamental importance is the nature of the conformational change upon actomyosin binding. One approach that could answer this question is the identification of the state, in which myosin appears to be weakly bound to actin.

Coates et al. (1985) have observed a weakly and a strongly bound acto.S1 state in their pressure jump studies and have shown that temperature, ionic strength and the presence of organic solvent had a marked effect on the two individual steps of the reaction. In this thesis the effect of these parameters have been examined in more detail in order to understand the nature of the reaction in each step. By using the differential effect of

various conditions it was possible to trap some of the acto.S1 complex in the weakly attached state. Stabilizing this state may allow the determination of the acto.S1 structure in solution, which can be compared to the strongly attached state and to structures identified in muscle fibres. Evidence of structural changes in muscle fibre has come from two different conformations observed under non-physiological conditions: a weakly bound state at low ionic strength relaxing solutions and a strongly bound rigor state (Brenner et al., 1982). This idea of two cross-bridge populations is compatiable with many of the structural and mechanical properties of contracting muscle (Huxley & Kress, 1985).

The nature of the structural changes, however, remained undefined. It may involve the actomyosin interface such that the two proteins "roll" past each other, a gross change in shape or size of a single myosin head or "melting" of part of the S2-coiled-coil as suggested by Harrington (1971). In this thesis the thermodynamics of the acto.S1 interaction have been examined in an attempt to ascertain the type of structural changes.

Stabilizing the acto.S1 complex in the weakly attached state

Different solvent conditions were employed in chapter 3 to trap the weakly bound acto.S1 state. Using different monovalent anions at low ionic strength (0.1M) and in the presence of organic solvents showed a negligible effect on the equilibrium constant (K_oK_1) of the weakly bound state. An equilibrium constant of approx 10^5 M^{-1} was observed, which is in agreement with results reported by Coates et al. (1985) for 0.1M

chloride. Increasing the concentration of acetate and possibly of proprionate to 0.5M and the presence of DMSO and ethylene glycol showed no significant change in K_oK_1. This is compatible with observations by Tregear et al. (1984) who have reported that organic solvents have a "stabilizing" effect on acto.S1 in the weakly bound state. However, the presence of chloride ions (and probably bromide and bicarbonate, since these anions gave similar indications) at concentrations well above 0.1M did destabilize the attached state by increasing the rate, at which the two proteins dissociated. There is no direct information to what this effect can be assigned to specifically. It could be due to a change in conformation of actin, S1 or simply in the interaction between the two with no large scale structural change of either species (Harrington, 1971). A clue to these observations is given by Warren et al. (1966) and Stafford (1985) who have reported the same effectiveness of monovalent ions and ionic strength on myosin stability and interpreted their results with the removal of water from the protein.

Electrostatic interactions seem to play an important role in the association of actin and S1 as the affinity of the complex and the rate constant of the association are dependent on ionic strength and solvents. As shown in chapter 3 the association rate constant decreased by a factor of 3-4 on increasing ionic strength and addition of organic solvents. The effect of these parameters on the association rate has previously been reported by White & Taylor (1976) and Konrad & Goody (1982) and was described as an ion-paired charge interaction. However, the

formation of the attached state is a complex reaction and this effect on the formation of a collision complex can not be distinguished from the effect on the rate of transition to the attached state. Yet, these experiments have shown that increases in ionic strength (except for chloride, bromide and bicarbonate) or the addition of organic solvents have very little effect upon the weakly attached state and can hence be used to find conditions where the fraction of attached myosins in the "rigor-like" state can be reduced.

The effect of different experimental conditions on the "rigor-like" acto.S1 state

The effect of monovalent anions at high ionic strength and organic solvents on the acto.S1 isomerization step was also investigated in chapter 3. Using pressure relaxation technique showed that ionic strength at 0.5M and the presence of 40% ethylene glycol or 20% DMSO decreased the equilibrium constant K_2 by a factor of 5 - 6 to a value of approx 20 (table 3.2). Under all these conditions more than 95% of the acto.S1 complex remained in the "rigor-like" complex, which did not allow for structural studies to be carried out of the two states.

Previously, Geeves & Jeffries (1988) have shown that the weakly attached state of the acto.S1 is not affected by ADP but ADP markedly reduces the equilibrium constant K_2 of the isomerization step. In chapter 4 different experimental conditions were used in the presence of nucleotide. Since the fluorescence of pyrene-labelled actin reports the isomerization step specifically (Coates et al., 1985), steady state experiments

were used for direct determination of the fraction of bound actin in the two states. Results in chapter 4 show that the combination of ionic strength and ADP reduced the strongly attached state significantly (K_2 approx 1.6; conditions: 0.5M KCl, 1mM ADP, 20°C, pH 7), leaving approx 60% of the acto.S1 complex in the "rigor-like" state. Complete occupancy of the acto.S1 complex in the attached state by this method was, however, limited by the high protein concentration and the weak binding of actin to S1. The decrease in K_2 with increasing chloride concentration was much larger compared to acetate or proprionate concentration. Replacing chloride with acetate or proprionate in the presence of 1mM ADP showed an approx 30 fold and an approx 5 fold decrease in K_2, respectively. This phenomenon was attributed to a specific chloride effect on the binding of nucleotide to the nucleotide binding site of S1 and was further investigated by stopped flow displacement experiments (chapter 4). Results, however, were inconclusive and a possible answer of the effect of chloride is given by the idea that acetate and proprionate are less effective in removing water from the macromolecules. Previously, Von Hippel & Wong (1962) have shown the degree of hydration of collagen decreases with increasing electrolyte concentration and monovalent anions of the order $CH_3COO^- < Cl^- < Br^-$.

The evidence presented here support the view that major conformational changes occur in the acto.S1 complex and that this conformational change is sensitive to the nucleotide bound to S1. Studies by Eccleston & Bayley (1980) and Shriver & Sykes (1981), using various methods have observed local changes in the

myosin.nucleotide and acto.S1 binding, respectively but no gross structural change of any one species was reported. It may be inferred that the overall conformation in this state is more compact than in the nucleotide-free AM state. Normally proteins, which take up compact conformation are associated with a net increase in weak interactions within the molecule (e.g. hydrogen bonds, van der Waals contact, charge-charge interactions) that contribute to the enthalpy value (Bagshaw & Reed, 1976).

Results in chapter 3 and 4 have shown that the differential effect of ionic strength, solvent and nucleotide can be used to increase the portion of actin bound myosin (S1) in the weak [A-M] state. Although these conditions have not stabilized most of the acto.S1 in the weakly attached state (< 60%), using the different parameters may allow for some studies to be carried out. Future work, e.g. could involve the use of PPi or AMP.PNP in an attempt to completely occupy the acto.S1 complex in the weakly attached state.

Conformational changes associated with the formation of the weakly attached acto.S1 complex

It has been shown in chapter 3 that temperature affects the equilibrium constant K_oK_1 of the weakly attached state and the rate of association K_ok_{+1} markedly. The effect of temperature on the rate of acto.S1 binding has been well documented in the past (Trybus & Taylor, 1980; Marston, 1982; Criddle et al., 1985). Results from experiments in chapter 3 showed that the rate of association of acto.S1 in 0.1M acetate was reduced similarly over a 20°C temperature range as observed in 0.1M chloride by Coates

et al. (1985). Plotting the rate constants against temperature in an Arrhenius graph indicated a break in the slope at approx 10°C (fig. 3.6). The thermodynamic data in table 3.5 showed large differences in entropy below and above the critical temperature, indicating some change in order of this reaction step. Sofar linear Arrhenius plots have been reported for acto.S1 binding in chloride buffer and structural transitions have been suggested because of the large temperature dependence of this reaction (Highsmith, 1977). Konrad & Goody (1982) have regarded the association of actin and myosin (S1) as an entropy-driven process and interpreted the entropy change with a less ordered water structure surrounding the proteins. The results presented here give support to the idea of a structural or phase change of the acto.S1 binding reaction.

The association reaction of actin to S1 was also examined by temperature jump method. A simple modification to a standard thermostated stopped flow machine was carried out, which allowed it to be used as a temperature jump apparatus. This apparatus, which is described in detail in chapter 5, has a sample size of 300ul and can produce temperature jumps both above and below ambient temperature. Temperature jumps larger than 10°C were achieved in less than 150msec, which made it useful for the range of times for acto.S1 binding reactions to be measured. Results from acto.S1 binding experiments in chapter 5 were in good agreement with data achieved in the stopped flow apparatus and in the pressure jump machine by Geeves & Halsall (1986) at 20°C and at 5°C in chapter 3.

Findings in chapter 3 and 5 support the idea that some conformational change occurs in the acto.S1 binding reaction. The high temperature dependence of this reaction, the observation of a breakpoint in the Arrhenius plot and the thermodynamic data in table 3.5 suggest that this process is more complex than a simple binding reaction.

Conformational changes associated with the transition of acto.S1 from the weakly to the "rigor-like" complex

Analysis of the amplitudes of the pressure sensitive step K_2 allowed volume changes to be calculated (table 3.2) to obtain information of the conformational changes and thermodynamics involved. Results in chapter 3 indicated that high ionic strength and organic solvents caused a reduction in volume from approx $100cm^3/mol$ (0.1M KCl) to approx $50cm^3/mol$, which is probably be due to changes in water structure inferred by these parameters. Volume changes of this size imply a substantial rearrangement of the hydration sphere around the protein complex or the interface between the proteins (Gutfreund, 1972; Heremans, 1982). This can be attributed to a conformational change in at least one of the two proteins or the contact area between them and since ionic, polar and hydrophobic groups interact with acto.S1, these have a strong influence on the volume (Kodama, 1985). Hydrophobic interactions are of particular interest as they have a marked influence on the stability when macromolecules are interacting (Von Hippel & Schleich, 1969b). Although little is known about volume changes associated with the hydrophobic interactions. The transfer of non-polar molecules from non-polar

to polar surroundings results in a decrease of molar volume of the solute. It is believed that the hydrophobic hydration is a cooperative phenomenon, in which the exact microstructure of water is very important for the occupied volume. Changes in microstructure when two molecules associate in a hydrophobic interaction, however, is not particularly well understood (Ben-Naim, 1980).

Several pieces of evidence suggest that the myosin head (S1) consists of at least two structural domains and the interaction of these domains appear to be altered upon binding to actin (Vibert, 1988; Vibert & Cohen, 1988). Results in chapter 3 can not give direct evidence that myosin (S1) undergoes a delocalised change of conformation. The source for thermodynamic changes seems to be displacement of water from the surface areas of the two proteins that come in contact during association. Charged and/or hydrophobic side chains are probably involved in the interaction. Borejdo (1983) mapped the hydrophobic sites of myosin and actin and results suggested that either hydrophobic interaction or actin binding are important to induce a shift in the macrostate. Studies by fluorescence resonance energy transfer (FRET) have also reported substantial conformational changes upon actin binding to S1 but have given no direct information on where in the structure of actin or S1 this change takes place (Trayer & Trayer, 1983; Bhandari et al. 1985;).

The effect of different temperatures on the equilibrium constant K_2 of the acto.S1 complex was also investigated in the search for clues of the type of conformational changes involved. The results in chapter 3 from pressure jump experiments (table

3.4) showed that temperature increased K_2 by a factor of approx 2 when decreased from 20°C to 2°C. Calculating the volume change for this temperature range from amplitude changes of the pressure sensitive step K_2 indicated a similar change in volume observed for high ionic strength and solvents (table 3.3). Kinetic methods give no direct information on the nature of the structural change, they do provide thermodynamic data, which can give an indication of the type of structural change. An important parameter for the discussion of pressure-temperature relationship is ΔV. As ΔV is temperature dependent, it also controls the pressure dependence of ΔS through the relationship;

$$d(\Delta G) = -\Delta S x dT + \Delta V dp$$

Using above the equation and from the Maxwell relation, the enthalpic contribution (more negative or less positive) becomes dominant in stabilizing the acto.S1 conformation when the volume changes with increasing temperature. This effect has been reported for other protein-protein interactions (Greaney & Somero, 1979). Paladini & Weber (1981) explained this phenomenon with an increase of free volume or dead space between the associated protein subunits and the trapping of solvent at the interface between proteins. As shown in chapter 3 (ΔH) becomes less positive with an increase in temperature, making (ΔS) less positive at higher temperature. This can be attributed to diminishing water structure and protein conformational change (Eagland, 1975).

Correlation of biochemical and mechanical events

As previously discussed by Coates et al. (1985) and also shown in chapter 3 high pressure reduces the equilibrium constant K_2 of the isomerization step by a factor of 1.5 - 2. If this step is the molecular basis of force generation then a reduction in tension in muscle is predicted. Fortune et al. (1989) have used pressure perturbation method on muscle fibre and observed a depression on maximally Ca^{2+} activated skinned fibres at high pressure. Geeves & Ranatunga (1990) monitored a pressure-induced decrease in tetanic tension of intact fibres. These findings are compatible with the model of Geeves et al. (1984), which suggested that the isomerization is closely linked to the tension generating event in muscle fibre. The change in sensitivity in the fibre system to increases in hydrostatic pressure is consistent with the step identified in solution (Coates et al. (1985); chapter 3). This suggests that hydrostatic pressure is principally perturbing the transition between the attached cross-bridge and a rigor-like tension-bearing state in fibre systems.

If the transition from the "attached" to the "rigor-like" conformation of the acto.S1 is closely linked to the power stroke of the cross-bridge (Geeves et al., 1984) and solvents and high ionic strength reduce K_2 of the isomerization step in solution as demonstrated in chapter 3 then an effect on the tension in muscle is also expected. Previous observations by Gulati & Babu (1982) have demonstrated that an increase in KCl concentration causes a decrease in isometric tension generation in skinned fibres. Clarke et al. (1980) published data that the presence of 50% ethylene glycol decreased rigor tension in insect flight muscle.

These results support the idea that changes identified in the transition step in solution can be correlated to changes in tension generation in muscle fibre.

Results in chapter 6 have indicated that high pressure does not affect calcium binding to troponin C in solution significantly. Under the assumption that the effect of pressure on TnC is no different in muscle fibre, this would imply that the increase in twitch tension observed by Geeves & Ranatunga (1990) upon pressurisation cannot be due to changes in calcium affinity to the regulatory proteins. The augmentation of twitch tension at high pressure can, therefore, be the result of either the release of calcium from the sarcoplasmic reticulum or due to a shift in the inhibitory function of the regulatory proteins. The idea of calcium release from the sarcoplasmic reticulum at 10MPa pressure rise can be tested e.g. by injecting TnC_{DANZ} into muscle fibres. The shift in the inhibitory function of the (actin)$_7$Tn/Tm unit at high pressure can also be evaluated, using the results presented in chapter 6.

Fortune *et al.* (1989) and Geeves & Ranatunga (1990) have both observed that pressure induced a decrease in maximally calcium-activated tension in skinned muscle fibre and in tetanic tension in intact muscle fibre, respectively. This effect has been interpreted as the consequence of a specific effect of pressure on cycling cross-bridges. Results presented in chapter 6 have shown that not only the binding of calcium to TnC (< 3%) but also the binding of calcium to EGTA (< 1%) is insignificantly affected by high pressure. This observation would, therefore, allow

pressure perturbation experiments to be performed in skinned muscle fibre at low calcium concentration, using EGTA buffers with no perturbation of the free[Ca^{2+}]. If, under these conditions pressure perturbation causes a tension increase, then this is likely be due to a shift in the inhibitory function of the regulatory proteins.

CONCLUSION

Although the experimental approach of the study of purified acto.S1 in solution compared to muscle fibres is different, the correlation of biochemical findings to *in vivo* observations gives support of the two step binding model proposed by Geeves *et al.* (1984). It has been shown that conformational changes occur upon the binding of acto.S1 to form the weakly attached state and that the transition between this state and the "rigor-like" state involves structural changes sufficient to account for the force generating event. The various experimental conditions, which influence the transition in solution also affect force generation. However, for this transition to be fully identified as the force generating event, it must be coupled with the ATP product release. Solution studies have given little direct information sofar on the acto.S1 ADP.Pi state as a result of minimal binding of phosphate to the complex (Sleep & Hutton, 1980). Isotope exchange experiments have provided a method of monitoring this step in solution and sofar limited information on an intact system has been obtained (Webb *et al.*, 1986). Correlation of these findings in solution and intact muscle are the ultimate test of this model.

The potential of pressure relaxation method for the study of acto.S1 in solution has been demonstrated in this work and its application to measure cross-bridge events in muscle fibre has been referred to. This perturbation method not only provided information about rates of acto.S1 interaction but also gave indications of volumetric behaviour of these proteins. From the concentration dependence of the specific volume, information was obtained on the protein-protein interactions. The amplitudes of displacement from equilibria at different reactant concentrations and at different temperature changes were used to calculate equilibrium constants and thermodynamic parameters, respectively, which provided clues of structural changes. All this information proved valuable in the elucidation of the acto.S1 binding mechanism and make this method a powerful tool. Since the understanding of mechanical force on molecular level remains a major aim of muscle research, perturbation method used on isolated proteins in solution and on muscle fibres can, therefore, make a valuable contribution towards this aim. Using this technique, several challenging questions to date could be addressed and results could be correlated with findings in muscle fibres; e.g. the cooperative behaviour of the $(actin)_7$Tn/Tm unit in the presence of calcium. The elucidation of the overall mechanism could give an answer, at which step Tm/Tn affects the actin binding, ATPase rate and subsequent Pi-release; or the possibility of the cooperative binding of the two heads of S1 (HMM) to actin. The difference in behaviour of the two heads in the kinetic ATP-cycle could have significant consequences on

isometric tension in muscle fibre.

Having shown in this thesis that conformational changes do occur upon binding of actin to S1 to form the weakly attached state followed by changes to form the rigor-like state, future work could involve e.g the use of rapid-freeze-etching methods to observe these conformational changes in a high resolution electron microscope. Although the different experimental treatments have not achieved complete occupation of the weakly attached state, using this method could allow for studies of the two interacting proteins to be carried out and results could be compared with published data on whole muscle fibre.

REFERENCES

Adelstein, R.S. & Eisenberg, E. (1980) Actomyosin, Ann. Rev. Biochem. 49, 921-956

Amos, L.A., Huxley, H.E., Holmes, K.C., Goody, R.S. & Taylor, K.A. (1982) Structural evidence that myosin heads may interact with two sites on F-actin, Nature (London) 299, 467-469

Applegate, D. & Reisler, E. (1984) Nucleotide-induced changes in the proteolytically sensitive regions of myosin subfragment 1, Biochemistry 23, 4779-4783

Ashley, C.C., Griffiths, P.J. & Potter, J.D. (1988) The mobility of TnC_{DANZ} following injection into barnacle muscle fibres, J. Physiol. 399, 20p

Bagshaw, C.R. (1982) Muscle Contraction, Chapman & Hall, London, UK

Bagshaw, C.R. & Reed, G.H. (1976) Investigations of equilibrium complexes of myosin subfragment 1 with the magnesium ion and adenosine diphosphate using magnetic resonance techniques, J. Biol. Chem. 251, 1975-1983

Baker, T.S. & Winkelmann, D.A. (1986) In: Proceedings of 44th. annual meeting EMSA (G.W. Bailey ed.) pp.26-29, San Francisco Press, San Fransisco

Balint, M., Wolf, I., Tarcsafalui, A., Gergely, J. & Sreter, F.A. (1978) Essential SH groups of myosin, Arch. Biochem. Biophys. 190, 793-799

Baylor, S.M., Chandler, W.K. & Marshall, M.W. (1983) Sarcoplasmic reticulum calcium release in frog skeletal muscle fibres estimated from arsenazo III calcium transients, J. Physiol. 344, 625-666

Baylor, S.M., Hollingworth, S., Hui, C.S. & Quinta-Ferreira, M.E. (1985) Calcium transients from intact frog skeletal muscle fibres simultaneously injected with metallochromic dyes, J. Physiol. 365, 70p

Baylor, S.M., Hollingworth, S., Hui, C.S. & Quinta-Ferreira, M.E.(1986) Properties of metallochromic dyes arsenazo III, antipyralazo III and azo I in frog skeletal muscle fibres at rest, J. Physiol. 377, 89-141

Ben-Naim, A. (1980) In: Hydrophobic Interactions, Plenum, New York, USA.

Bhandari, D.G., Trayer, H.R. & Trayer, I.P. (1985) Resonance energy transfer evidence for two attached states of the actomyosin complex, FEBS Lett. 187, 160-166

Biosca, J.A., Travers, F. & Barman, T.E. (1983) A jump in an Arrhenius plot can be the consequence of a phase transition. The binding of adenosine triphosphate to subfragment 1, FEBS Lett.153, 217-220

Bock, R.M., Ling, N.S., Morell, S.A. & Lipton, S.H. (1956) U.V. absorption spectra of Adenosine 5'triphosphate and other related 5'ribonucleotides, Arch. Biochem. Biophys. 62, 253-264

Borejdo, J. (1983) Mapping of hydrophobic sites on the surface of myosin and its fragments, Biochemistry 22, 1182-1187

Brenner, B., Schoenberg, M., Chalovich, J.M., Greene, L.E. & Eisenberg, E.(1982) Evidence for cross-bridge attachment at low ionic strength, Proc. Natl. Acad. Sci. USA79, 7288-7291

Brown, D.E.S. (1934a) The effect of rapid changes in hydrostatic pressure upon the contraction of skeletal muscle, J. cell. comp. Physiol. 4, 257-281

Brown, D.E.S. (1934b) The effect of rapid compression upon events in the isometric contraction of skeletal muscle, J. cell. comp. Physiol. 8, 141-157

Burghardt, T.P., Ando, T. & Borejdo, J. (1983) Evidence for cross-bridge order in contraction of glycerinated skeletal muscle, Proc. Natl. Acad. Sci. U.S.A. 80, 7515-7519

Clarke, M.L., Rodger, C.D., Tregear, R.T., Bordas, I. & Koch, M. (1980) The effect of ethylene glycol and low temperature on the structure and function of insect flight muscle, J. Muscle Res. Cell Motil. 1, 195-196

Clarke, M.L. & Spudich, J.A. (1977) Nonmuscle contractile proteins: The role of actin and myosin in cell motility and shape determination, Ann. Rev. Biochem. 46, 797-822

Coates, J.H., Criddle, A.H. & Geeves, M.A. (1985) Pressure relaxations of actomyosin.S1, Biochem. J. 232, 351-356

Collins, J.H. & Elzinga, M. (1975) The primary structure of actin from rabbit skeletal muscle, J. Biol. Chem. 250, 5915-5920

Collins, J.H., Greaser, M.L., Potter, J.D. & Horn, M.J. (1977) Determination of the amino acid sequence of TnC from rabbit skeletal muscle, J.Biol. Chem. 252, 6356-6362

Collins, J.H., Potter, J.D., Horn, M.J., Wilshire, G. & Jackson, N. (1973) The amino acid sequence of rabbit skeletal muscle TnC: Gene replication and homology with calcium binding proteins from carp and hake muscle, FEBS Lett. 36, 268-273

Cooke, R. (1986) The mechanism of muscle contraction, Critical Reviews in Biochemistry 21, 53-118

Cooke, R. & Pate, E. (1985) The effect of ADP and phosphate on the contraction of muscle fibres, Biophys. J. 48, 789-798

Cooper, J.A., Walker, S.B. & Pollard, J.D. (1983) pyrene actin: Documentation of the validity of a sensitive assay for actin polymerization, J. Muscle Res. Cell Motil. 4, 253-262

Craig, R. (1977) Structure of A-segments from frog and rabbit skeletal muscle, J. Mol. Biol. 109, 69-73

Criddle, A.H. (1985) Actomyosin subfragment 1 interaction in the presence and absence of nucleotides as studied by fluorescent labelling and phosphate medium exchange, PhD thesis, Bristol University

Criddle, A.H., Geeves, M.A. & Jeffries, T. (1985) Pyrene-actin and myosin interactions, Biochem. J. 232, 343-349

Czerlinski, G.H. (1966) In: Chemical Relaxation, Marcel Dekker, New York, USA.

Czerlinski, G.H., Gibbson, Q. & Staerk, H. (1964) paper WB2, 8th. Ann. Meeting Biophys. Soc., Chicago

Dantzig, J.A., Lacktis, J.W., Homsher, E. & Goldman, Y. E. (1987) Mechanical transients initiated by photolysis of caged Pi during active skeletal muscle contraction, Biophys. J. 51, 3a

Davis, J.S. & Gutfreund, H. (1976) The scope of moderate pressure changes for kinetic and equilibrium studies of biochemical systems, FEBS Lett. 72, 199-207

Eagland, D. (1975) In: Water a comprehensive treatise (F. Franks ed.) Vol.4, Chapter 5, Plenum, New York-London

Ebashi, S. & Ebashi, F. (1964) A new protein component participating in the superprecipitation of myosin, J. Biochem. (Tokyo) 55, 604-620

Ebashi, S. & Kodama, A. (1966) Native tropomyosin-like action of troponin on trypsin-treated myosin B, J. Biochem. (Tokyo) 60, 733-735

Eccleston, J.F. & Bayley, P.M (1980) Circular diφchroic spectra of 6-thio guanosine nucleotides and their complexes with myosin subfragment 1, Biochemistry 19, 5050-5056

Egelman, E.H. (1985) The structure of F-actin, J. Muscle Res. Cell Motil. 6, 129-151

Eigen, M. (1963) The effects of salts on free energies of nonpolar groups in model peptides, Pure Appl. Chem. 6, 97-115

Eigen, M. & DeMaeyer, L. (1963) In: Technique of organic chemistry (S.L. Fries, E.S. Lewis, & A. Weissberger eds.)vol. VIII, part II, pp. 895-1054, Wiley (Interscience) New York, USA.

Eisenberg, E. & Greene, L.E. (1980) The relation of muscle biochemistry to muscle physiology, Ann.Rev.Physiol.42,293-309

Eisenberg, E. & Hill, T.L. & Chen, Y. (1980) Cross-bridge model of muscle contraction, Biophys. J. 29, 195-229

Eisenberg, E. & Hill, T.L. (1985) Muscle contraction and free energy transduction in biological systems, Science 227, 999-1006

Elzinga, M., Collins, J.H., Kuehl, W.M. & Adelstein, R.S. (1973) Complete amino acid sequence of actin from rabbit skeletal muscle, Proc. Natl. Acad. Sci. U.S.A. 70, 2687-2691

Endo, M. & Ebashi, S. (1966) Localisation of native tropomyosin in relation to striation patters, J. Biochem. (Tokyo) 60, 425-436

Finlayson, B., Lymn, R.W. & Taylor, E.W. (1969) Hydrolysis of nucleotide triphosphates by myosin during the transient state, Biochemistry 8, 811-819

Flicker, P.F., Phillips, G.N. & Cohen, C. (1982) Tn and its interactions with tropomyosin, J. Mol. Biol. 162, 445-450

Fortune, N.S., Geeves, M.A. & Ranatunga, K.W. (1988) The effect of hydrostatic pressure on rabbit glycerinated muscle fibre tension, J. Physiol. 401, 10p

Fortune, N.S., Geeves, M.A. & Ranatunga, K.W. (1989) Pressure sensitivity of active tension in glycerinated rabbit psoas muscle fibre: effects of ADP and phosphate, J. Muscle Res. Cell Motil. 10, 113-123

French, T.C. & Hammes, G.G. (1969) The temperature-jump method, Methods in Enzymology XVI, 3-30

Fuchs, F. & Briggs, F.N. (1968) The site of calcium binding in relation to the activation of myofibrillar contraction, J. Gen. Physiol. 51, 655-676

Geeves, M.A. (1990) The dynamic interaction of actin myosin association and the cross-bridge model of muscle contraction, review submitted to Biochem. J.

Geeves, M.A. (1989) Dynamic interaction between actin and myosin subfragment 1 in the presence of ADP, Biochemistry 28, 5864-5871

Geeves, M.A., Goody, R.S. & Gutfreund, H. (1984) Kinetics of

acto.S1 interactions, J. Muscle Res. Cell Motil. 5, 351-361

Geeves, M.A. & Gutfreund, H. (1982) The use of pressure perturbation to investigate the interaction of rabbit muscle myosin subfragment 1 with actin in the presence of MgADP, FEBS Lett. 140, 11-15

Geeves, M.A. & Halsall, D.J. (1986) The dynamics of the interaction between myosin subfragment 1 and pyrene-labelled thin filaments from rabbit skeletal muscle, Proc. R. Soc. Lond. B 229, 85-95

Geeves, M.A. & Halsall, D.J. (1987) Two-step ligand binding and co-operativity, Biophys. J. 52, 215-220

Geeves, M.A. & Jeffries, T.E. (1988) The effect of nucleotide upon a specific isomerization of actomyosin subfragment 1, Biochem. J. 256, 41-46

Geeves, M.A., Jeffries, T.E. & Millar, N.C. (1986) ATP-induced dissociation of acto.S1. Characterization of an isomerization of the ternary acto-S1-ATP complex, Biochemistry 25, 8454-8458

Geeves, M.A. & Ranatunga, K.W. (1987) Effects of pressure on muscle tension, Proc. R. Soc. Lond. B232, 217-226

Geeves, M.A. & Ranatunga, K.W. (1990) Effect of hydrostatic pressure on isometric contractions of intact fibre bundles isolated from rat muscles, J. Physiol. 425, 16p

Giles, R. (1987) Volume regulation in cells of euryhaline invertebrates, Curr. Topics Membr. Transp. 30, 205-247

Goldman, Y.E., Dantzig, J.A., Hibberd, M.G. & Trentham, D.R. (1983) Ca^{2+} dependence of tension transients initiated by photolysis of caged adenosine triphosphate in rabbit skinned muscle fibres, J. Physiol. 341, 38p

Goldman, Y.E., Hibberd, M.G., McCray, J.A. & Trentham, D.R. (1982) Relaxation of muscle fibres by photolysis of caged adenosine triphosphate Nature (London) 300, 701-705

Graceffa, P. & Lehrer, S.S. (1980) The excimer fluorescence of

pyrene-labelled tropomyosin, J. Biol. Chem. 255, 11296-11300

Greaney, G. S. & Somero, G.N. (1979) Effects of anions on the activation thermodynamics and fluorescence emission spectrum of alkaline phosphatase: Evidence for enzyme hydration changes during catalysis, Biochemistry 18, 5322-5332

Greaser, M.L. & Gergely, J. (1971) Reconstitution of troponin activity from three protein components, J. Biol. Chem. 246, 4226-4233

Greaser, M.L. & Gergely, J. (1973) Purification and properties of the components from troponin, J. Biol. Chem. 248, 2125-2133

Greene, L.E. & Eisenberg, E. (1980) Dissociation of the actoSubfragment 1 complex by AMPPNP, ADP and pyrophosphate, J. Biol. Chem. 255, 543-548

Greene, L.E. & Eisenberg, E. (1980a) Cooperative binding of myosin subfragment 1 to actin-troponin-tropomyosin complex, Proc. Natl. Acad. Sci. U.S.A. 77, 2616-2620

Griffiths, P.J., Potter, J.D., Coles, B., Strang, P. & Ashley, C.C. (1984) Fluorescence changes from single striated muscle fibres injected with labelled troponin C (TnC_{DANZ}), FEBS Lett. 176, 144-150

Gulati, J. & Babu, A. (1982) Tonicity effect on intact muscle fibres: Relation between force and cell volume, Science 215, 1109-1111

Gutfreund, H. (1972) Enzymes: Physical Principles, Wiley-Interscience, London, UK.

Harold, F.M. (1986) Vital Force: A study of bioenergetics, W.H. Freeman & Co., New York. USA

Harrington, W.F. (1971) A mechamochemical mechanism for muscle contraction, Proc. Natl. Acad. Sci. U.S.A. 68, 685-689

Harrington, W.F. & Rodgers, M.E. (1984) Myosin, Ann. Rev. Biochem. 53, 35-73

Hartsborne, D.J. & Mueller, H. (1969) Preparation of troponin and tropomyosin from natural actomyosin, Biochim. Biophys. Acta 175, 301-309

Hartsborne, D.J. & Pyun, H.Y. (1971) Calcium binding by the troponin complex and the purification and properties of troponin A, Biochim. Biophys. Acta 229, 698-711

Haselgrove, J.C. (1972) X-ray evidence for a conformational change in the actin-containing filaments of vertebrate striated muscle, Cold Spring Harbour Symp. Quant. Biol. 37, 341-352

Heremans, K. (1982) High pressure effects on proteins and other biomolecules, Ann. Rev. Biophys. Bioeng. 11, 1-22

Herzberg, O. & James, M.N.G. (1985) Common structural framework of the two Ca^{2+}/Mg^{2+} binding loops of TnC and other Ca^{2+} binding proteins, Biochemistry 24, 5298-5302

Hibberd, M.G. & Trentham, D.R. (1986) Relatioships between chemical and mechanical events during muscular contraction, Ann. Rev. Biophysics Biophys. Chem. 15, 119-161

Highsmith, S. (1976) Interactions of the actin and nucleotide binding sites of subfragment 1, J. Biol. Chem. 251, 6170-6172

Highsmith, S. (1977) The effects of temperature and salts on myosin subfragment 1 and F-actin association, Arch. Biochem. Biophys 180, 404-408

Hirami, K. (1979) Kinetics of fast enzyme reactions, Halsted press, Division of Wiley, New York, USA.

Hodges, R.S., Sodek, J., Smillie, L.B. & Jurasek, L. (1972) Tropomyosin: Amino acid sequence and coiled-coil structure, Cold Spring Harbour Symp. Quant. Biol. 37, 299

Hofmeister, F. (1888) Die Beteiligung geloester Stoffe an Quellungsvorgaengen, Arch. Exp. Pathol. Pharmakol. 24, 247-256

Hole, C.J., (1980) The ATP dependent calcium pump of skeletal muscle sarcoplasmic reticulum, PhD thesis, Bristol University

Horwitz, J., Bullard, B. & Mercola, D. (1979) Interaction of troponin subunits, J. Biol. Chem. 254, 350-355

Huxley, A.F. (1957) Muscle structure and theories of contraction, Prog. Biophys. Biochem. 7, 255-318

Huxley, A.F. & Niedergerke, R. (1954) Interference microscopy of living muscle fibres, Nature (London) 173, 971-973

Huxley, A.F. & Simmons, R.M. (1971) Proposed mechanism of force generation in striated muscle, Nature (London) 233, 533-538

Huxley, H.E. (1957) The double array of filaments in cross-striated muscle, J. Biophys.Biochem. Cytol. 3, 631-648

Huxley, H.E. & Hanson, J. (1954) Changes in the cross striations of muscle during contraction and stretch and their structural interpretation, Nature (London) 173, 973-976

Huxley, H.E. & Kress, M. (1985) Cross-bridge behaviour during muscle contraction, J. Muscle Res. Cell Motil. 6, 153-161

Iio, T. & Kondo, H. (1981) Fluorescence titration and fluorescence stopped flow studies on skeletal troponin C labelled with fluorescent maleimide reagent or dansylaziridine, (Tokyo) 90, 163-175

Irving, M. (1987) In: Fibrous protein structure (J.M. Squire & P.J. Vibert eds.) pp.495-528, Academic press, London, UK

Irving, M. & Peckham, M. (1986) Birefringence as a probe of cross-bridge orientation in demembranated muscle fibres, J. Physiol. 377, 95p

Ishii, Y. & Lehrer, S.S. (1990) Excimer fluorescence of pyrenyliodoacetamide-labeled tropomyosin: A probe of the state of tropomyosin in reconstituted muscle thin filaments, Biochemistry 29, 1160-1166

Johnson, J.D., Charlton, S.C. & Potter, J.D. (1979) Fluorescence stopped flow analysis of Ca^{2+} exchange with TnC, J. Biol. Chem. 254, 3497-3502

Johnson, J.D., Collins, J.H. & Potter, J.D. (1978) Dansylaziridine labelled TnC, J. Biol. Chem. 253, 6451-6458

Johnson, J.D. & Potter, J.D. (1978) Detection of two classes of Ca^{2+} binding sites in TnC with circular diochroism and tyrosine fluorescence, J. Biol. Chem. 253, 3775-3777

Kabsch, W. & Holmes, K.C. (1990) The structure of the actin-DNA'ase 1 complex at 3 Angstrom resolution and the derived structure of F-actin, Biophys. J. 57, 397a

Kao, J.P.Y. & Tsien, R.Y. (1988) Ca^{2+} binding kinetics of fura-2 and azo-1 from temperature-jump relaxation measurements, Biophys. J. 53, 635-639

Karn, J., Brenner, S. & Barnett, L. (1983) Protein structural domains in the Caenorhabditis elegans unc-54 myosin heavy chain gene are not separated by introns, Proc. Natl. Acad. Sci., U.S.A. 80, 4253-63

Kauzmann, W. (1959) Some factors in the interpretation of protein denaturation, Adv. Protein Chem. 14, 1-63

Kay, C.M. & Brahms, J. (1963) The influence of ethylene glycol on the enzymatic adenosine triphosphatase activity and molecular conformation of fibrous muscle proteins, J. Biol. Chem. 238, 2945-2949

Kodama, T. (1985) Energetics of muscle ATPase reactions, Physiol. Reviews 65, 467-551

Konrad, M. & Goody, R.S. (1982) Kinetic and thermodynamic properties of the ternary complex between actin, myosin and AMPPNP, Eur. J. Biochem. 128, 547-555

Kouyama, T. & Mihashi, K. (1981) Fluorimetry study of N-(1-pyrenyl)iodoacetamide labelled F-actin, Eur. J. Biochem. 114, 33-38

Kress, M., Huxley, H.E., Faruqi, A.R. & Hendrix, J. (1986) Structural changes during activation of frog muscle studies by time resolved X-ray diffraction, J. Mol. Biol. 188, 325-42

Laemmli, U.K. (1970) Cleavage of structural proteins during the

assembly of the head of bacteriophage T4, Nature (London) 227, 680

Lehrer, S.S. (1975) Intramolecular crosslinking of tropomyosin via disulphide bond formation: Evidence for chain register, Proc. Natl. Acad. Sci. U.S.A. 72, 3377-3381

Lin, T. (1978) Fluorimetric studies of actin labelled with dansylaziridine, Arch. Biochem. Biophys. 185, 285-299

Londesborough, J. (1980) The pH and temperature dependence of the activity of high K_m cyclic nucleotide phosphodiesterase of bakers's yeast, J. Biol. Chem. 255, 9262-9270

Low, P.S. (1985) In: Transport processes -Iono -and Osmoregulation (R. Giles & M. Giles-Baillien eds.) Springer Verlag, Berlin

Lymn, R.W. & Taylor, E.W. (1971) Mechanism of ATP hydrolysis by actomyosin, Biochemistry 10, 4617-4624

Marayama, K., Matsuno, A., Higuchi, H., Shimaoka, S., Kimura, S. & Shimizu., T. (1989) Behaviour of connectin (titin) and nebulin in skinned muscle fibres released after extreme stretch as revealed by immunoelectron microscopy, J. Muscle Res. Cell Motil. 10, 350-359

Margossian, S.S. & Lowey, S. (1978) Interaction of myosin subfragments with F-actin, Biochemistry 17, 5431-5439

Margossian, S.S. & Lowey, S. (1982) Preparation of myosin and its subfragments from rabbit skeletal muscle, Methods in Enzymology 85, 55-71

Marston, S.B. (1982) Formation and dissociation of actomyosin complexes, Biochem. J. 203, 453-460

Marston, S.B. & Tregear, R.T. (1984) Modification of the interactions of myosin with actin and 5'adenylyl-imidodiphosphate by substitution of ethylene glycol for water, Biochem. J. 217, 169-177

McLachlan, A.D. (1984) Structural implications of myosin amino acid sequence, Ann.Rev. Biophys. Bioeng. 13, 167-189

Millar, N.C. (1984) Kinetics of actomyosin interactions in rabbit skeletal muscle, PhD thesis, Bristol University

Millar, N.C. & Geeves, M.A. (1983) The limiting rate of the ATP-mediated dissociation of actin from rabbit skeletal muscle myosin subfragment 1, FEBS Lett. 160, 141-148

Millar, N.C. & Homsher, E. (1990) The effect of phosphate and calcium on force generation in glycerinated rabbit skeletal muscle fibers. A steady state and transient kinetic study, Ann. Rev. Physiol., submitted

Mornet, D., Bertrand, R., Pantel, P., Audemard, E. & Kassab, R. (1981a) Structure of the actin-myosin interface, Nature (London) 292, 301-306

Mornet, D., Pantel, P., Bertrand, R., Audemard, E. & Kassab, R. (1981b) Isolation and characterization of the trypsin modified myosin-S1 derivatives, FEBS Lett. 123, 54-58

Mushtaq, E. & Greene, L.E. (1989) Effect of ethylene glycol on the interaction of different myosin subfragment 1-nucleotide complexes with actin, Biochemistry 28, 6478-6482

Nakatani, H. (1985) Contruction of Up-and-Down temperature-jump apparatus, Anal. Biochemistry 149, 87-90

Nandi, P.K. & Robinson, D.R. (1972a) The effects of salts on the free energy of the peptide groups, J. Amer. Chem. Soc. 94, 1299-1307

Nandi, P.K. & Robinson, D.R. (1972b) The effects of salts on the free energies on nonpolar groups in model peptides, J. Amer. Chem. Soc. 94, 1308-1318

O'Brien, E.J., Couch, J., Johnson, G.R.P. & Morris, E.P.(1983) In: Actin structure and function in muscle and non-muscle cells (C.G. dos Remedios & J.A. Barden eds.) Academic press, Sydney, Australia

Owen, J.D. (1976) The determination of the stability constant for calcium/EGTA, Biochim. Biophys. Acta 451, 321-325

Paladini, A.A. & Weber, G. (1981) Pressure-induced reversible

dissociation of enolase, Biochemistry 20, 2587-2593

Pardee, J.D. & Spudich, J.A. (1982) Purification of muscle actin, Methods in Enzymology 85, 164-181

Pate, E. & Cooke, R. (1989) A model of cross-bridge action: the effects of ATP, ADP and Pi, J. Muscle Res. Cell Motil. 10, 181-196

Pearlstone, J.R., Carpenter, M.R., Johnson, P. & Smillie, L.B. (1976) Amino-acid sequence of tropomyosin binding component of rabbit skeletal muscle troponin, Proc. Natl. Acad. Sci. U.S.A. 73, 1902-1907

Phillips, G.N., Fillers, J.P. & Cohen, C. (1986) Tropomyosin crystal structure & muscle regulation, J.Mol. Biol.192, 111-131

Pohl, F.M. (1968) Einfache Temperatursprung-methode im Sekunden - bis Stundenbereich und die reversible Denaturierung von Chymotrypsin, Eur. J. Biochem. 4, 373-377

Potter, J.D. (1982) Preparation of troponin and its subunits, Methods in Enzymology 85, 241-263

Potter, J.D. & Gergely, J. (1975) The calcium and magnesium binding sites on troponin and their role in the regulation of myofibrillar adenosine triphosphatase, J. Biol. Chem. 250, 4628-4683

Potter, J.D., Hsu, F.J. & Pownall, H.J. (1977) Thermodynamics of Ca^{2+} binding to troponin C, J. Biol. Chem.252, 2452-2454

Potter, J.D. & Johnson, J.D. (1982) In: Calcium and cell function (W.Y. Cheung ed), Vol. II, Academic press, New York, USA

Poulsen, F.R. & Lowy, J. (1983) Small angle X-ray scattering from myosin heads in relaxed and rigor frog skeletal muscles, Nature (London) 303, 146-152

Rosenfeld, S.S. & Taylor, E.W. (1984) The ATP'ase mechanism of skeletal & smooth muscle acto.S1, J. Biol. Chem. 259, 11908-11925

Rosenfeld, S.S. & Taylor, E.W. (1985a) Kinetic studies of calcium and magnesium binding to TnC, J. Biol. Chem. 260, 242-251

Rosenfeld, S.S. & Taylor, E.W. (1985b) Kinetic studies of calcium binding to regulatory complexes from skeletal muscle, J. Biol. Chem. 260, 252-261

Ross, P.D. & Scruggs, R.L. (1964) Electrophoresis of DNA III. The effect of several univalent electrolytes on the mobility of DNA, Biopolymers 2, 231

Ross, P.D. & Subramanian, S. (1981) Thermodynamics of protein association reactions: Forces contributing to stability, Biochemistry 20, 3096-3102

Shriver, J.W. & Sykes, B.D. (1981) P-31 nuclear magnet evidence for two conformations of myosin S1-nucleotide complexes, Biochemistry 20, 2004-2012

Siemankowski, R.F. & White, H.D. (1984) Kinetics of the interaction between actin, ADP and cardiac myosin S1, J. Biol. Chem. 259, 5045-5053

Siemankowski, R.F., Wiseman, M.O. & White, H.D. (1985) ADP dissociation from actomyosin subfragment 1 is suffiently slow to limit the unloaded shortening velocity in vertebrate muscle, Proc. Natl. Acad. Sci. U.S.A. 82, 658-662

Sivaramakrishnam, M. & Burke, M. (1982) The free heavy chain of vertebrate skeletal myosin subfragment 1 shows full enzymatic activity, J. Biol. Chem. 257, 1102-1105

Sleep, J.A. & Hutton, R.L. (1980) Exchange between inorganic phosphate and adenosine 5'-triphosphate in the medium by actomyosin subfragment 1, Biochemistry 19, 1276-1283

Sleep, J.A. & Smith, S.J. (1981) Actomyosin adenosine triphosphatase and muscle contraction, Curr. Topics Bioeng. 11, 239-286

Stafford, W.F. (1985) Effect of various anions on the stability of the coiled coil of skeletal muscle myosin, Biochemistry 24, 3314-3321

Starr, R. & Offer, G. (1982) Preparation of C-protein, H-protein, X-protein and Phosphofructokinase, Methods in Enzymology 85, 130-138

Stein, L.A., Schwarz, Jr., R.P., Chock, P.B. & Eisenberg, E. (1979) Mechanism of acto.S1 ATP'ase. Evidence that adenosine triphosphate hydrolysis can occur without dissociation of the actomyosin complex, Biochemistry 18, 3895-3909

Stewart, M. & Edwards, P. (1984) Length of myosin rod and its proteolytic fragments determined by electron microscopy, FEBS Lett. 168, 75-78

Suck, D., Kabsch, W. & Mannherz, H.G. (1981) Three dimensional structure of actin:DNA'ase 1 complex at 6 Angstroms resolution, Proc. Natl. Acad. Sci. U.S.A. 78, 4319-4323

Sutoh, K. (1983) Mapping of actin-binding sites on the heavy chain of S1, Biochemistry 22, 1579-1585

Tanford, C., Buckley, C.E., Paritosh, K.D. & Lively, E.P. (1962) Effect of ethylene glycol on the conformation of alpha-globulin and beta-lactoglobulin, J. Biol. Chem. 237, 1168-1171

Trayer, H.R., Levine, B.A. & Trayer, I.P. (1985) Differential binding of rabbit fast muscle subfragment 1-isoenzymes to regulated actin in the presence of Ca^{2+}, J. Muscle Res. Cell Motil. 6, 81p

Trayer, H.R. & Trayer, I.P. (1983) Fluorescence energy transfer between the myosin subfragment 1 isoenzymes and F-actin in the absence and presence of nucleotides, Eur. J. Biochem. 135, 47-49

Tregear, R.T., Terry, C.S. & Sayers, A.J. (1984) The process of muscle relaxation by the combined action of MgAMPPNP and ethylene glycol, J. Muscle Res. Cell Motil. 5, 687-696

Trentham, D. R., Eccleston, J. & Bagshaw, C.R. (1976) Kinetic analysis of ATP'ase mechanisms, Quart. Rev. Biophys. 9, 217-281

Trinick, J., Knight, P. & Whiting, A. (1984) Purification and properties of native titin, J. Mol. Biol. 180, 331-356

Trybus, K.M. & Taylor, E.W. (1980) Kinetic studies of the co-operative binding of S1 to regulated actin, Proc. Natl. Acad. Sci. U.S.A. 77, 7209-7213

Vanderkerckhove, J. & Weber, K. (1979) The amino acid sequence of actin from chicken skeletal muscle actin and chicken gizzard smooth muscle actin, FEBS Lett. 102, 219-222

Vibert, P. (1988) Domain structure of the myosin head in correlation-averaged images of shadowed molecules, J. Muscle Res. Cell Motil. 9, 147-155

Vibert, P. & Cohen, C. (1988) Domains, motions and regulation in the myosin head, J. Muscle Res. Cell Motil. 9, 296-305

Von Hippel, P.H. & Schleich, T. (1969a) In: Biological Macromolecules (G. Fasman & S. Timasheff eds.) Vol. II, 1969, Marcel Dekker, New York, USA.

Von Hippel, P.H. & Schleich, T. (1969b) Ion effects on the solution structure of biological macromolecules, Accounts Chem. Res. 2, 257-265

Von Hippel, P.H. & Wong, K.Y. (1962) The effect of ions on the kinetics of formation and stability of the collagen-fold, Biochemistry 1, 664-670

Wagner, P.D. & Stone, D.B. (1983) Myosin heavy chain, light chain recombinations and interactions between two classes of light chain, J. Biol. Chem. 258, 8876-8886

Wang, S.M. & Greaser, M.L. (1985) Immunocytochemical studies using a monoclonal antibody to bovine cardiac titin on intact and extracted myofibrils, J. Muscle Res. Cell Motil. 6, 293-312

Warren, J.C. & Cheatum, S.G. (1966) The effect of various salt conditions on myosin, Biochemistry, 5, 1702-1707

Warren, J.C., Stowring, L. & Morales, M.F. (1966) The effect of structure-disrupting ions on the activity of myosin and other enzymes, J. Biol. Chem. 241, 309-316

Webb, M.R., Hibberd, M.G., Goldman, Y.E. & Trentham, D.R. (1986)

Oxygen exchange between Pi in the medium and water during ATP hydrolysis mediated by skinned fibres from rabbit skeletal muscle, J. Biol. Chem. 261, 15557-15564

Weeds, A.G. & Taylor, R.S. (1975) Separation of subfragment 1 isoenzymes from rabbit skeletal muscle myosin, Nature (London) 257, 54-56

West, J.J., Nagy, B. & Gergely, J. (1967) The effect of EDTA on the spectral properties of adenosine triphosphate-ADP and ITP G-actin, Biochem. Biophys. Res. Commun. 29, 611-619

White, H.D. (1977) Magnesium binding to acto-myosin.S1 and acto-heavymeromyosin, Biophys. J. 17, 40a

White, H.D. & Taylor, E.W. (1976) Energetics and mechanism of actomyosin ATP'ase, Biochemistry 15, 5818-5826

White, S.P., Cohen, C. & Phillips, G.N. (1987) Structure of co-crystals of Tm and Tn, Nature (London) 325, 826-828

Wilkinson, J.M. & Grand, R.J.A. (1975) The amino acid sequence of troponin I from rabbit skeletal muscle, Biochem. J. 149, 493-496

Winkelmann, D.A. Meekel, H. & Rayment, J. (1985) Packing analysis of crystalline S1, J. Mol. Biol. 181, 487-501

Woledge, R.C., Curtin, N.A. & Homsher, E. (1985) In: Energetic aspects of muscle contraction, Academic press,London and Orlando.

Zot, A.S. & Potter, J.D. (1987a) Effect of Mg^{2+} on the Ca^{2+} dependence of ATPase and tension development of fast skeletal muscle, J. Biol. Chem. 262, 1966-1969

Zot, A.S. & Potter, J.D. (1987b) Structural aspects of troponin-tropomyosin regulation of skeletal muscle contraction,Ann. Rev. Biophysics Biophys. Chem. 16, 535-559

APPENDIX 1 The ratio of perturbation amplitude for the two-step binding reaction

Consider the reaction:

$$A + B \underset{}{\overset{K_1}{\longleftrightarrow}} C \overset{K_2}{\longleftrightarrow} D$$

If "i" denotes initial concentrations and "f" the concentration after the perturbation then the equilibrium constants K_1 and K_2 can be derived as follows:

$$K_1{}^i = \frac{C^i}{A^i B^i} \quad (1) \qquad K_1{}^f = \frac{C^f}{A^f B^f} \quad (2)$$

$$K_2{}^i = \frac{D^i}{C^i} \quad (3) \qquad K_2{}^f = \frac{D^f}{C^f} \quad (4)$$

if Δ represents the change in concentration upon perturbation then:

$$C^i = C^f + \Delta C \quad (5) \qquad D^i = D^f + \Delta D \quad (6)$$

combining 1, 2 and 5 then:

$$C^f + \Delta C = (K_1{}^f + \Delta K)\ (A^f + \Delta A)\ (B^f + \Delta B)$$

if the product of two Δ terms is negligible, and $\Delta B = \Delta C$ then:

$$\Delta C = K_1{}^f \Delta A\ (A^f + B^f) + \Delta K_1{}^f A^f B^f \quad (7)$$

similary, combining 3,4 and 6 :

$$\Delta D = \Delta C K_2^f + C^f \Delta K_2^f \quad (8)$$

conserving A,

$$\Delta A + \Delta C + \Delta D = 0$$

from 8

$$\Delta A + \Delta C + \Delta C K_2^f + \Delta C^f \Delta K_2^f = 0$$

using expression (7) then:

$$-\Delta A = \frac{\Delta K_1 A^f B^f (1+K_2^f) + C^f \Delta K_2^f}{1 + K_1^f (A^f + B^f)(1 + K_2^f)} \quad (9)$$

(7) and (9) gives:

$$\Delta C = \frac{\Delta K_1^f A^f B^f - C \Delta K_2^f K_1^f (A^f + B^f)}{1 + K_1^f (A^f + B^f)(1+K_2^f)} \quad (10)$$

as $\Delta D = -\Delta A - \Delta C$ then ΔD, using 9 & 10

$$\Delta D = \frac{\Delta K_1^f K_2^f A^f B^f + C^f \Delta K_2 (1+K_2 (A^f+B^f))}{1 + K_1^f (A^f + B^f)(1+K_2^f)}$$

if ΔK_1 is zero, that is, pressure only perturbs the second reaction then:

$$\Delta D = \frac{C \Delta K_2^f (1+K_1 (A^f+B^f))}{1 + K_1^f (A^f + B^f)(1+K_2)}$$

This equation describes the change in amplitude of D, this is composed of two phases. The fast phase is described by:

$$\frac{C\Delta K_2}{1 + K_2}$$

The slow phase is then the total amplitude minus the fast phase:

$$\frac{C\Delta K_2{}^f K_2{}^f}{(1+K_2)\ (\ 1+K_1{}^f)\ (A^f + B^f)(1+K_2{}^f)}$$

the ratio of the two phases is then:

$$\frac{1+ K_1{}^f (A^f+B^f)(1+K_2{}^f)}{K_2{}^f}$$

APPENDIX 2 Determining the K_d for metal-indicator complexes

For 1:1 Metal:Indicator binding

The dissociation constant for a metal-indicator complex (K_d) was estimated from a plot of [metal] vs. [metal]/ΔA, where ΔA is the molar absorbance change of the indicator upon addition of the metal.

For the equilibrium metal-indicator = $metal^-$ + $indicator^-$

$$K_d = \frac{[metal^-]_f \, [indicator^-]_f}{[metal\text{-}indicator]} \quad ....(1)$$

$$[indicator^-]_f = [indicator]_t - [metal\text{-}indicator] \quad ... \quad (2)$$

Where $[indicator^-]_f$ and $[metal^-]_f$ are the concentrations of indicator and metal <u>free</u> in solution, and $[indicator]_t$ and $[metal]_t$ are the <u>total</u> concentrations of indicator and metal, i.e. free plus bound. Substituting for $[indicator^-]_f$ from (2) into (1) gives:

$$K_d = \frac{[metal^-]_f([indicator]_t - [metal\text{-}indicator])}{[metal\text{-}indicator]} \quad ...(3)$$

The [metal-indicator] is directly related to the absorbance change by the Lambert-Beer-law

$$[metal\text{-}indicator] = \Delta A/\varepsilon$$

when the cell path length is 1cm and ε the molar absorption

coefficient. For low indicator concentrations the concentration of metal bound will be low and $[\text{metal}^{-}]_f \approx [\text{metal}]_t$. Making this assumption and substituting for [metal-indicator] in (3), and rearranging gives:

$$[\text{metal}]_t = \frac{[\text{metal}]_t\,[\text{indicator}]_t}{\Delta A/\varepsilon} - K_d$$

Therefore from a plot of $[\text{metal}]_t$ vs. $[\text{metal}]_t/\Delta A$ the K_d for the complex can be obtained from the negative intercept of the ordinate.

APPENDIX 3 Computer programme written by Dr. D.J. Halsall for the determination of volume changes

```
JPR£2
JLIST

 10  PRINT "VOL"
 15  PRINT : PRINT
 20  PRINT " A + S <==>AS<==>AS*"
 30  PRINT "          K1     K2"
 35  PRINT : PRINT
 37  INPUT "R*T (ATM*K) ,2.26*E4 A
     T23'C)";R: PRINT : PRINT
 40  INPUT "KD UM ";KD:KD = KD * 1
     E - 6: INPUT " K1 ";K1
 45  PRINT : PRINT "1/KD * K1 =  "
     1 / (KD * K1): PRINT
 49  PRINT : INPUT " K2 ";K2: PRINT

 50  INPUT "AO UM";AO: INPUT "SO U
     M";SO
 55  PRINT : PRINT
 60 AO = AO * 1E - 6:SO = SO * 1E -
     6
 70  REM  EQ CONC
 75  PRINT
 80 B = KD + AO + SO:C = AO * SO
 90 Q =  SQR (B ^ 2 - 4 * C)
100 X = (B - Q) / 2
110 AS = X / (K2 + 1):DAS = K2 *
     X / (K2 + 1)
120 S = SO - X:A = AO - X
125  PRINT " EQ CONC M": PRINT
130  PRINT "S="S: PRINT "A="A: PRINT
     "AS="AS
140  PRINT "AS*"DAS
150  PRINT : PRINT
200  INPUT "AMP MM ";AM: INPUT "F
     ULL SCALE MM ";FS: INPUT "Y
     SCALE V ";FV: INPUT "SIGNAL
     V ";V
210 F = V / (A + AS + (.3 * DAS))

230 DSA = (AM * FV) / (F * FS * .
     7)
235  PRINT : PRINT
240  PRINT "CHANGE IN AS* ="DSA"M
     "

300  REM  D = A+AS)P,E=S + AS )P
310 D = A + AS + DSA
320 E = S + AS + DSA
340  REM  EQ
350 I = (1 / K1) + D, + E:G = D *
     E
360 H =  SQR (I ^ 2 - 4 * G)
370 PAS = (I - H) / 2
375  PRINT : PRINT : PRINT "CONC
     AT HIGH PRESSURE M": PRINT
380  PRINT "AS  = "PAS
400 SAP = DAS - DSA: PRINT "AS* =
     "SAP
410 KP2 = SAP / PAS
420  PRINT "K2= "KP2
423  PRINT : PRINT
425  INPUT "P.JUMP ATM= ";DP
427  PRINT
429  REM  T = 2.5'C
430 VC = (( LOG (K2) -  LOG (KP2)
     ) * R) / DP
431  PRINT "VOL CHANGE ="VC" CC P
     ER MOLE"
435  PRINT : PRINT
436  PRINT : PRINT "<1> K2 CALC":
      PRINT "<2> PRINT": GET H$
437 H% =  VAL (H$): ON H% GOTO 46
     0,440: GOTO 437
440  PRINT "<1> RESTART WITH SAME
      K'S": PRINT "<2> RESTART": PRINT
     "<3> PRINT": PRINT
450  GET A$:A% =  VAL (A$): ON A%
      GOTO 50,35,500: GOTO 450
460  INPUT " FAST AMPLITUDE MM ";
     AF
465  PRINT
470 CAS = (AF * FV) / (FS * F * .
     7)
480 KB = (SAP - CAS) / (PAS - CAS
     ): PRINT "K2 ="KB: GOTO 440
500  PR£ 1: POKE 1657,80
510  PRINT "AO ="AO" SO ="SO" AMP
      ="AM" SCALE ="FS" YSCALE =
     "FV" SIGNAL ="V
520  PRINT "P.J ="DP"
550  PRINT : PRINT "VOL CHANGE ="
     VC" CC PER MOLE  K2 ="KB: PRINT

560  PR£ 0: GOTO 440
```